Towards osteochondral regeneration with human bone marrow derived mesenchymal stromal cells in a functionalized hydrogel system

Inauguraldissertation zur Erlangung der Würde eines Doktors der Philosophie vorgelegt der Philosophisch-Naturwissenschaftlichen Fakultät der Universität Basel von

Chiara Alessandra Noëmi Stüdle
von Luzern, LU

Basel, 2018

Genehmigt von der Philosophisch-Naturwissenschaftlichen Fakultät auf Antrag von

Prof. Dr. Rolf Zeller, Prof. Dr. Ivan Martin und PD Dr. Martin Ehrbar

Basel, 14.11.2017

Prof. Dr. Martin Spiess,
The Dean of Faculty

Table of content

Abbreviations

ACs	Articular chondrocytes
BM	Bone marrow
BMSCs	Bone marrow derived mesenchymal stromal cells
bTGFß3	Biotinylated TGFß3
CC	Chondrogenic differentiation capacity
ChM	Chondrogenic medium
CM	Complete medium (with 10 % FBS)
COL	Collagen
DGA	Differential gene expression analysis
ECM	Extracellular matrix
FG	Fast green
GAG	Glycosamino glycan
HM	Hypertrophic medium
hu	human
IF	Immunofluorescence
IHC	Immunohistochemistry
ms	mouse
NCs	Nasal chondrocytes
OM	Osteogenic medium
P	passage
PEG	Poly(ethylene glycol)
SafO	SafraninO
TE	Tissue engineering

Summary

There is the need of alternative treatment strategies for osteochondral injuries that include a defect of articular cartilage and the underlying bone. Human bone marrow derived mesenchymal stromal cells (BMSCs) due to their ease of isolation and multipotent differentiation capacity have been investigated for a long time as cell source candidate for osteochondral tissue engineering. However, their clinical application has been hampered by several limitations most importantly such as intrinsic tendency to acquire a (pre-) hypertrophic chondrogenic phenotype leading to endochondral ossification in vivo, lack of spatial control of the differentiated cell phenotypes and vast donor-to-donor variability, as well as unpredictability of differentiation outcome potentially due to the crude isolation procedure and lack of selective markers.

Part I of the thesis addressed the optimization of the protocol to generate endochondral bone by BMSCs and the assessment of the formation of bone-cartilage composites by combination of BMSCs with nasal chondrocytes (NCs). To this end, an enzymatically cross-linked and cell-degradable poly(ethylene glycol) (PEG) based hydrogel system served as a scaffolding material. By functionalization of the hydrogel with TGFß3 employing an affinity binding strategy, encapsulated BMSCs were induced to undergo endochondral ossification resulting in the efficient formation of ossicles including a cortical rim and bone marrow upon immediate subcutaneous implantation in immunocompromised mice. This demonstrated that the otherwise needed lengthy in vitro culture step can be circumvented. In bi-layered hydrogels endochondral ossification of BMSCs occurred similarly to the single-layered configuration, while NCs formed cartilaginous tissue, however, unexpectedly acquired hypertrophic features under the influence of the TGFß3 from the BMSC-layer. Replacing TGFß3 with BMP-2 allowed the formation of an osteochondral construct including hyaline cartilage corroborating the potential of our approach to generate cartilage-bone composites. In future, these bi-layered gels need to be tested in an orthotopic model with special focus on how an interface closely resembling the native one can be generated.

Part II of the thesis aimed at elucidating the existence of an expanded BMSC subpopulation with superior chondrogenic differentiation potential. It was hypothesized that retrospective analysis of single clones with high chondrogenic capacity have a different gene expression profile than clones with low capacity and that differential gene expression would guide to prospectively isolate superior chondrogenic potential clones from bulk BMSCs. For one of the tested donors a segregation of clones of high and low CC based on their transcriptomic profile could be observed.

Comparison of sorted multiclonal BMSCs based on CD56/NCAM1 - the most promising surface marker identified by the transcriptomic analysis - in chondrogenic in vitro culture assays showed a trend of better chondrogenesis in the CD56$^+$ cells, however, it necessitates confirmation with additional donors. In a further analysis of clones from other donors, intra-donor variability compromised the revelation of transcriptional signatures of clones with high versus low chondrogenic capacity. In future, RNA sequencing as well as cell sorting are required to be performed at earlier time points to exclude confounding effects from extensive cell expansion. Ultimately, identification of a cell subset with superior chondrogenic potential may aid to develop improved BMSC based osteochondral tissue engineering approaches.

1 Introduction

1.1 Articular cartilage

1.1.1 Structure

Articular cartilage, a connective tissue of hyaline cartilage type covers the bone surface of diarthrodial joints. Its major function is to transmit load and to allow smooth articulation of the joints. It is composed of extracellular matrix (ECM) mainly based on collagens and proteoglycans and is scarcely populated by one cell type, the chondrocyte. Articular cartilage is not vascularized and does not contain nerves. The nutrition happens solely through diffusion from the synovial space or the subchondral bone plate [1].

Articular cartilage has a zonal organization (Figure 1), from top to bottom there is the superficial (SZ), the middle/transitional (TZ), the deep/radial zone (RZ), the calcified cartilage (CC), the subchondral bone plate (SB) and the subchondral spongiosa. The line visible in H&E staining between the RZ and the calcified cartilage is called tidemark (T). The whole structure is a few millimeters thick. From the SZ to the RZ the cell density decreases, in the SZ the cells have a flattened, whereas in the other zones the cells have a rounded morphology and in the RZ they are arranged in columns of 5-8 cells oriented perpendicular to the joint surface. The content of glycosamino glycan (GAGs) increases from the surface to the deeper zones, as well as the thickness of the collagen fibers, which are parallel to the surface in the SZ, of mixed orientation in the TZ and perpendicular to the surface in the RZ [2].

The ECM can be divided into three regions, depending on the distance to the chondrocyte, the pericellular, the territorial matrix and the interterritorial matrix forming the largest region. Collagens (Col) mainly of type II and marginally of type I, IV, V, VI, IX, and XI account for 60% of the dry weight of the articular cartilage ECM [1]. Collagens have a very specific protein structure, namely they are composed of a repetitive Gln-Pro-hydroxyPro-tripeptide alpha-chain forming triple helices, which arrange in fibers of 50-110 µm in diameter from the SZ to the RZ as measured by scanning electron microscopy [3]. Proteoglycans contribute 10-15 % to the dry weight of the ECM. They are composed of small protein cores heavily decorated with long linear GAGs of up to 100 monosaccharides. Due to their high negative charge they are responsible for the high osmotic

pressure within articular cartilage and thereby providing it with high physical strength. The main proteoglycan in articular cartilage is aggrecan [1].
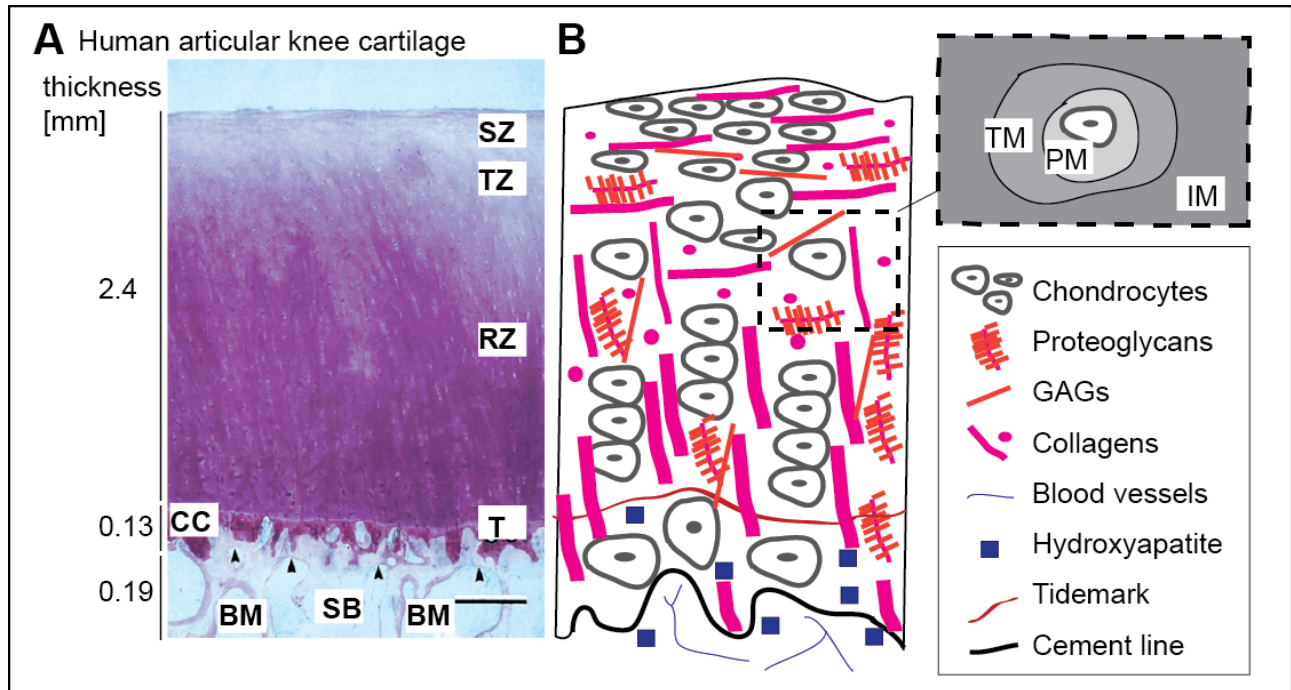

Figure 1: Zonal organization of articular cartilage. A) Human articular cartilage from the femoral condyle stained with McNeil's Tetrachrome, basic Fuchsine and Toluidine Blue O, scale bar: 500 µm. On the left the average thicknesses of the respective layers are indicated in mm (adapted from [2]). B) Schematic drawing of articular cartilage. SZ: superficial zone, TZ: transitional zone, RZ: radial zone, T: tidemark, CC: calcified cartilage, SB: subchondral bone, BM: bone marrow, PM: pericellular matrix, TM: territorial matrix, IM: interterritorial matrix.

1.1.2 Development

During limb development two different cartilage types are formed, i) the stable articular cartilage and ii) the transient cartilage of the cartilage anlage and the growth plate that is eventually replaced by bone tissue (Figure 3). The development of articular cartilage is linked to joint formation, which morphologically manifests first in the so-called interzone. It is a cell band interrupting the cartilaginous condensations at the prospective joint sites that is demarcated by down-regulation of chondrogenic genes such as ColII and Sex-Determining Region Y-Box 9 (Sox9), as well as up-regulation of growth differentiation factor 5 (GDF-5) (a member of the bone morphogenetic protein (BMP) superfamily), wingless-type MMTV integration site family 9a (Wnt9a) and Wnt4, and the BMP antagonists chordin and noggin [4-6] (Figure 3C). The precise molecular mechanisms governing the induction of interzone formation are not completely known yet. Clearly, Wnt signaling, in particular Wnt9a secreted from interzone cells, plays an important role since its

10

ectopic application caused heterotopic joint-like structures [7, 8]. However, it has been demonstrated that Wnt is not a requisite for joint induction, but rather it is involved in the regulation of joint integrity by inhibiting chondrogenesis and by regulating indian hedgehog (Ihh) expression [9]. Ihh in turn is not only involved in controlling the phenotype of growth plate chondrocytes, but it also seems to be implicated in joint formation [10]. Additionally, tight regulation of BMP signaling is crucial for joint formation [11]. Lineage tracing studies demonstrated that articular cartilage and the other joint related structures, but not growth plate cartilage, directly originate from GDF-5^{+} interzone cells [12]. Later, conditional lineage tracing of the progeny of GDF-5^{+} cells revealed that joint development necessities a continuous influx of cells contributing to the GDF-5 lineage, since a single tamoxifen administration was insufficient to label all joint cells at late embryonic days [13]. These experiments also showed that through the temporal induction of new GDF-5^{+} cells the lineage divergence is controlled. Early traced interzone cells contributed to different joint tissues than temporally later traced ones, which developed to articular chondrocytes [13, 14]. What is the driver of the temporal lineage specification and the precise population of cells replenishing the GDF-5^{+} interzone cells still remains elusive. In contrast, Ray et al. demonstrated by pulse-chase DNA-labeling experiments and lineage tracing of the progeny of ColII^{+} cells that the proliferating chondrocytes within the cartilage anlage not only contribute to transient chondrocytes, but also to the proliferation deficient interzone cells and proposed that inhibition of BMP signaling by noggin expressed by cells directly next to the presumptive joint site directed this lineage segregation [15] (Figure 3D). Articular cartilage adopts its unique structure postnatal, it is controversial whether cell proliferation plays a role [16] or if it is rather governed by cellular rearrangements and cell volume increase [14].

Whether we can extrapolate from the precise understanding of the development, more specifically from how the lineage bifurcation into stable and transient cartilage is decided, to treatment strategies advancing cartilage regeneration remains to be answered.

1.1.3 Repair and current treatment strategies

Cartilage has very limited self-repair capacities due to its avascular nature, low proliferative activity of resident chondrocytes and dense ECM network not allowing for cell migration. Articular cartilage injuries are classified according to how deep the injury penetrates the tissue. In partial thickness defects, the injury affects the tissue above the tidemark, in full thickness defects the subchondral bone plate is exposed and in osteochondral defects the injury goes beyond the subchondral bone

plate and can even penetrate the subarticular spongiosa [17]. Lack of treatment or insufficient repair can cause the degenerative disease osteoarthritis that leads to functional loss of the joint articulation. Interestingly, by analysis of the degree of post-translational modifications of cartilage ECM proteins Catterall et al. observed that in human osteoarthritic knee cartilage the modified to unmodified collagen ratio was much lower than in osteoarthritic hip suggesting that knee cartilage is biologically "younger" than hip cartilage thanks to a higher repair response by producing more new ECM protein. This study suggested the existence of intrinsic healing responses at least in certain joints; the very important question remaining is how they can be enhanced in order to prevent joint degeneration [18].

Surgical interventions to treat articular cartilage injuries include bone marrow stimulatory techniques, which allow the formation of a bone marrow clot at the defect site, mosaic plasty that encompasses the transfer of osteochondral pieces from a less weight bearing region, or the implantation of previously harvested and expanded articular chondrocytes directly (ACI, autologous chondrocyte implantation (ACI)) or with the help of a collagen and/or GAG based scaffold, (matrix associated ACI ((MACI)) [19]. Mosaic plasty is not often applied because of limited donor site availability and very high donor site morbidity. Bone-marrow stimulatory techniques, as well as the implantation of ACs often result in the formation of fibrocartilage that is rich in ColI and has inferior mechanical properties, hence can induce osteoarthritis. Moreover, for the treatment based on autologous ACs the donor site morbidity and the need for a two-step surgical procedure is also an issue [20]. Meta-reviews comparing ACI with microfracture procedures did not reveal whether one technique is superior over the other [21, 22]. Neither did various clinical studies show whether one technique is better than the other in a certain scenario [20]. Absence of consent is based on different reasons, mainly maybe due to lack of standardization. A promising approach for an alternative treatment strategy is tissue engineering (TE) (described in section 1.3.2) by e.g. using an alternative cell source with reduced donor site morbidity such as MSCs harvested from the bone marrow (discussed in section 1.3.2.1.2).

If there is only one defect with a size smaller than 1 cm in an otherwise healthy human (knee) joint, it can heal. Also in animal models there are the non-critical-size defects. Although, a recent study in rat demonstrated that even small defects that healed on short term could cause joint wide alterations such as increased catabolism and subchondral bone plate advancement at later time points [23]. Are these defects filled thanks to increased anabolic activity of the neighboring cells eventually concomitant with limited proliferation? If yes, what are the stimuli for them and why do

they lack or are insufficient in critical size defects? Or are there specific cells in the articular cartilage or the neighboring tissues such as the synovium or the infra-patellar fat pad that could be activated to contribute to repair? What is more, what is the precise origin of the cells forming repair tissue (sometimes stated to be very good) in small and pre-clinical animal models if acellular materials are implanted in critical-size defects? E.g. to date, a number of studies have addressed the use of acellular natural or synthetic scaffolds decorated with growth and/or chemotactic factors in order to improve the homing of endogenous cells for cartilage regeneration [24-26]. Studies assessing the effectiveness of repair between material-based treatments of defects with and without subchondral bone involvement (it is important to differentiate the two scenarios, since in the latter case bone marrow derived progenitor cells have facilitated access to the injury site) should be combined with cell tracing studies in order to find out which cells exactly are attracted by the diverse functionalized scaffolds implanted. A few studies have recently led to the identification of putative joint progenitor cells. They were defined based on characterization of the joint site by looking for slow-cycling proliferative cells and for numerous stem cell markers, as well as specific traits e.g. transforming growth factor beta receptor (TGFßR) II [27] or proteoglycan (Prg) 4 expression [16] in combination with in vitro colony-forming-unit and differentiation assays. These cells localized to various joint tissues such as the superficial zone of articular cartilage, the infra-patellar fat pat, the synovium and the groove of ranvier, and were shown to persist also in the (young) adult organism [6].

1.2 Bone

1.2.1 Structure

Bone gives mechanical structure to soft tissues, houses hematopoiesis and controls blood calcium levels. It has a hierarchical structure (Figure 2). Macroscopically there is cortical (compact) and trabecular (cancellous) bone. The ends of long bones consist of a cortical rim and a trabecular interior at the epiphysis and cortical bone at the diaphysis, while flat bones have a shelf of cortical bone and a trabecular interior. Trabecular bone is less dense, more porous and the lamellae are more irregularly distributed than in cortical bone. The lamellae are sheets of mineralized ColI fibers that in cortical bone are centrally arranged around the haversian canal containing nerves, blood and lymphatic vessels and together form the osteon [28]. During development and bone healing upon endochondral ossification woven bone (primary bone) is formed first. It is characterized by rapid calcification, thinner collagen fibers and overall a less organized structure of the lamellae. Later it is remodeled into secondary (compact and cancellous) bone [29]. The primary cell that

builds up the bone ECM is the osteoblast. It develops from mesenchymal precursors and either once embedded into the mineralized matrix it becomes an osteocyte or at the bone rim it stays as a quiescent bone lining osteoblast. The osteocytes are star-shaped cells with long extrusions that allow cell-cell communication through gap junctions. They sense the mechanical status of the surrounding bone and guide remodeling by osteoclasts. Osteoclasts, monocyte-derived multinucleated cells acidify the microenvironment in order to dissolve the hydroxyapatite crystals and secrete various enzymes such as metalloprotease 9 (MMP9) or cathepsin K to degrade the decalcified ECM [30]. ColI, the major organic component of bone, arranges as fibrils in arrays and may play a role, although not fully elucidated yet, in initiation of the formation and in governing the orientation and size of hydroxyapatite crystals [31]. Other ECM proteins are osteopontin, osteocalcin or bone sialoprotein (BSP) that are implicated in cell-ECM interactions and also play a role in bone mineralization [32].
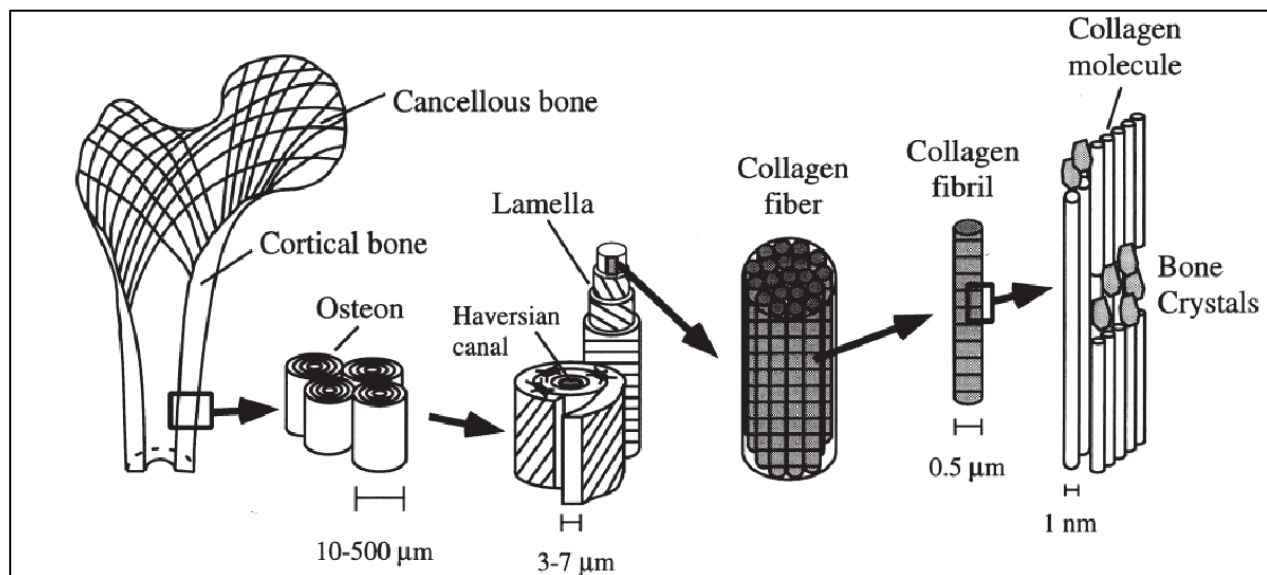
Figure 2: Hierarchical organization of bone. Cortical bone is composed of osteons that in the middle contain blood vessels and nerve fibers and contain the lamella in which the connected osteocytes reside and are built up by calcified ColI fibers. These fibers are aggregates of collagen fibrils which in turn are aggregates of collagen triple helices (adapted from [28]).

1.2.2 Development

Bone tissue has three different embryonic origins and develops trough two different processes. While the bones of the extremities develop from lateral plate mesoderm, ribs and the vertebra originate from rostral paraxial mesoderm through the somites and the craniofacial bones mainly develop from neural crest cells descending from the neuroectoderm. The first two undergo

endochondral ossification (Figure 3), in which first a cartilage template is formed that is subsequently remodeled into bone and the latter undergoes mainly intramembranous (direct) ossification, which lacks the cartilage intermediate step [33].

1.2.2.1 Endochondral ossification

The transfer of different parts of the chicken limb bud to ectopic sites led to the identification of two different organizing cell centers within the limb bud. The apical ectodermal ridge (AER) at the distal tip governs the specification of the proximal-distal axis, and the zone of polarizing activity (ZPA) within the posterior mesenchyme determines the anterior-posterior axis [34-36]. The AER secretes fibroblast growth factors (FGFs) and Wnts, the inner mesenchymal cells produce BMP-4 and its inhibitor Gremlin-1 (Grem1) and the main signal of the ZPA is sonic hedgehog (Shh). Initial high levels of mesenchymal BMP-4 induce Grem1 expression that allows the secretion of the FGFs by the AER, which in turn initiates the secretion of Shh by the ZPA. Shh keeps the Grem1 levels high, while BMP-4 decreases and allows the AER to produce more FGF initiating an intricate loop that connects the two axes of the limb and additionally is responsible for digit number specification. It terminates (automatically) because of progenitor cell proliferation causing a shift out of the influence of the morphogens [37]. The mesenchymal cells under the influence of the AER stay undifferentiated and proliferate (Figure 3A). As soon as they are not under the influence of the AER anymore the chondrogenic program by high BMP-4 and consequently Sox9 activity can be induced [38] (Figure 3B). Deletion of Sox9 in pre-condensating mesenchyme showed that the transcription factor is necessary to establish the osteochondropogenitor lineage, since in absence of it, the limb bud mesenchymal cells were stuck [39]. After condensation and induction of ColII and aggrecan, Sox9 in concert with other transcription factors such as Sox5 and 6 drives chondrogenesis by further inducing expression of chondrogenic ECM genes and by supporting the proliferation of the newly formed chondrocytes [39]. This applies for the inner cells, while the outer rim stays uncommitted and forms the perichondrium, which is a few cell layers thick and which with the formation of the primary ossification center (POC) becomes the periosteum.

Ihh specifically expressed by pre-hypertrophic chondrocytes together with parathyroid related protein (PTHrP) expressed by the perichondrium at the distal tip establish a negative feedback loop that governs proliferation and differentiation of the chondrocytes and thereby controls pre- and postnatal bone growth [40]. The chondrocytes within the limb bud are organized along the proximodistal axis as different phenotypes. From the distal to the proximal end there are resting,

proliferating chondrocytes arranged in columns, pre-hypertrophic chondrocytes expressing Ihh and the hypertrophic chondrocytes expressing ColX and being up to 8 fold bigger than the other chondrogenic phenotypes [41] (Figure 3D). This pattern of different chondrocyte phenotypes persists as the cartilaginous growth plate up to adolescence allowing long bone growth to occur. Against the initial notion that Sox9 inhibits hypertrophic differentiation of chondrocytes, conditional deletion of Sox9 through the enhancer of aggrecan demonstrated that Sox9 is not only driving chondrocyte proliferation and expression of major ECM molecules, but also activates expression of the hypertrophic marker ColX and inhibits premature osteoblast differentiation of pre-hypertrophic chondrocytes by inhibiting ß-catenin [42].

For the establishment of the cartilage anlage angiogenesis does not play a role, in contrast the O_2 sensitive transcription factor hypoxia inducible factor 1-alpha (Hif1α) directly contributes to the persistent expression of Sox9 in the post-condensed mesenchyme and therefore is an important factor driving the transition from pre-chondrocytes to chondrocytes [43]. For the induction of bone tissue formation vascularization is crucial, if vascular endothelial growth factor (VEGF) was inhibited systemically by administration of one of its soluble receptors, the vascular pattern in growth plate of juvenile mice was disrupted and the remodeling into bone did not proceed, while the hypertrophic zone became enlarged [44]. With vascular invasion and the expression of Receptor Activator of NF-κB Ligand (RANKL) by hypertrophic chondrocytes, as well as matrix degrading MMPs (mostly MMP13) chondroclasts and osteoclasts are recruited that initiate the degradation of the cartilage ECM and therefore facilitate the deposition of woven bone matrix [45] (Figure 3E).

Until recently because increased abundance of apoptotic bodies was observed in the hypertrophic zone, it was assumed that the majority of hypertrophic chondrocytes are removed by apoptosis and bone tissue is laid down exclusively from progenitors originating from the perichondrium and periosteum. In fact, inducible lineage tracing of ColX expressing cells (hypertrophic chondrocytes) showed that those cells contributed to ColI expressing osteoblasts in the primary ossification center and they persisted till postnatal days, as well as that during postnatal growth the hypertrophic chondrocytes from the growth plate also contributed to osteoblast and sclerostin positive osteocytes in trabecular, cortical and endosteal bone [46]. Park et al. then showed that at the cartilaginous-osseous junction there are small osterix (Osx) positive cells descendent of ColX^{+} cells, which were called the chondrocyte-derived osteoprogenitors (CDOPs), it was proposed that the large cell size loss from hypertrophic chondrocytes to the CDOP could happen through

autophagy [47]. The contribution of CDOPs to prenatal bone was measured to be higher than in postnatal bone [47]. These experiments strongly suggested that endochondral bone cells not only originate from the perichondrium/ periosteum, but also from hypertrophic chondrocytes throughout life (Figure 3E).

The regulation of the transition of proliferative to hypertrophic chondrocytes is a highly complicated process and many more signaling molecules than the previously mentioned Ihh-PTHrP feedback loop have been attributed to play a role such as FGF9 and 18 expressed by perichondrial cells [48, 49] and BMP-2 and 4 expressed by pre- and hypertrophic chondrocytes [50]. Their receptors BMPRIα and ß are expressed throughout all chondrogenic phenotypes and the deletion of them in transient chondrocytes showed that BMP signaling fosters chondrogenic differentiation by inducing Ihh and antagonizing FGF signaling. Furthermore, in absence of the BMP pathway the terminal differentiation was inhibited and osteoblastogenesis did not progress [51]. While Sox9 is the chondrogenic transcription factor, pre- and hypertrophic chondrocytes up-regulate Runt Related Transcription Factor 2 (Runx2), which directly induces the expression of hypertrophic chondrocyte related marker proteins such as VEGF, MMP13 and ColX [52]. In pre-osteoblasts Runx2 functions upstream of the transcription factor Osx, both of them are indispensable for osteoblastogenesis, since genetic deletion of them ablated differentiation to osteoblasts and in absence of Runx2 no expression of Osx was observed [53]. Osteoblastogenesis is dependent on Wnt canonical signaling [54], BMPs [55] and others [52].

The mechanism underlying the induction and formation of the secondary ossification center (SOC) is much less known then of the POC. Within the resting chondrocytes cartilage channels invaginate from the perichondrium that allow blood vessel ingrowth and bone progenitor recruitment [56]. Genetic ablation studies have demonstrated that thyroid hormone [57], various MMPs [56], insulin growth factor 1 (IGF-1) [58] and VEGF [59] are essential for the commencement of secondary ossification (Figure 3F). The resting chondrocytes around the cortical canals become also hypertrophic. How the regulation is governed that the adjacent articular cartilage is not affected by the massive cartilaginous matrix degradation with the formation of the SOC and what is the trigger of the resting chondrocytes to secrete high amounts of VEGF and finally to undergo hypertrophy is not understood yet.
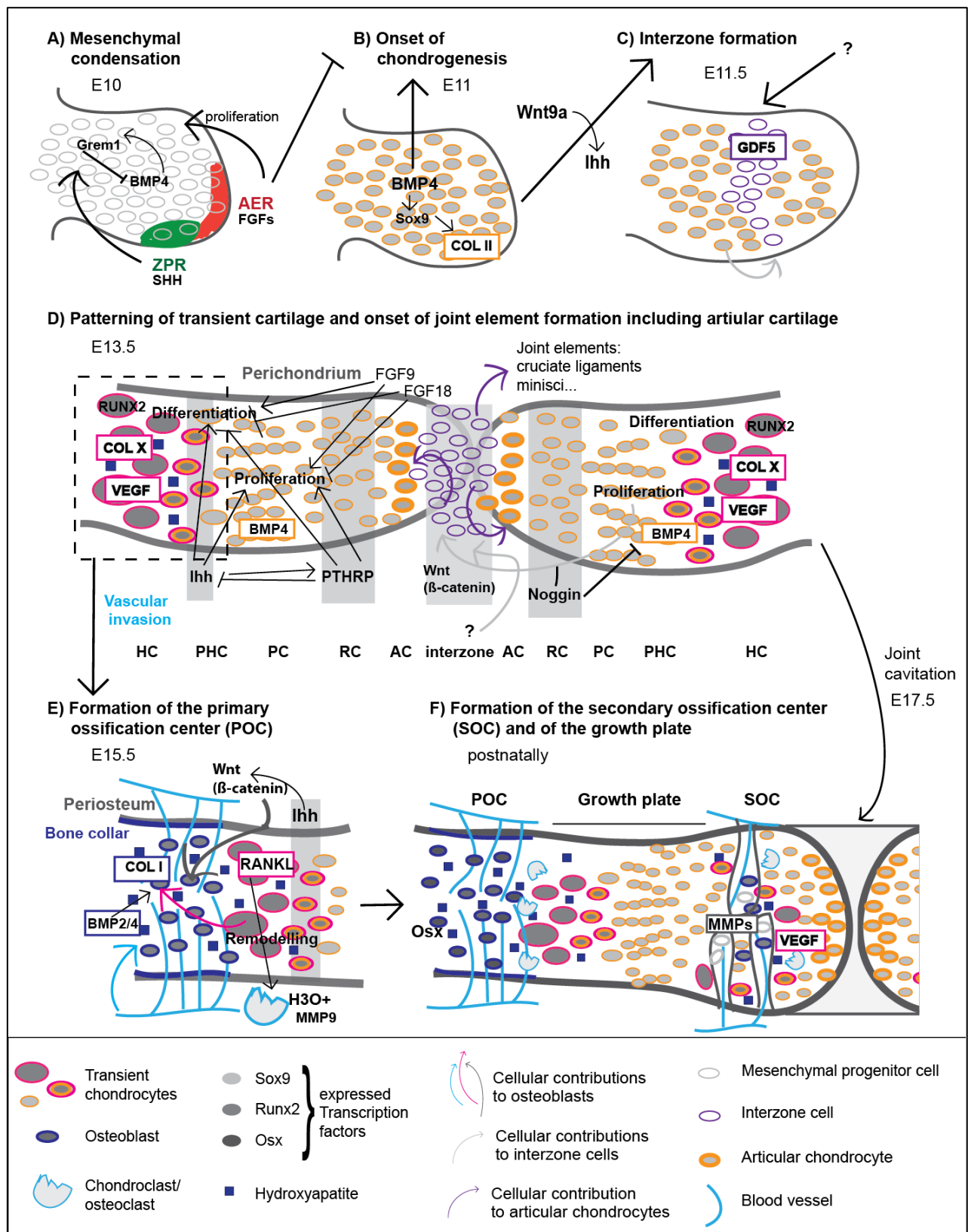
Figure 3: Simplified schematic representation of endochondral ossification of long bones and of the development of articular cartilage. A) Chondrogenesis in the limb bud starts with the condensation of mesenchymal precursors under the influence of high BMP-4 through up-regulation of cell adhesion molecules such as NCAM1 (CD56)

and N-cadherin. **B)** Sox9 expression is induced that up-regulates chondrogenic matrix molecule expression. **C)** Within the chondrogenically differentiating limb bud the interzone forms that localizes at the prospective joint site. **D)** These GDF5$^+$ and Sox9$^-$ interzone cells give progressively rise to all joint elements including articular cartilage (AC). At the same time the cartilage anlagen of the bone patterns into different phenotypes: Resting (RC), proliferating (PC), pre- and hypertrophic chondrocytes (PHC/HC). A tight balance of PTHrP, IHH, FGF and BMP signaling controls chondrocyte proliferation and maturation. **E)** With the ingrowth of blood vessels osteogenesis commences (primary ossification center, POC), perichondrial and hypertrophic chondrocytes contribute to osteoblasts. **E)** Shortly before birth, the joint cavity becomes apparent and the secondary ossification center (SOC) forms upon formation of perichondrial invaginations the so-called cartilage canals at the epiphysis. The growth plate persists till adolescence as long as the bones are growing.

1.2.2.2 Intramembranous ossification

Like endochondral, intramembranous ossification starts with the condensation of mesenchymal cells, but which then directly differentiate towards Runx2 positive osteoblasts and immediately secrete a woven bone ECM. Initial bone formation comes along with rapid proliferation of mesenchymal cells [60]. Day et al. observed that genetic ablation of Wnt signaling within the mesenchymal precursors caused ectopic chondrogenesis not only at the sites of endochondral ossification but also in the regions where normally intramembranous ossification occurs. Their experiments demonstrated that the mesenchymal population normally giving raise to direct ossification also has bipotential differentiation capacities and that high canonical Wnt activity (which was shown to be downstream of IHH signaling) decides for osteoblastogenesis instead of chondrogenesis [54].

1.2.3 Repair and current treatment strategies

Bone has good native healing properties. The healing process starts with bleeding at the fracture site resulting in hematoma formation and recruitment of inflammatory cells (platelets, macrophages etc.) that debride, secrete various growth and inflammatory factors; followed by vasculogenesis and high cell proliferation. In the inside a soft callus composed of avascular cartilage forms that develops into woven bone (hard callus) resembling the endochondral ossification process during development, while from the periosteum through intramembranous ossification directly a hard callus arises. The osteoblasts from the hard callus secret macrophage colony-stimulating factor (M-CSF) and RANKL, two major activator for osteoclasts, which execute the last step, the bone remodeling step, in which the woven bone is converted to cortical and trabecular bone [61, 62].

One of the main questions is the origin and mechanisms of recruitment of the stem/ progenitor cells that contribute to soft and hard callus formation. It is thought that they originate from MSCs in the bone marrow, adipose tissue and the periosteum [63]. A lot of effort has been done on the characterization of these putative MSCs by in vitro or homeostatic in vivo studies, but not in injury settings. Marecic and co-worker addressed injury conditions, more particularly they investigated the existence of a bone progenitor cell that is particularly active and has undergone a phenotypic switch upon skeletal injury. They based their study on their previously identified mSSC [64] and indeed 7 days post-fracture this population isolated from the digested injured bone peaked. Compared to the same population isolated from healthy animals, the fractured population showed enhanced in vitro and in vivo osteogenic potential, as well as higher CFU-F frequency and less apoptosis. CD49f (integrin alpha 6) expression was identified to mark activated mSSC [65]. What mechanism activates these cells and whether that could be exploited to improve bone healing in non-union fractures remains the issue of future investigations. Furthermore, there is a line of evidence that BMSCs contributing to fracture repair keep regional information from the development by their specific Hox gene expression profile and that only the progenitors of the specific region are implicated in the fracture repair [66]. This opens a new dimension to the origin of the cells responding to bone injuries. It would be interesting to know, how this positional information by specific Hox gene expression imparts cues for differentiation and whether it has any relationship to the regenerative function of BMSCs in tissue engineering applications.

Despite the good healing capacities of bone, there are circumstances where the regenerative process is impaired such as in case of congenital defects, of big bone loss due to tumor resection or trauma induced non-union fractures. The gold standard treatment of non-union fractures has been autologous bone grafting mostly with cancellous bone from the iliac crest. So far, bone autologous grafts have been the only bone substitute with osteogenic, osteoinductive and osteoconductive properties and seems to be a quite successful treatment strategy, however, there are limited donor site availability and diverse donor site morbidities such as chronic pain or infections, while cadaveric allografting suffers from increased incidence of fractures and infections [67, 68]. For these reasons alternative treatment options have been investigated including bone marrow aspirate implantation, allografting with decellularized bone chips, injection of synthetic calcium phosphate based materials, application of platelet rich plasma, recombinant BMP-2 or combinations thereof. Clinical studies including sufficient control groups have been lacking, therefore a putative superiority of another method over autografts could not be demonstrated so far [69]. Last, there remains the promising alternative of bone tissue engineering, which is discussed in section 1.3.3.

1.3 Tissue engineering (TE)

1.3.1 Paradigm

TE has been employed and investigated before, however in 1987 it was defined the way it is still applicable today, as well: "Tissue engineering is the application of the principles and methods of engineering and life sciences toward the fundamental understanding of structure-function relationships in normal and pathologic mammalian tissue and the development of biological substitutes to restore, maintain, or improve function." [70] An important publication in reflecting and summarizing the current attempts in the science of TE that time proposed it as an alternative treatment strategy to organ or tissue transplantation in case of organ or tissue loss or failure [71]. That time highlighted important future directions of TE research are still the main focus nowadays. These include the thorough understanding of mechanisms driving cell differentiation, also particularly the role of the ECM, the identification of the most suitable cell source, effective large-scale cell culture systems, the design of natural or synthetic biocompatible materials, including implementation of sustained delivery systems for biological stimulants that are able to support cellular functions and finally in vitro systems, which are predictive for in vivo out-comes [71].
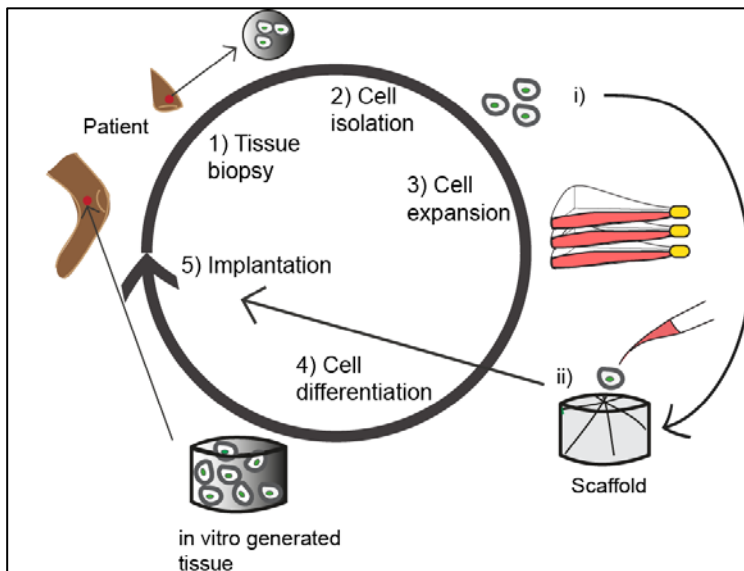
Figure 4: Tissue engineering (TE) paradigm. The classical TE work flow is composed of the following steps: harvesting stem/progenitor cells from a biopsy of the patient (1), isolating (2), expanding (3) and seeding them on a scaffold for in vitro directed tissue formation (4) and finally implanting the tissue graft back to the patient at the site of tissue damage (5). It can be altered by i) skipping the cell expansion step and directly seeding the isolated cells on the scaffold and/or by ii) circumventing the in vitro 3D culture step by immediately implanting the cells within a scaffold with tissue inducing cues.

Classically, TE is based on an appropriate cell source (stem/progenitor cells), a material that acts as a structural and possibly functional support and as a cell delivery tool, as well as a mix of soluble factors inducing differentiation. This can be summarized as the following paradigm (Figure 4): Cells are harvested

from a patient's biopsy, expanded, seeded on a scaffold for differentiation and tissue formation in vitro and the resulting constructs are implanted back to the patient. For clinical settings this procedure is rather unpractical due to long in vitro culture times, which are connected to high cost and risk of contamination and which would also necessitate development of sophisticated closed, fully automated systems. Therefore, the paradigm was adjusted to omit the in vitro culture steps partially (as investigated in the frame of my thesis, see part I) or fully [72] and let the tissue directly develop in situ by delivering all the necessary stimuli in the scaffold. Often, retrieval of autologous cells necessities a surgical procedure that may be related to various side effects and risks and is limited by donor site availability. For that reason, the TE paradigm has been adapted even more rigorously by skipping the cellular part and instead implanting only an instructive material (it can be a synthetically processed one [73-78] or decellularized tissue [79]) that directly at the site of implantation induces recruitment of local stem/progenitor cells and induces their differentiation to build up a tissue.

Unfortunately, TE in the sense of the in vitro generation of an immediate tissue replacement upon implantation has not led to an as broad success as postulated 25 years ago due to manifold reasons such as lack of standardization, reproducibility, efficacy, safety and/ or cost-effectiveness. But maybe most importantly insufficient understanding and inappropriate implementation of molecular mechanisms regulating tissue morphogenesis, growth and regeneration have led to a paradigm change in order to increase the robustness of TE, and to foster its clinical translation. We do not only speak from TE but rather about developmental engineering or even developmental re-engineering [80, 81]. Instead of cocktails of soluble factors empirically determined, concepts known from the development of the underlying tissue are applied e.g. the spatiotemporally controlled stimulation of key signaling factors. Furthermore, they are applied with consideration of the adult system (e.g. the state of commitment of the adult cell source in comparison to the counterpart during development) and the injury setting such as mechanical parameters, oxygen tension and the presence of inflammation, respectively.

1.3.2 Cartilage tissue engineering

1.3.2.1 Cell sources

1.3.2.1.1 Chondrocytes

Articular chondrocytes represent the first-choice cell source for cartilage TE. However, there is high donor site morbidity and due to limited biopsy size the cells have to be expanded massively that reduces their chondrogenic phenotype and also re-differentiation potential, which is further diminished with higher donor age [82].

A promising alternative chondrocyte source is the nasal septum, from which nasal chondrocytes (NCs) can be isolated. The cartilage of the nasal septum (together with the one of the nasal lobe) gives stiffness to the nose and its ECM like the one of articular cartilage is mainly based on ColII, has a high GAG content and shows absence of ColI and only traces of ColX [83]. NCs have high proliferative, and robust, less donor- and age- dependent re-differentiation capacities in vitro and in vivo and do not cause donor site morbidity [84-86]. What is more, when in co-culture with ACs or implanted in joints, NCs adapted their hox gene profile, which is because of their neural crest origin different from the one of ACs, demonstrating their developmental plasticity [87]. In full thickness defects in goats engineered NC derived cartilage was found to majorly contribute to the hyaline cartilage repair tissue and to efficiently integrate with the subchondral bone [88].

Considering the good chondrogenic differentiation capability of NCs it would be important to further characterize the (intra- and inter-donor) homogeneity of them and whether the tissue contains only fully differentiated cells or whether there are also (quiescent) progenitors present that can be activated to augment tissue formation even more. Interestingly, comparison of nasal septum cells outgrowth cultures to the more commonly enzymatically isolated NCs showed differences in terms of clonogenicity, migratory behavior, cell surface expression (after culture on plastic) leading the authors to propose them as more progenitor-like compared to the digestive cell fraction. However, in chondrogenic conditions these cells secreted higher amounts of ColI and did not prove to be more useful then the digestive fraction, at all [89].

1.3.2.1.2 Bone marrow-derived stem/stromal cells (BMSCs)

1.3.2.1.2.1 Definition

The identity of MSCs is a highly debated topic. Already the meaning of the acronym is not clear and ranges from mesenchymal stromal and/ or stem cells to multipotent stem cell and moreover is used for cells derived from a broad range of tissue types, such as adipose tissue, bone marrow, umbilical cord blood, the amniotic membrane, synovial tissue, skeletal muscle, liver and heart tissue [90]. Most importantly, it cannot be defined by a ubiquitous surface marker phenotype, neither differentiation potential. The mesenchymal and tissue stem cell committee of the international society for cellular therapy attempted to define minimal criteria for "the" MSCs as the plastic adherent cells that are after culture under standard conditions lineage negative (CD45, CD34, CD14 or CD11b, CD79alpha or CD19 and HLA-DR), positive for CD73, CD90 and CD105 (>95 %) and have tri-lineage in vitro differentiation potential to adipocytes, chondrocytes and osteocytes [91]. However, these properties do not solve the above-mentioned issues and what is more, they introduce an additional problem, namely the definition of a cell purely based on in vitro conditions. Historically, in the 1960's Friedenstein et al. showed that whole mouse bone marrow transplanted ectopically in diffusion chambers depending on the cellular density applied (sometimes) formed bone of host origin [92, 93]. Later, bone marrow was plated (in the specific case of this report on collagen gels) and the adherent cells, denoted as the stromal fraction, formed clones (colony-forming unit fibroblasts (CFU-F)). The clones were implanted on these collagen gels subcutaneously or under the renal capsule in mice and 15 % of the implanted clones formed a bone organ inclusive marrow or only bone tissue, respectively and the remaining ones just formed some kind of connective tissue [94]. Based on these experiments and others the idea of the bone marrow stromal stem cell was grown, which is capable to make bone, reticular, stromal and adipogenic tissue [95, 96].

Since then many questions arose: what is the identity of the cell in the bone marrow giving rise to the CFU-Fs and to different skeletal phenotypes; where is it located in situ: can a specific surface marker panel describe/isolate it; and does it really have self-renewing properties and therefore can be considered as a true stem cell? Since it is generally thought that "the" BMSC has the highest clonogenic property, mostly, the approach of finding prospective markers that select for the (total) CFU-Fs in low density cultures of CD45⁻ bone marrow mononuclear cells (BMNCs) has been followed. Consequently, several single surface markers were proposed to demarcate these cells e.g. Stro-1 [97], CD271 [98], CD49a [99] and CD146 [100]. CD146/MCAM in the bone marrow localized to adventitial reticular cells of sinusoids. When these clones (consisting of all cells

24

expressing CD146) were combined and implanted on hydroxyapatite carriers bone organs formed including bone marrow containing cells lining the sinusoids. In contrast CD146$^-$ cells were able to form bone, but without a hematopoietic compartment. CFU-Fs were generated from the human cells derived of the CD146$^+$ ossicles, of which 100% expressed CD146. These experiments demonstrated that among BMNCs there are cells, which have high clonogenic properties, self-renewal capacities, are bone forming cells, important for establishing the hematopoietic niche and supposedly overlapping to the CD146$^+$ cells of mural type on sinusoids in human bone marrow [100]. Attempting to combine the two well-described markers CD146 and CD271, Tormin et al. sorted from CD45$^-$CD271$^+$ (0.03 % of BMNCs) the CD146$^+$ and CD146$^-$ cells and found CFU-Fs in both populations. Both populations showed in vitro tri-lineage differentiation potential and implantation of cultured multiclonal populations with hydroxyapatite granules ectopically generated bone organs with bone marrow. In situ, CD271/CD146 double positive cells localized sub-endothelial on sinusoids while the CD271 only cells were found within the endosteum. Both were found in close proximity with CD34$^+$ HSCs. This proposed that there are BMSCs at different locations forming possibly distinct HSC niches [101]. Several other combinations of CD271$^+$ cells were proposed to more selectively isolate BMSCs including MSCA-1$^+$CD56$^+$ [102], CD90$^+$CD106$^+$ [103], and CD140a$^-$ [104, 105].

Other groups have used the murine system to find "the" BMSC prospectively. CD140a$^+$Sca1$^+$ was found to mark the highest CFU-F cells, in vitro they had tri-lineage potential and in vivo after tail vein injection, the cells homed to the bone marrow and seemed to contribute to maintain the hematopoietic niche [106]. Coincidentally, nestin:GFP cells were observed to localize as perivascular non-hematopoietic, non-endothelial cell subpopulation close by to the rare CD150$^+$CD48$^-$Lin$^-$ HSCs [107]. Further investigations demonstrated that they marked a BMSC, since they were clonogenic, had in vitro multilineage differential potential, self-renewal capacities by serial transplantation experiments on hydroxyapatite carriers, HSC niche supportive functions and since they contributed to osteoblast lineages under homeostatic conditions [107]. On the search of surface markers that stain specifically nestin:GFP cells Pinho et al. discovered PDGFRa$^+$CD51$^+$ cells to be the corresponding cell population [108]. Later, a mouse skeletal stem cell (mSSC) was defined by AlphaV$^+$Thy$^-$6C3$^-$CD105$^-$CD200$^+$ and isolated from collagenase digested femurs. Seven descendent cell phenotypes were identified giving raise to bone, cartilage and stroma in a hierarchical manner. Specific signals could bias the phenotype of the progeny [64]. Nusspaumer et al. recently investigated the appearance and frequency of the most important described markers of MSCs in mice over time. PDGFRa$^+$CD51$^+$ was the largest subset of mesenchymal limb cells detected in mice during development and with the highest abundance

shortly after birth. These cells consisted of the PDGFRa$^+$ Sca1$^+$ cells, the CD200$^+$ mSSCs and a third cell population. The first subpopulation arose earlier in development than the CD200$^+$ one and could be further divided into four populations based on CD73 and CD90 expression. Although the CD90$^-$ subfraction performed best in in vitro trilineage assays, the chondrogenically pre-differentiated CD90$^+$ cells gave raise to bone organoids upon subcutaneous implantation in nude mice suggesting it to be a mice counterpart of the human BMSC [109].

Several recent studies by using mouse genetic models gave valuable information about how the in vivo functional properties, marker phenotype of skeletogenic BMSCs and developmental origin are related with each other. Zhou et al. used leptin receptor (LepR) for fate mapping BMSCs in vivo. LeptR$^+$ cells gave rise to almost the total CFU-F of the bone marrow, were positive for pro-HSC niche factors and formed skeletal lineages in vitro and upon transplantation in vivo. LepR$^+$ cells were observed postnatal around sinusoids and arterioles and contributed majorly to bone and marrow adipocytes after fracture in adult mice, but did not contribute to cartilage during development [110]. Grem1 expressing cells (0.0025 % of BMNCs) were found to overlap with high bone marrow CFU-F. Lineage tracing of these cells originally found in the metaphysis demonstrated that they contributed to growth plate, articular cartilage and stromal cells during development and to bone and cartilage under homeostatic or fractured conditions in adult mice. Adipocytes did not form neither in vitro nor in vivo. Grem1$^+$ cells did not overlap neither with perisinusoidal Nes:GFP, nor with LepR$^+$ cells therefore suggesting them to be a complementary skeletal stem cell of a reticular type [111]. Recently, a report demonstrated that the Hox gene profile that plays a crucial role in patterning during development was maintained throughout adulthood in mesenchymal progenitors in the bone marrow and cells lining the periosteum, while in differentiated cells Hox expression was downregulated. Hoxa11EGFP cells overlapped with LeptR$^+$ and PDGFRa$^+$CD51$^+$ and responded to injury by proliferation and contributed to cartilage and bone tissue of the callus and this in a regional specific way [66].

In conclusion, there is increasing evidence that a skeletal stem cell exist in vivo. However, the relationship between the different multipotent stem cell types described and their contribution to tissue formation, hematopoietic niche formation during development, and homeostasis and regeneration of skeletal tissues as well as maintenance of the hematopoietic stem cell niche during adulthood needs further investigations. Understanding more deeply the signals governing function and steering differentiation of these cells may provide valuable information for therapy options in skeletal regeneration and hematopoietic dysfunctions. Still, in the human system no surface

marker combination is generally acknowledged for the prospective isolation of BMSCs and that may limit the successful utilization of BMSCs for TE strategies to heal bone and cartilage defects.

1.3.2.1.2.2 Chondrogenic differentiation of BMSC in vitro and in vivo

Due to their ease of isolation (by culturing non-fractionated bone marrow aspirates on plastic), high proliferative capacities and their osteogenic and chondrogenic differentiation potential for the last 20 years BMSCs have been a popular cell source tested for cartilage TE approaches [81]. Most simply, chondrogenesis of BMSCs is triggered by centrifugation of an aliquot of 0.25-0.5×10^6 cells and subsequent culture of these pellets under serum-free conditions in presence of TGFß1 or 3, ascorbic acid and dexamethasone [112] or in various scaffolds. TGFß-induced differentiation of BMSCs typically induces concomitant expression of hypertrophy-associated genes such as ColX, BSP, MMP13, ColI and osteopontin, and stable cartilage matrix genes such as ColII and aggrecan. If implanted subcutaneously in immunodeficient mice, BMSCs- derived cartilage unlike that of expanded articular chondrocytes shows phenotypic instability namely calcification and features of endochondral ossification [113]. While this inherent tendency to undergo hypertrophy and endochondral ossification can be exploited for bone TE applications (see section 1.3.3) or hematopoietic niche modeling [114, 115], it represents the biggest limitation for cartilage repair. So far, no protocol has acquainted general acceptance among the scientific community that reliably generates hyaline-like cartilage from BMSCs and still it is not known whether at all it is possible. Furthermore, the donor-to-donor variability of chondrogenic in vitro differentiation potential and intrinsic heterogeneity are other major issues namely, only approximately 30 % of single-cell derived clones have the capacity to chondrogenically differentiate [116].

How does the pre-mature hypertrophic differentiation of chondrogenically stimulated BMSCs observed in vitro and at ectopic sites actually relate to the chondrogenic differentiation in an orthotopic environment? In 2002, the first clinical trial reporting the usage of cultured BMSCs for the repair of a defect in the femoral condyle was reported [117]. Since then many other clinical trials using cultured BMSCs [117-119], fresh BM aspirate or a concentrate of fresh BM [120-123] were published. The main focus of these studies was the assessment of the suitability and safety of the cells alone and not any other parameter such as specific scaffold design or growth factor delivery for induction of chondrogenic differentiation. In pre-clinical models such as the sheep [124-126], goat, horses pigs and minipigs the effect of expansion, 3D-pre-culture and or growth factor co-delivery was not thoroughly compared, neither. Considering the cartilage phenotype achieved in

the repair tissue there were no consistent results. However, rather fibrosis - increased ColI synthesis in the cartilaginous repair tissue- and not hypertrophic differentiation of the cells represented the main problem reported in the clinical trials (also when bone marrow stimulatory techniques were applied) and in pre-clinical models [127].

Underlying oncept of approach	Treatment	Scaffold	In vitro outcome	In vivo outcome (subcutaneous nude mice)	Ref.
PTHrP suppresses hypertrophic maturation during endochondral ossification [40]	TGFß1 + PTHrP or TGFß1 and after 3 weeks + PTHrP	- - (pellet)	6 weeks: down-regulation of Col II, GAGs and Col X (catabolism induced?)	4 weeks: calcification	[128]
Load bearing environment enhances cartilage ECM accumulation	Dynamic compressive loading in ChM for 10 weeks.	Hyaluronic acid hydrogel	10 weeks: significant down-regulation of Col X and MMP13, and calcification content.	--	[129]
Whole genome gene array analysis comparing GP with AC→ Dkk1, FRZ (canonical Wnt inhibitors) and Grem1 enriched in AC	TGFß1 for 1 weeks, and then + recombinant Dkk1, Frz or Grem1 for 2-4 weeks	-- (pellet)	3 and 5 weeks: no inhibition of chondrogenesis, delay of calcification, significant down-regulation of hypertrophic genes	--	[130]
Permanent cartilage arises and persists at hypoxia, while endochondral ossification necessities vascular invasion [44].	2.5 % O_2 for 5 weeks versus normoxia, (and 3 weeks hypoxia + 2 weeks normoxia)	-- (pellet) for in vitro Alginate gel for in vivo	5 weeks: more ECM synthesis, hypertrophic genes down-, AC- and glycolysis-related genes up regulated (continuous low O_2 was necessary for the observed effects).	5 weeks: inhibited calcification, no fuchsin positivity, no vessel invasion.	[131]
"	Transduction with human sFLK1 (soluble VEGFR)	ColI sponge	No in vitro culture (no difference to naïve cells)	4-12 weeks: spontaneous chondrogenesis, no Col X and no vessels observed.	[132]
Combination of FGF and Wnt that induces proliferation of limb bud mesenchymal progenitors [38] and Wnt that later drives osteogenesis [54].	Expansion phase with WNT3a and FGF2, chondrogenic phase with WNT inhibitor (IWP2) (for 5 weeks)	-- (pellet)	5 weeks: Expansion with Wnt and FGF enhanced chondrogenicity, IWP2 treatment lowered hypertrophy (Col X induced, but not further increased from 3 to 5 weeks)	8 weeks: hypertrophic gene expression and calcification reduced, no bone, more Col II-rich cartilage.	[133]
Sequential stimulation with FGF2, 9 and 18 (mimicking embryonic development) can obviate hypertrophy.	2 weeks ChM, + 2 weeks ChM + FGF9 or 18	-- (pellets)	Pro-anabolic effect and reduction of hypertrophy mediated genes (signaling through FGFR3, overriding disadvantageous signaling through FGFR1), some differences between FGF9 and 18 observed.	--	[134]
Cartilage deep zone maturation and calcification guide development of stable cartilage in the upper zones.	3 weeks ChM in transwell insert and well, + 7 weeks ChM in transwell insert and HM in well	-- (transwell cultures, insert cultured with ColI)	10 weeks: mineralization only in the lower part, Col II/Col X throughout the construct.	4 weeks: Calcification and bone formation in the lower part, tidemark formation is questionable, while there is cartilage with lubricin at the surface in the upper part (Col X was not assessed anymore).	[135]
Inhibition of BMP by noggin allows the formation of embryonic AC [15].	2 weeks Alk1-3 (BMP receptors) inhibitor in ChM + 2 weeks HM (only for in vitro)	-- (pellet) for in vitro ColI sponge for in vivo	2 weeks: down-regulation of hypertrophic genes, slight down-regulation of ColI, up-regulation of AC related genes, no Col X at protein level 4w: inhibition of hypertrophy maintained even in HM	8 weeks: no signs of endochondral ossification (Col X and I, vascularization) were not observed.	P. Oc-chetta, manuscript in preparation

Table 1: Summary of protocols tested in order to reduce hypertrophic differentiation of BMSCs during in vitro and in vivo chondrogenesis. ChM: chondrogenic medium (+ TGFß), HM: hypertrophic medium (+ glycerophosphate to induce calcification). Implantation was performed after the treatment described in the second row.

Nevertheless, if an in vitro generated BMSC based chondrogenic graft should serve for implantation, it must not have hypertrophic traits; otherwise it would fail to contribute to functional articular cartilage regeneration. For that reason, several groups have tried different approaches for inhibiting or reducing the hypertrophic phenotype of chondrogenically differentiating BMSCs as summarized in Table 1. Most of these studies exploited findings from development and thus highlighted the potential of a developmental inspired approach, however also showed that for more robust outcomes the implementation of a combination of factor may be necessary.

1.3.2.1.3 Embryonic stem cells (ESCs) and induced pluripotent stem cells (iPSCs)

Step-wise developmental-oriented protocols were devised to generate chondrocytes from human/mouse ESCs and/or iPSCs [136-141]. ESCs are only suited to study the minimal medium compositions for following the developmental steps of chondrogenic differentiation in an academic setting. In contrast, iPSCs that can be generated from every patient and do not have any ethical concerns could therefore represent a suitable cell source for cartilage repair if safety-related aspects had been excluded [142]. Several experimenters succeeded in controlling the differentiation towards stable hyaline cartilage tissue [136, 138, 141], however, even step-wise stimulation of PSCs did not always lead to the desired cartilage phenotype. It is not clear yet, following which developmental path leads to the most efficient cartilage formation and most particularly allows the specific differentiation to the desired cartilage phenotype.

### 1.3.2.2 Biomaterials - Chondrogenesis in hydrogels

Generally, biomaterials are classified based on their microstructures into sponges, microfibers, microspheres and hydrogels. All of these classes have been used as scaffolds in cartilage TE. Sponges are interconnected porous structures and are often fabricated by lyophilization of natural (collagens, GAGs) and synthetic polymers that are eventually cross-linked in order to improve mechanical stability [143]. Hydrogels of natural, synthetic or of mixed origin are particularly suitable biomaterials for chondrogenic cultures. They are insoluble, hydrophilic, chemically and/or physically cross-linked polymer 3D-matrices that are highly loaded with water and are permeable for solutes, thus resemble the basic ECM. They are very tunable in terms of matrix stiffness and functionalization in order to render them biologically active such that they are cell-degradable, cell-

adhesive, deliver and/or sequester growth factors or small molecules. The stiffness of the hydrogel depends on the concentration and size of monomers used and is linked to its cross-linking density and its mesh size. Naturally derived hydrogels are beneficial for their intrinsic biocompatibility, but can vary from batch to batch. The most commonly used natural hydrogels are based on the macromolecular chains of repetitive disaccharide units of GAGs such as hyaluronic acid, chitosan and alginate or are based on proteins such as fibrin, collagen or non-natural peptides. These monomers either jelly via spontaneous polymerization through self-assembly or are additionally modified for chemical cross-linking as described later for the synthetic hydrogels [144].

Synthetic hydrogels comprise poly(ethylene glycol) (PEG), poly(vinyl alcohol) (PVA), poly(2-hydroxethyl methacrylate) (PHEMA) and others [144] (Figure 5A). While PHEMA was one of the first synthetic hydrogels used in TE, PEG hydrogels are the most commonly used ones and I also used a hydrogel system based on PEG during my PhD thesis. Oligo(poly(ethylene glycol) fumarate (OPF) is an example of a PEG based oligomer to that through the fumarate a hydrolysis susceptible ester bond was introduced. This renders the hydrogel degradable. The polymerization mechanism through chemical cross-linking depends on the end functionalities introduced to the PEG monomers. It is either light-dependent and needs the presence of a photo initiator (PI) such as for radical homo-polymerization between PEG-acrylate (PEGDA) or -methacrylate monomers, or in radical reactions (with UV or visible light depending on the PI used) of PEG-acrylate or PEG-norbornene with a dithiol cross-linker (Figure 5B). To avoid radical polymerization, which can be cytotoxic, Michael type addition is employed, where the polymerization happens spontaneously through nucleophilic addition between a PEG-vinyl sulfone or a -maleimide and a dithiol cross-linker (Figure 5B) [145].

The enzymatically polymerized PEG hydrogel, used in part I of the thesis consisted of eight-armed (40 kPa) monomers functionalized with a glutamine donor or a lysine acceptor peptide, two substrates of transglutaminase factor XIII (thrombin, that naturally is implicated in blood clot formation). The lysine peptide contained an MMP1-sensitive stretch to render the hydrogel cell-degradable [146]. The hydrogels can be functionalized with RGD or streptavidin (for biotinylated growth factor immobilization) also in a factor XIII-dependent manner (Figure 5C). At the monomer concentration used here (1.5 % w/v) hydrogels have a storage modulus (G') of 94 Pa, a phase angle of 12.7 and according the theory of Flory-Rehner the mesh size was calculated to be 40 nm [147]. This hydrogel does not reach the stiffness of articular cartilage. Intended to serve only as temporal support for the cells to lay down new ECM a similar stiffness is not necessary [143].
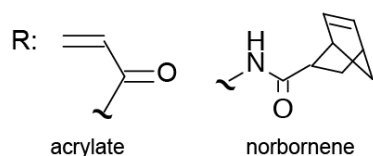
A **Synthetic hydrogel chemistries**

PEG PVA PHEMA OPF
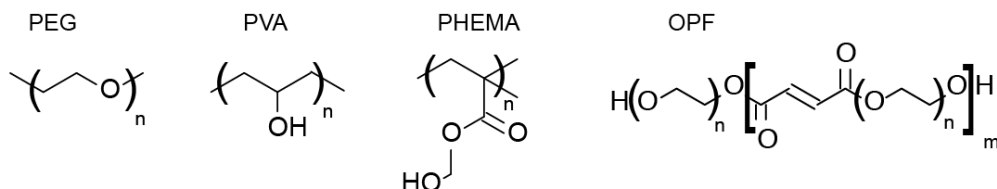
B **Chemical cross-linking strategies**

i) Light induced radical polymerization of PEGDA (chain growth mechanism)

$$\xrightarrow[\text{PI}]{h\nu}$$
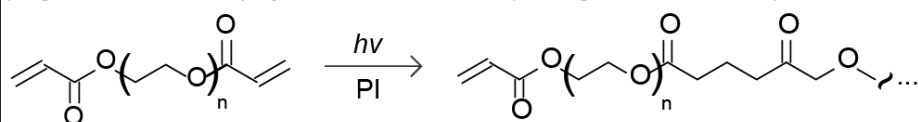
ii) Light induced thiol-en reaction of differentially functionalized PEG with PEG-dithiol (step growth mechansim)

$$\xrightarrow[\text{PI}]{h\nu}$$
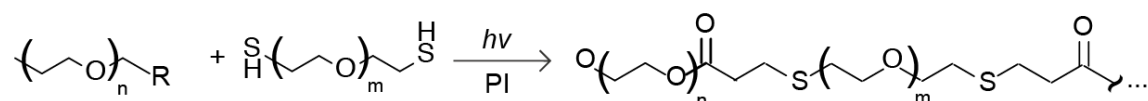
(cross-linking shown with acrylate)

R:

acrylate   norbornene

ii) Michael-type conjugation of PEG vinyl sulfone with PEG-dithiol (step growth mechansim)
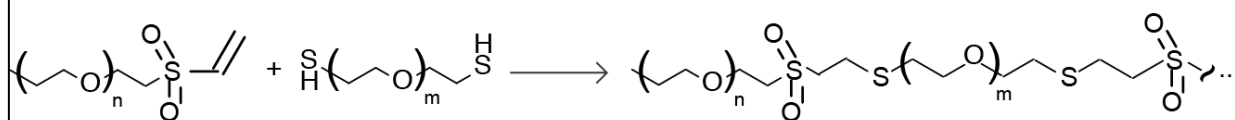
C **Enzymatic 8-armed PEG system**

$R_{1/2}$ $R_{1/2}$ $R_{1/2}$ $R_{1/2}$ $R_{1/2}$ $R_{1/2}$

$R_{1/2}$ R_1: $R_{1/2}$

R_2:

factor XIII, Ca2+
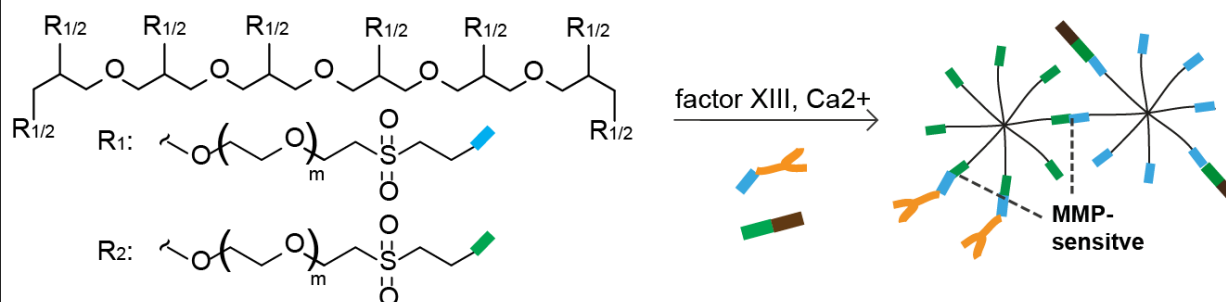
MMP-sensitve

Glutamine acceptor peptide:

H-**NQEQVSPL**-ERCG-*NH$_2$*

MMP-sensitive lysine donor peptide:

Ac-**FKGG**-**GPQG§IWGQ**-ERCG-*NH$_2$*

Cell adhesive peptide:

Ac-**FKGG**-RGDSPG-*NH$_2$*

Additional functionalization:

H-**NQEQVSPL**-Streptavidin

Figure 5: Synthetic hydrogels and their cross-linking strategies. A) Basic chemical structure of the most common hydrogel monomers. n indicates the number of arms [144]. PEG: poly(ethylene glycol), PVA: poly(vinyl alcohol), PHEMA: poly(2-hydroxethyl methacrylate) (PHEMA), OPF: oligo(poly(ethylene glycol) fumarate). **B)** Chemical cross-linking occurs through chain growth (simple light-induced radical polymerization of acrylate groups) or through step growth mechanism (light induced radical polymerization of acrylate or norbornene with dithiol cross-linkers, or light independent Michael type addition (nucleophilic addition) with e.g. vinyl sulfone and a dithiol cross-linker). PI: photo initiator [145]. The chain growth polymerization is faster leading to less regular and less mechanically stable network structures, whereas the step growth polymerization has slower kinetics and leads therefore to more homogenous structures with higher mechanical stability [144]. **C)** The system used in my PhD project: 8-armed PEG (40 kDa) is functionalized through Michael type addition with either a glutamine (in red) containing or a lysine (in red) containing peptide that are cross-linked by transglutaminase factor XIII. Additionally an MMP-sensitive peptide (in bold, §: cleavage site) for cell-mediated hydrogel degradability was added. By adding to the hydrogel-pre-polymerization mix other functionalities such as the fibronectin derived RGD peptide or streptavidin the hydrogel becomes cell-adhesive or can immobilize growth factors (if biotinylated growth factors are added) [146, 148].

Degradability of the PEG hydrogel and the presence of cell-adhesive peptides or functional groups with affinity for cartilaginous ECM proteins were assessed whether they have beneficial effects on chondrogenic differentiation. Either the PEG hydrogel is degraded non-specifically through hydrolysis such as of ester bonds in a photo polymerized PEG-polylactic acid diacrylate hydrogel [149] or OPF, or in a cell-mediated manner by being cross-linked with protease-cleavable cross-linkers [150-153]. Degradability allowed higher secretion and better distribution of ECM proteins and therefore fostered chondrogenesis [150, 153], while the cells survived equally well regardless of the degradability of the underlying hydrogel [151]. In combination with cell-adhesive peptides MMP-cleavable hydrogels increased cell proliferation and chondrogenesis of human BMSCs, in absence of the cell-adhesive peptides MMP cleavage sites did not prove to be advantageous [152]. Most commonly the cell-adhesive peptide RGD is incorporated in the hydrogel. It was originally discovered in fibronectin, but is also present in other ECM proteins and is recognized by almost half of all integrin receptors [154]. In four-armed MMP-sensitive PEG cross-linked by the GAG heparin, RGD significantly enhanced cartilage ECM deposition of porcine ACs directly implanted in vivo, while surprisingly the ColII binding motif CWYRGRL did not have any beneficial effect on matrix accumulation and distribution, but rather lowered the quality of chondrogenesis compared to RGD [155]. In vitro RGD induced cell spreading of human BMSCs and enhanced chondrogenesis, while CWYRGRL did not improve it [155]. The cell-adhesive peptide GFOGER found on collagens induced higher GAG secretion and higher ColII and aggrecan mRNA expression of BMSCs than RGD in vitro in four-armed MMP-sensitive PEG hydrogels [152]. An additional important parameter that can be varied in PEG hydrogels is their mechanical strength, stiffness, this either by varying the initial monomer concentrations, the monomer molecular weight (changing the arm length) or the arm number. 2D cultures of BMSCs on hydrogels with differential

stiffness showed a poised differentiation behavior, namely that stiffer hydrogels induced rather osteogenic and softer hydrogels chondrogenic or adipogenic differentiation [156]. But how is the more relevant 3D chondrogenesis affected by the mechanical properties of the hydrogel? In a study that aimed to generate an osteochondral construct in vitro by using BMSCs and PEG-diacrylate hydrogel of a graded stiffness (a compressive modulus of 48 kPa in the cartilage, 100 in the interface and 345 kPa in the bone part was measured) as well as varying RGD concentrations and presence of chondroitin-sulfate showed that the stiffness plus the biochemical cues alone did not induce different MSC phenotypes; secretion of ColI, II and X was the same throughout all layers. However, interestingly dynamic mechanical loading reduced ColX expression. Due to the differential stiffness there was a lower strain in the bone part leading to higher ColX expression there [157]. In conclusion, the question is not whether the hydrogel should be degradable or not, but how fast it should be degradable. Moreover, it is not yet as clear how to adjust the stiffness of the hydrogel in order to achieve a significant beneficial effect on the chondrogenic phenotype while providing sufficient mechanical support.

1.3.2.3 Growth factor delivery for chondrogenic differentiation

For simple localized delivery of growth factors in particular hydrogels, there are currently numerous techniques available (Figure 6). Growth factors can be physically incorporated or most importantly immobilized to the hydrogel network by covalent [158] or by affinity binding [159, 160]. The appropriate technique depends on the cross-linking strategy used and on the particular growth factor to be immobilized, e.g. presence of reduced and surface accessible cysteines, sensitiveness to further chemical modifications or short linker distances, etc. Specific tethering of the growth factors allows their controlled release by e.g. utilizing MMP-sensitive linkers [161]. Cartilage is naturally exposed to mechanical loading, therefore, systems in which growth factor release is governed mechanically might open the possibility for temporally adjusted growth factor release after implantation. Accordingly, Moghadam et al. showed that cyclic loading of a hydrogel consisting of thermo sensitive nanoparticles and a physically entrapped drug triggers within a few minutes a temperature-mediated shrinkage of the nanoparticles that resulted in higher permeability of the hydrogel and thereby facilitated release of the drug [162]. Furthermore, affinity binding offers the possibility of manipulating the activity of the growth factor. If a receptor or a receptor derived peptide is incorporated in the hydrogel, it can serve to sequester growth factors [159].
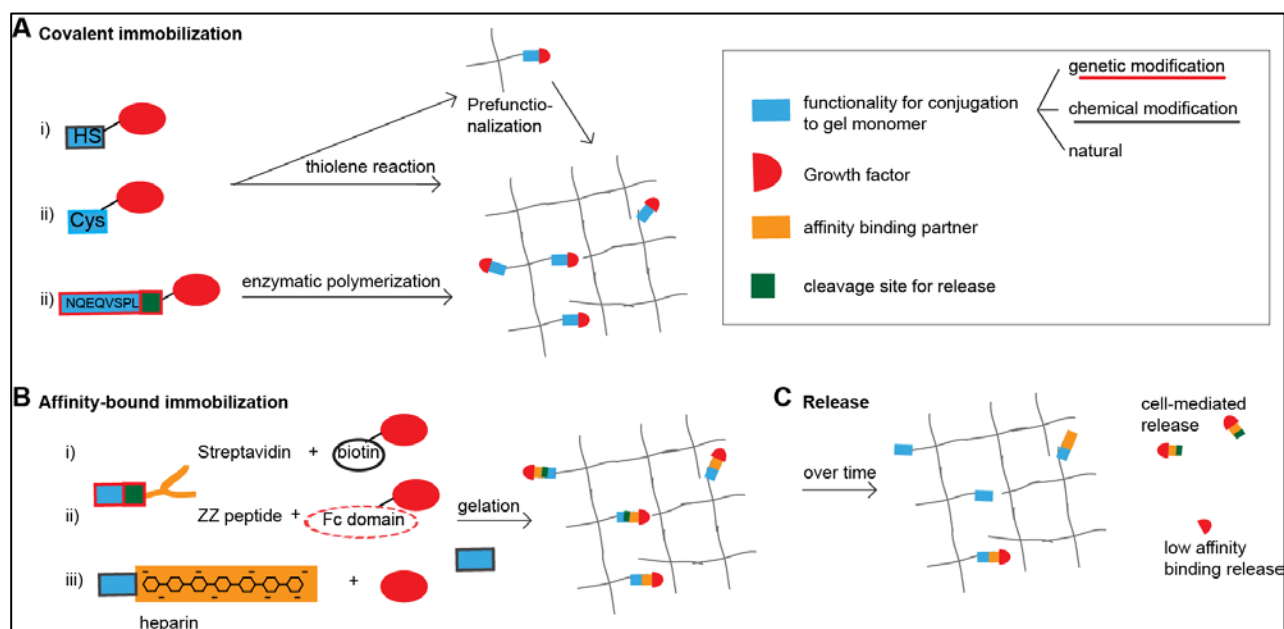
Figure 6: Basic growth factor immobilization in hydrogels. A) Growth factors (GFs) (naturally bearing a free cysteine (i) or thiolated (ii)) are immobilized covalently through Michael type addition or radical thiolene conjugation into PEGDA, -norbornene, or -vinyl sulfone and this either directly during gelation or as a step beforehand for more controlled GF functionalization of the hydrogel monomers and avoiding an interference with the gelation process. In case of an enzymatic polymerization system the growth factor was conjugated to the enzyme substrate genetically (iii). **B)** GFs can also be indirectly immobilized through an affinity binding partner such as i) streptavidin, ii) ZZ-peptide or a GAG e.g. heparin. In i) GFs need to be chemically modified (biotinylated), in ii) the modification is done genetically by cloning a FC domain to the recombinant GF or the protein to be immobilized already contains it, while in iii) the native affinity of certain GFs to ECM components such as GAGs is exploited and no additional modification is necessary. Alike with direct binding the affinity-binding partner is incorporated into the hydrogel network during gelation or conjugated to the gel monomer in a previous step. **C)** Specific GF immobilization also aims at tuning its release. Through incorporation of protease sensitive linkers or based on the affinity of the GF to its binding partner the release kinetics can be adjusted.

TGFß, the main inducer of chondrogenesis, has been tested to be immobilized in various hydrogels aiming at achieving a highly localized and effective growth factor delivery at the site of cartilage injury. McCall et al. demonstrated that the covalent incorporation of thiolated TGFß1 into a PEGDA-based hydrogel did not hamper its activity and was suitable to induce chondrogenic differentiation of human BMSCs to a similar extent or even higher compared to soluble growth factor application as measured by accumulated GAG and ColII staining [163]. Likewise in MMP-degradable PEG-norbornene-based hydrogels, covalently tethered TGFß1 induced ECM secretion by human BMSCs - swine articular chondrocytes co-cultures within two weeks of in vitro culture time [153]. Sustained release of adsorbed TGFß1 from self-assembling peptide hydrogels was achieved and resulted in the chondrogenesis of equine BMSCs within two weeks similarly to when delivered soluble, but with a 10-fold lower TGFß1 concentration [164]. Re'em et al. tethered

TGFß1 to a sulphated alginate scaffold through affinity binding and BMSCs in there underwent chondrogenic differentiation in the subcutaneous pockets of nude mice within three weeks [165].

Many experimenters thoroughly characterized the release kinetics of the factor from their scaffold mostly in acellular conditions. Does the factor really need to be released for biological activity and to what extent are the release kinetics altered when there are cells present and if the scaffold was implanted in vivo? How long should the cells be able to sense the provided factor(s) and what are the ideal concentrations; do different concentrations elicit even a different response? These are important points that have not been investigated sufficiently, yet. Introduction of a triple MMP-sensitive linker to the streptavidin in the hydrogel system used here in the thesis, aimed at increasing biotinylated growth factor release from the hydrogel. Indeed, when BMP-2 was immobilized through this degradable streptavidin linker, in vitro C2C12 cells and BMSCs exhibited enhanced osteogenic differentiation by means of ALP expression and activity compared to when a non-MMP-sensitive linker was used indicating that the mode of growth factor delivery can influence the cell response [161]. In canonical TGFß signaling, upon ligand binding the heteromer of type I and II receptors (TßRI and TßRII) forms and TßRII phosphorylates TßRI, which triggers down-stream signaling via Smad2/3 and Smad4 [166]. TßRI and II are constitutively endocytosed and ligand binding does not alter the dynamics of receptor internalization. It seems that ligand-mediated endocytosis (which is only possible when the immobilized growth factor was released) is not necessary for TGFß signaling, however, the signaling strength can be enhanced in early endosomes of clathrin-mediated endocytosis, while receptors being localized to lipid rafts and undergoing caveolin-mediated endocytosis are prone for degradation shutting off the TGFß signal [166]. Thus, it seems that TGFß does not need to be released in order to be (more) active. In situ the plasma activity of TGFß is prolonged through non-covalent association with its latency associated protein (LAP) (which is called the small latent complex (SLC)) and matrix bound through the binding to latent TGFß binding proteins as the large LC. TGFß becomes bioactive only ones proteolytically or mechanically liberated from LAP [167]. Interestingly, Place et al. addressed, whether delivering TGFß in its form as SLC immobilized in a PEGDA cross-linked hyaluronic acid hydrogel thus mimicking its natural presence in the tissue, has a beneficial effect on chondrogenesis. Although in vitro chondrogenesis of bovine ACs was induced the cell number decreased and the cartilage matrix was of inferior composition compared to soluble TGFß stimulation suggesting that in this in vitro system the chondrocytes were not able to activate the latency associated TGFß sufficiently [168].

1.3.3 Bone tissue engineering

Traditionally, bone has been generated through direct (intramembranous) ossification most commonly with BMSCs and mineralized substrates [169]. Besides BMSCs, MSCs from adipose tissue (ADSCs) are increasingly more investigated for bone TE applications. Isolation of adipose tissue by liposuction causes less donor site morbidity than harvesting a bone marrow aspirate and more cells can be isolated [170]. Upon expansion of collagenase digested liposuction biopsies ADSCs can be retrieved, they show good osteogenic differentiation capacity [171] and also undergo endochondral ossification after implantation of hypertrophically differentiated cell pellets at an ectopic site [172]. Moreover, adipose tissue has the potential of intraoperative usage; by enzymatic digestion of the liposuction the stromal vascular fraction can be isolated, it is a heterogeneous population of adipocytes, MSCs, endothelial cells and macrophages. By seeding it on ceramic scaffolds its utility to generate de novo bone tissue in a rat calvarial defect model and in osteoporotic humerus fractures in a first in human trial was demonstrated [72].

In order to overcome the limits of the direct osteogenic TE strategies by BMSCs, namely graft tissue necrosis due to insufficient vascularization, researcher have moved to use a more developmentally inspired approach and to generate bone through the endochondral route [169]. Chondrocytes bear intrinsic resistance to hypoxia and hypertrophic chondrocytes secrete pro-angiogenic and pro-osteogenic factors. Studies investigating the endochondral path demonstrated that BMSC based constructs after chondrogenic priming in scaffold-free or -aided in vitro cultures remodeled spontaneously into ossicles consisting of cortical and trabecular bone and bone marrow mostly in ectopic [114, 115, 173-177] and also in orthotopic settings [178-180]. Several different scaffold systems were used, from scaffold-free relying on self-aggregation approaches over ColI sponges, to collagen/GAG scaffolds, calcium phosphate based carriers and Polylactic co-glycolic acid (PLGA). Also the applied in vitro culture protocols were variable, not only did the composition of the used media vary, but most importantly the culture time (2-6 weeks) and the presence of a switch from chondrogenic to hypertrophic conditions. It is still unclear, which timing leads to the most efficient outcome in vivo in terms of frank bone formation. Scotti et al. reported that more mature hypertrophic tissue (cultured for a longer time in vitro) resulted in more efficient ossicle development [114] and Yang et al. did not observe more bone formation in relation to 2, 3 or 4 weeks of in vitro culture in ChM in PLGA, nor in hydroxyapatite/tricalcium phosphate scaffolds [177]. Neither it is known yet to what extent the in vitro chondrogenic differentiation capacity that varies largely from donor to donor, is reflected in the bone formation efficiency in vivo. From a translational perspective, circumventing the in vitro pre-culture step would greatly facilitate the

faster generation of the graft and massively reduce the production costs. Indeed, Dang et al. designed a system based on TGFß1-loaded gelatin micro particles allowing for a fast release by cell secreted collagenases and BMP-2-loaded mineral coated hydroxyapatite micro particles allowing a slow release due to the low dissolution rate of the mineral coat for the induction of undifferentiated BMSCs aggregates to undergo endochondral ossification directly after implantation [181]. These BMSC based cell sheaths containing the micro particles with all the possible growth factor combinations were after 2 days (this time was needed for the self-aggregation process) implanted in 5 mm sized rat calvarial defects. After four to eight weeks clearly the dual growth factor delivered constructs performed the best as measured by μCT, the defect was filled 50 % with real bone and the bridging to the adjacent host bone was achieved also in the widest area of the defect. The BMP-2 only group reached similar levels, while the TGFß group showed much worse results, but still better than the empty microspheres group. Histological analysis demonstrated that the cells followed endochondral ossification route since ColII, I and X could be detected including in the control group, although to varying degrees. After eight weeks very little human specific ColI was observed in all the groups, also there were only a few ALU-positive human cells left. This strongly indicated that the new bone was formed by recruited rat cells and that surprisingly the empty micro particle very efficiently induced spontaneous hypertrophic cartilage differentiation, but this was apparently not enough to trigger osteogenic differentiation of the attracted rat cells because after eight weeks the human cells had vanished [182]. In part I of the thesis we tested whether chondrogenic differentiation directly in vivo triggered by TGFß that is delivered with the scaffold is enough to induce endochondral ossification of BMSCs. In contrast to Dang et al. we do not necessitate any pre-culture (the cells could even be directly injected to the defect site).

1.3.4 Osteochondral tissue engineering

Osteochondral defects arise as a consequence of trauma or disease (osteochondritis dissecans, osteonecrosis). The main challenges for osteochondral TE are the localized induction of differentiation to cartilage and bone tissue, respectively, the successful integration of the two tissues (ideally mimicking the native junction with calcified cartilage as an intermediate tissue) and generally that the scaffold provide sufficient mechanical stability and/or has the ability to degrade concomitantly with the deposition of new ECM [17].

In the last 20 years, hundreds of studies have assessed cartilage-bone composites for the repair of osteochondral defects. In Table 2 there is a summary of 20 of these studies. Although it is a random selection it should represent the different approaches, which have been undertaken so far. Reports assessing osteochondral tissue formation only in vitro showed that a shorter individual pre-culture time is beneficial for improved cartilage to bone integration [183] or that a layer of non-differentiated cells is necessary for improved integration [184]. Real osteogenic differentiation cannot be observed in vitro, therefore a study aiming at generating an osteochondral construct and stopping with in vitro results is incomplete. Studies using the subcutaneous model have failed to generate fully differentiated bi-layered tissues, either the cartilage was not of stable phenotype and/or the bone tissue was not mature yet due to suboptimal cell source selection, insufficient stimuli or insufficient in vivo maturation time, respectively [185-189]. Still the subcutaneous model would be appropriate to indicate the potential of the multilayered scaffolds and the used cell source to form a (properly integrated) cartilage-bone composite even in a challenging environment before testing it in an orthotopic set-up. Because different animal models, sizes of osteochondral defects and time points were selected as experimental set-up, as well as the histological evaluation process followed differential criteria the cross comparison of the studies at an orthotopic site is difficult. Nevertheless, some interesting points can be mentioned. First, studies comparing their scaffolds in an acellular versus a cell-laden manner and studies implanting their scaffold only in an acellular way in an osteochondral defect did not observe a worse outcome compared to the condition with cells [73-78, 190]. This means that either the seeding of the cells did not happen in a sufficient way, not an appropriate cell source was used or also that absence of pre-culture to form already a tissue might have impacted the absence of a beneficial effect of the cells on the repair tissue. Implantation of labeled cells in these studies would have indicated the direct contribution of the donor cells to the formation of the repair tissue. Furthermore, these results indicated that in goats and rabbit osteochondral defects host cells (of whatever origin) could be attracted sufficiently. Second, in studies of no pre-culture (sometimes due to absence of seeded cells) for the induction of localized differentiation rather the differential scaffold mechanical and material composition was harnessed [73, 191-193] than co-delivery of growth factors [77, 78, 194]. This indicates that either the physical parameters are good enough, while biochemical parameters such as growth factors are not necessarily needed or that the neighboring environment e.g. paracrine factors exert a good enough influence on the differentiation of the loaded or recruited cells. In rare cases it was even relied solely on the effect of the neighboring tissue, namely when the scaffold had a single monophasic structure [75, 190, 195]. Unfortunately, these studies did not so precisely assess to what extent the typical structural organization (such as ECM protein distribution) of the cartilage and at the interface to the bone was reproduced by the repair tissue. This actually would

be crucial to better understand the parameters fostering the recreation of the native structural features of the tissue. Third, the influence of the pre-culture, whether in 2D or 3D and in a combined or separated manner etc., is not fully understood, yet. He et al. observed that longer in vitro pre-culture in chondrogenic medium led to a better outcome [195], however it has to be noted that they implanted a monophasic construct. Last, it is evident that steps ahead in terms of the experimental design could not really be observed over the time. The absence of accordance about what are the necessary stimuli (physical and biochemical), the optimal pre-culture time and the presence or absence of what cell source might be attributed to that most of the papers focus on one aspect, but there is a lack of big (complete) studies comparing all these different factors for one model and scaffold type.

Ref.	Cartilage		Bone		Interface	Pre-culture	In vivo Model	Outcome
	Material	Cell source	Material	Cell source				
[183]	PGA mashes	Bovine articular chondrocytes	PLGA/PEG 80:20	Bovine periosteal cells	Suture	Separate pre- culture in ChM and OM, resp. followed by combination in OM for 1-4 weeks	--	For increased integration, a less mature cartilaginous part is needed.
[73]	PGA/PLGA at different % + reinforced fibers (porous, two different stiffness)	Goat rib chondrocytes versus no cells	PGA at different % + bioglass or calcium sulfate (porous, of different stiffness)	Goat rib chondrocytes versus no cells	Glued together	2 days in CM	Goat osteochondral defect (3x 4mm), 16 weeks	Good hyaline cartilage and also subchondral bone restoration, no significant difference between groups with and without seeded cells. Better healing in the condyle than in the patellar groove (lower weight-bearing region). Higher stiffness materials for the cartilage part proofed to be better, while for the bone part surprisingly the stiffness did not influence the outcome.
[191]	Two different hyaluronan sponges coated with fibronectin	Rabbit BMSCs	Injectable CaP	--	Through hardening process of the CaP material	--	Rabbit osteochondral defect (3x 3mm), 4, 12 weeks	Cartilage-like tissue formed. The CaP gave mechanical support that promoted chondrogenesis in the upper part.

[185]	PLA sponge	Porcine articular chondrocytes	HA, cells seeded in fibrin glue	BMP-2 transduced human fibroblasts	PGA polymer film as a barrier for cell migration, PLA as a glue	--	Subcutaneously, nude mice, 4weeks	Bone plus bone marrow formed, cartilage only at the rim not inside the scaffold.
[192]	Collagen gel	Rabbit articular chondrocytes	ß-TCP	--	Integrated (through polymerization)	--	Rabbit osteochondral defect (4x 6mm), 8, 12, 30 weeks	Early to late time point, initially hyaline repair tissue was replaced by fibrocartilage. ß-TCP was resorbed after 12 w and replaced by new bone. No full integration with adjacent tissue.
[74]	Self-assembled ColI gel	Sheep articular chondrocytes or no cells	30 % ColI and 70 % HA	Sheep articular chondrocytes or no cells	Transition zone composed of 60 % ColI and 40 % HA	5 days	Sheep osteochondral defect (7x 9 mm), 24 weeks	Presence of cells did not improve cartilage and bone regeneration. Defects in both groups were filled with well-integrated hyaline like cartilage and subchondral bone tissue. Necessity of all three layers and whether the ratio of ColI:HA could be improved remain elusive.
[193]	PEGDA	Rabbit BMSCs	Allograft bone or 13-93 glass or porous tantalum metal	--	Chemical attachment	--	Rabbit osteochondral defect (3.2x 4 mm), 6, 12 weeks	Bioactive glass out-performed the other two materials in terms of bone-bone integration and (supporting) ColI positive repair cartilage.

[190]	OPF hydrogels plus/minus gelatin micro particles with TGFß1	Rabbit BMSCS or no cells	OPF plus/minus gelatin micro particles with TGFß1	Rabbit BMSCS or no cells	None (same scaffold)	--	Rabbit osteochondral defect (3x3 mm), 12 weeks	More subchondral trabecular bone with TGFß1, no improvement of cartilage properties with cells or cells and TGFß1 compared to the scaffold- only condition, rather more fibrous and fibrocartilage formation observed.
[184]	Collagen microspheres	Rabbit BMSCs chondroge-nically stimulated, 4 weeks	Collagen microspheres	Rabbit BMSCs, osteogenically stimulated, 4 weeks	Combination through undifferentiated BMSCs microencapsulated in collagen	ChM and/or OM, 2, 3 weeks	--	Layer of undifferentiated BMSCs bridging the cartilage and the bone was necessary for a better interface formation.
[194]	Alginate sulfate (porous sponge)/ hydrogel with affinity-bound TGFß1	Human BMSCs (only for in vitro evaluation)	Alginate sulfate (porous sponge)/ hydrogel with affinity-bound BMP-4	Human BMSCs (only for in vitro evaluation)	Through additive polymerization (directly injected in defect)	-- / OM for in vitro culture	Rabbit osteochondral defect (3x3 mm), 2-4 weeks	After 4 weeks the defects were fully filled with cartilage and underlying woven bone.
[75]	Coral aragonite scaffold with or w/o drilled channels and with or w/o impregnation with HAc	--	Coral aragonite scaffold with or w/o drilled channels	--	No interface (one scaffold)	--	Goat osteochondral defect (6x 8 mm), 24 weeks	Drilling channels and impregnating with HAc the cartilage part of the scaffold was pre-requisite for the regeneration of osteochondral tissue. Well-integrated hyaline-like cartilage was formed. Scaffolds almost fully degraded.

[76]	Segmented polyurethane, TGFß1 or BMP-2 loaded microspheres	--	PLGA	--	Integrated	--	Rabbit osteochondral defect (4.5x4 mm), 12-24 weeks	Slow release of the two factors within 6 weeks (measured in vivo non-invasively). Osteochondral tissue formed, no ColX detected in cartilage. No difference between the two growth factors.
[186]	Agarose hydrogel	Porcine articular chondrocytes	Agarose hydrogel	Porcine BMSCs	Through additive polymerization	ChM, 3 weeks	Subcutaneous implantation, 4 weeks	Calcification, ColI and X localized to the bony layer, however, time point to early to observe bone formation. Cartilage formed by chondrocytes. No graded interface.
[77]	OPF hydrogel with microspheres containing IGF-1	--	OPF hydrogel with microspheres containing BMP-2	--	Through additive polymerization	--	Rabbit osteochondral defect (3x 3 mm), 6, 12 weeks	Delivery of both growth factors did not overtly improve the repair cartilage tissue compared when only one was delivered. Hyaline: fibrocartilage, 50:50 was formed, also in the bone part there were remnants of fibrous tissue, bone mineral density improved with dual growth factory delivery.
[78]	Collagen/GAG scaffold absorbed FGF-18 or BMP-7	--	Collagen/GAG scaffold absorbed FGF-18 or BMP-7	--	No interface (one scaffold)	--	Sheep osteochondral defect (5.8x 6 mm), 24 weeks	FGF-18 out-performed the BMP-7 treated scaffold. Well-integrated hyaline cartilage was formed. Sometimes cartilage extended into the bone part.

[187]	Agarose hydrogel or self-assembled aggregate	Porcine BMSCs and various cell sources (…)	Alginate hydrogel	Porcine BMSCs	?	ChM, separate culture, 2 weeks; combination, 4 weeks	Subcutaneously, nude mice, 6 weeks	BMSCs calcified in vivo, no stable cartilage was formed. Too short time point in order to see nice bone formation.
[196]	Polyvinyl alcohol/ gelatin/ vanillin (PVA/G/V)	Rabbit BMSCS, chondrogenically pre-cultured	HA- polyamide-6	Rabbit BMSCS, osteogenically pre-cultured	Non porous PVA/G, integrated	OM, 1 week	Rabbit osteochondral defect (4x 6mm), 6, 12 weeks	Cell seeded constructs performed better at 6 and 12 weeks, the cartilage integrated undistinguishable with the host tissue, the subchondral bone as well. Donor cell contribution to tissue regeneration could be observed till 4 weeks, at later time points it was not investigated.
[188]	Highly porous poly (ε-caprolactone)	Bovine articular chondrocytes	Highly porous poly (ε-caprolactone) and HA particles	Bovine BMSCs	Integrated	--	Subcutaneously, nude mice, 9 weeks	(Good) and confined vascularization in bony layer, new bone tissue deposited around HA granules, chondrogenic matrix formed. No degradation/ remodeling of the scaffold was observed.
[189]	Coll hydrogel	Human BMSCs	Coll hydrogel with Mg/HA	Human BMSCs	Integrated	3 days, CM	Subcutaneously, nude mice, 4, 8 weeks	No delamination, organized homogenous cell colonization, some hints of differentiation.

| [195] | PGA/PLA | Porcine BMSCs | PGA/PLA | Porcine BMSCs | No interface (one scaffold) | ChM, 2, 4, 8 weeks | Porcine osteochondral defect (10x 4 mm), 24 weeks | The longer cultured the constructs were (more scaffold degradation), the better the repair (50 % of fully repaired defects in the 8 week-group). Cartilage (even though hypertrophic after in vitro culture) and subchondral bone formed and integrated with host tissue – localized differentiation was governed by the environment. |

Table 2: Summary of studies assessing the performance of osteochondral grafts in vitro and in in vivo ectopic and orthotopic models. OM: osteogenic medium, ChM: chondrogenic medium, CM: complete medium, the composition of the media delineated with the same name might not always be equal. PGA: Polyglycolic acid, PLGA: Polylactic co-glycolic acid, PLA: Poly-L-lactic acid, CaP: Calcium phosphate, HA: hydroxyapatite, TCP: Tricalcium phosphate, HAc: hyaluronicacid.

2 Thesis aims

2.1 Part I: Functionalized hydrogels to engineer in vivo osteochondral composites by spatially controlled induction of endochondral ossification

Traumatic joint injuries involving damage of articular cartilage and subchondral bone represent a clinical challenge with frequently unsatisfactory outcome. A promising alternative strategy to treat these defects could be the implantation of an engineered cartilage-bone composite. BMSC due to their ease of isolation, high proliferative capacities and chondrogenic and osteogenic differentiation potential have been extensively used for the generation of engineered grafts. However, the major hurdles in achieving chondrogenesis from BMSCs are their pre-mature adoption of a (pre-)hypertrophic phenotype that results in ossification along the endochondral route in an in vivo vascularized environment, and the vast donor to donor variability. Furthermore, the spatial organization of engineered cartilage could not be achieved, neither.
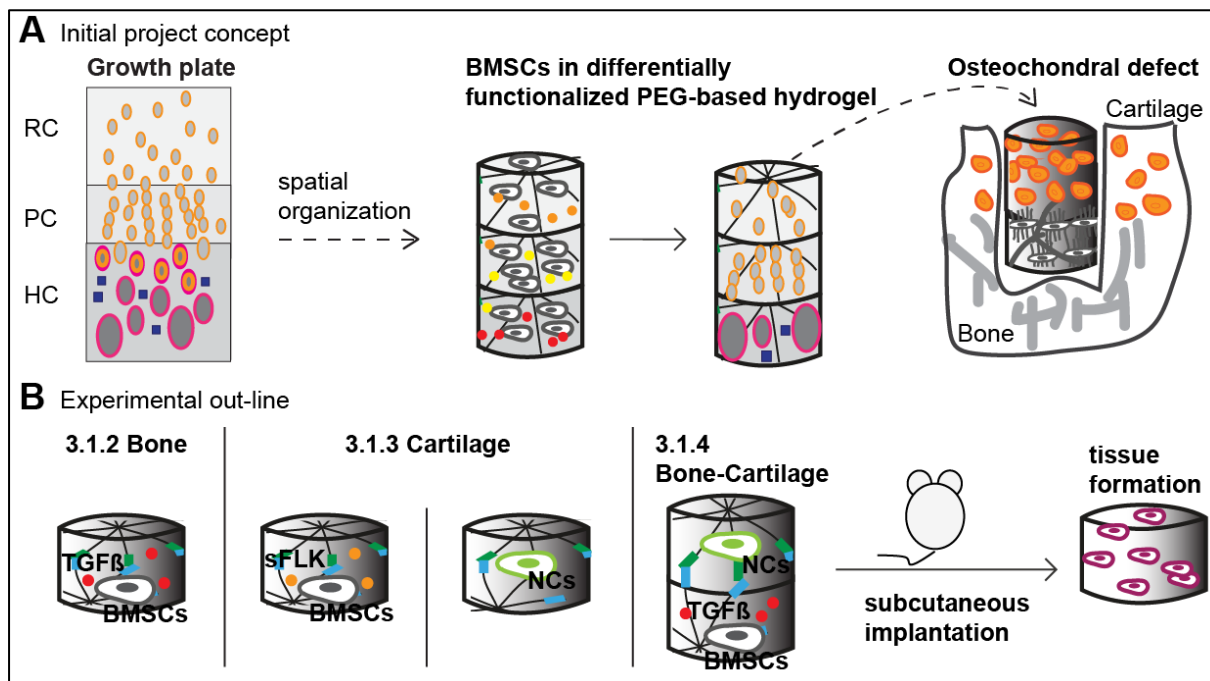

Figure 7: Schematic of the experimental approach of part I. A) Initial concept of the project. RC: resting, PC: proliferating, HC: hypertrophic chondrocytes. **B)** Components of the project that were assessed effectively (numbers indicate chapter). For the osseous layer BMSCs were encapsulated in PEG hydrogels containing (immobilized) TGFß3. For the cartilaginous layer, first, BMSCs transduced with sFLK were encapsulated and the possibility of

immobilizing sFLK or bevacizumab to the PEG hydrogel was assessed and second nasal chondrocytes (NCs) were encapsulated in non-functionalized hydrogels. For the formation of a bone-cartilage composite, BMSCs in a hydrogel layer containing (immobilized) TGFß3 were combined with NCs in a non-functionalized second layer. All hydrogel constructs were implanted subcutaneously in immunocompromised mice immediately after cell encapsulation for evaluation of their tissue formation potential.

During embryonic development and postnatal long bone growth the chondrocytes of the cartilage anlage in the limb bud and of the growth plate arrange in a pattern according to their maturation state i.e. resting, proliferating, pre-hypertrophic and hypertrophic, which is mediated by a specific spatiotemporal interplay of various signaling factors. It is possible that the absence of the spatial component in engineered cartilage could account for the lack of robust chondrogenesis by BMSCs. Therefore, we hypothesized that by applying a localized growth factor delivery a spatially controlled chondrogenic differentiation of BMSCs can be induced. Utilizing the PEG hydrogel system, a versatile tool to immobilize growth factors in a defined way, allows to test whether a transplantable growth plate-like structure can be generated from BMSCs by recapitulating certain developmental principles (Figure 7A). Specific goals of thesis part I were:

- Validation of PEG hydrogel as a suitable scaffold for in vitro chondrogenesis.
- Functionalization of PEG hydrogel with specific growth factors and proving their potential to induce the desired chondrogenic phenotype in vitro and in vivo.
- Combination of differentially functionalized PEG hydrogel layers to generate a bone-cartilage template in an in vivo ectopic environment.

2.2 Part II: Identification of a BMSC subpopulation with a superior chondrogenic differentiation capacity

Traditionally, BMSCs are isolated from bone marrow containing a mixture of hematopoietic and non-hematopoietic cells by their preference to adhere to plastic. This isolation procedure yields very heterogeneous cell populations and may account for the high inter-donor variability and unpredictability of chondrogenic differentiation out-come in functional assays. Several studies have tried to identify surface markers that select more pure BMSCs that enrich for the highest CFU-F forming cell population and show tri-lineage differentiation potential within the unfractionated bone marrow. Whether there is a sub-fraction of cells within culture expanded BMSCs that have a higher and less donor-dependent chondrogenic differentiation capacity has

remained elusive. Since single-cell derived clones of fresh bone marrow aspirates show a broad range of chondrogenic differentiation, we assessed whether the gene expression profile of clones with high and low chondrogenic capacity is different. Second, we anticipated that within the differentially expressed genes there are surface markers that potentially could guide to prospectively isolate a subpopulation with superior chondrogenic differentiation capacity. Ultimately, identification of such a cell fraction and reducing the variance in basic chondrogenic differentiation could further aid the process to develop BMSC based cartilage regeneration strategies. The specific aims of part II were (Figure 8):

- RNA sequencing of single cell derived clones with high and low chondrogenic differentiation capacity.
- Prospective isolation and chondrogenic assessment of sorted BMSCs from bulk expansion cultures based on specific surface markers identified by the transcriptomic analysis.
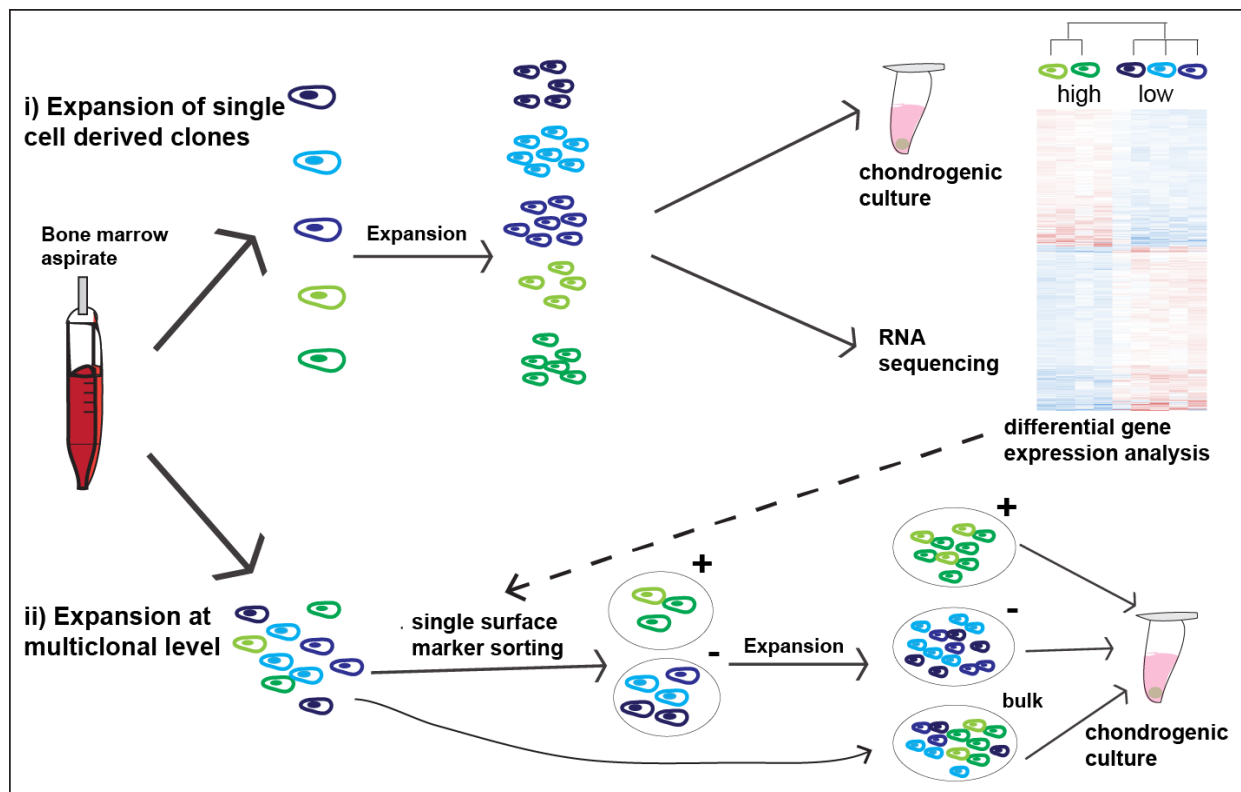

Figure 8: Experimental set-up of part II. Single cell-derived clones are isolated in order to address i) whether there is a correlation between the in vitro chondrogenic capacity of clones and their transcriptome and ii) to identify surface marker(s) that could be suited for prospective isolation of multiclonal BMSCs with a higher chondrogenic capacity.

3 Results and Discussion

3.1 Part I - Functionalized hydrogels to engineer in vivo osteochondral composites by spatially controlled induction of endochondral ossification

3.1.1 Validation of PEG hydrogel as a suitable scaffold for chondrogenesis of BMSCs

The suitability of the PEG-based hydrogels for in vitro chondrogenic differentiation of BMSCs was assessed and compared with scaffold-free pellet cultures. When 0.25×10^6 BMSCs (the same number as used for pellets) were encapsulated in the hydrogel of 10 µL volume, BMSCs formed a cartilaginous matrix rich of GAG and collagen type II (ColII) within two weeks of culture in chondrogenic medium containing TGFß3 (ChM) similarly to when cultured as pellets (Figure 9A). Compared to pellet culture the total amount of glycosaminoglycan (GAG) accumulated and the DNA content per construct was higher indicating for superior chondrogenesis and higher cell survival and/or proliferation (Figure 9B). In this system the presence or absence of the adhesion peptide RGD did not influence chondrogenic outcome, as the amount of accumulated GAG per construct was very similar with the three different RGD concentrations tested (Figure 9C). To test the impact of cell density on chondrogenesis, BMSCs were encapsulated at various cell densities from 1.6x to 50x 10^6 cells/mL of pre-polymerized gel solution. Clearly, the higher cell density the more GAG was deposited and below 12x 10^6 cells/mL chondrogenesis was suboptimal (Figure 9D). In order to monitor the degree of hydrogel degradation during chondrogenic culture, FITC was covalently incorporated into the hydrogel network. While directly after cell encapsulation the green fluorescence showed a homogeneous smooth pattern, with increasing culture time fluorescence disappeared directly around the cells and sometimes also in small areas indicating that the hydrogel was degraded in close proximity to the cells (Figure 9E). In summary, these experiments demonstrated that the here-used PEG system is well compatible with chondrogenic differentiation of BMSCs.
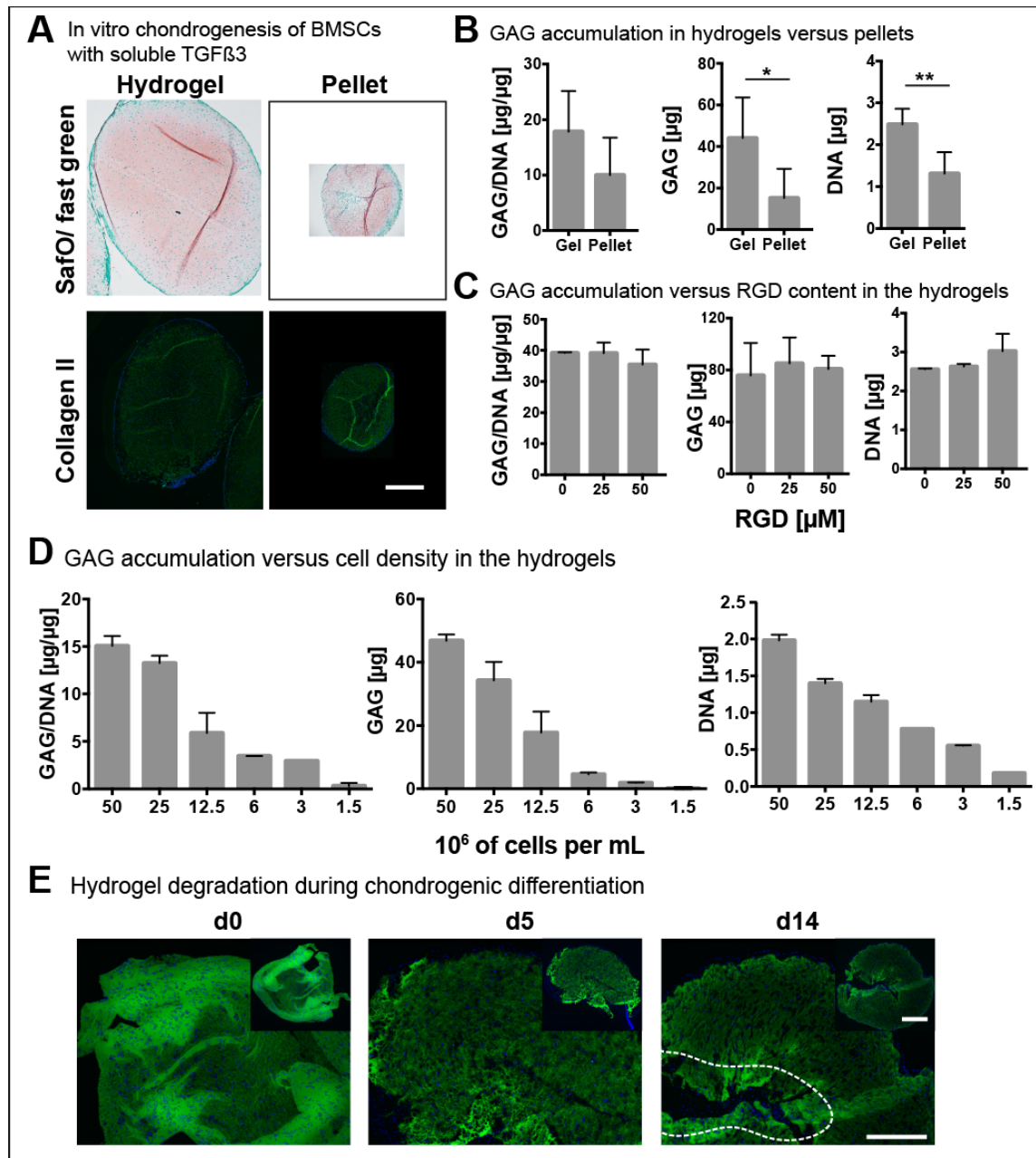
Figure 9: BMSCs underwent reproducible in vitro chondrogenic differentiation in PEG hydrogels in a cell density dependent way. A) 0.25x 10^6 BMSCs were encapsulated in 10 µL MMP-degradable PEG hydrogel containing RGD adhesion peptide or prepared as pellets and cultured for two weeks in ChM. SafraninO/fast green (SafO/FG) staining and IF for collagen type II (ColII) of paraffin sections are shown. **B)** Glycosaminoglycan (GAG) accumulation in hydrogels and pellets was quantified by DMMB assay and presented as total GAG normalized to total DNA content and as GAG per construct. N=6, 2 replicates each. Paired t-test, P-values = *0.0044, **0.001 **C)** BMSCs were encapsulated in PEG hydrogels containing 0, 25 µM or 50 µM RGD, respectively and cultured for two weeks in ChM. GAG and DNA content was quantified. N=3, 2 replicates each. **D)** GAG and DNA quantification of hydrogel constructs generated with various cell densities (1.5x 10^6 - 50x 10^6 cells /mL hydrogel) and cultured for two weeks in ChM. N=3, 2 replicates each. **E)** Hydrogel degradation was determined by visualizing enzymatically incorporated FITC
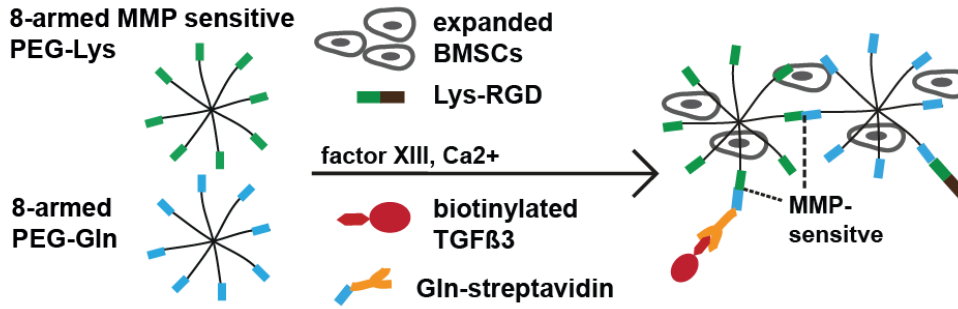
to the hydrogel network on cryosections from hydrogels cultured 0, 5 and 14 days in ChM. Green: FITC, blue: DAPI, encircled area indicates region with complete absence of FITC, but DAPI positivity indicative for replacement of the hydrogel by newly deposited matrix. Scale bars: 500 µm (low) and 200 µm (high magnification). N=1, two replicates each time point.
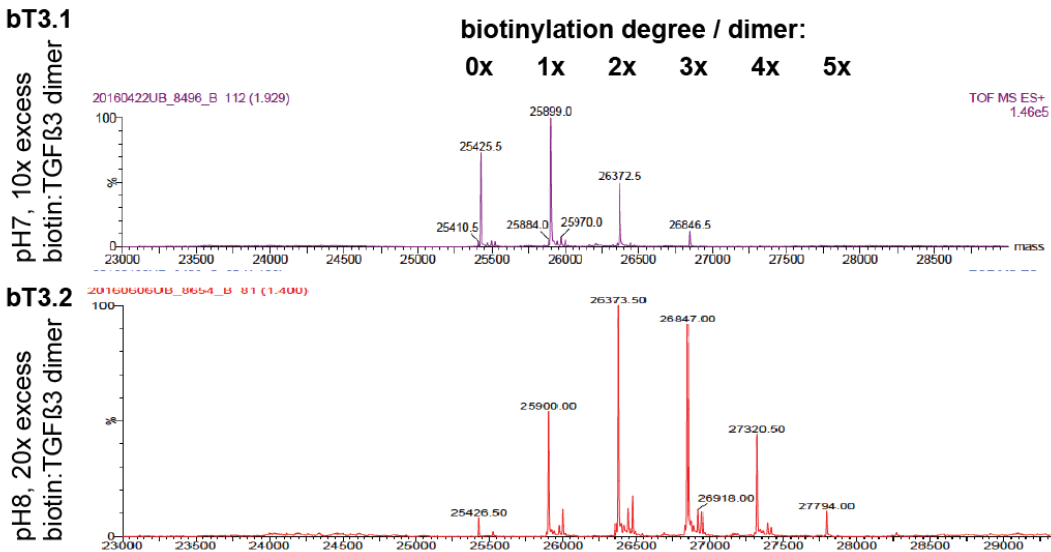
3.1.2 Osseous layer

3.1.2.1 Functionalization of PEG hydrogel with TGFß3

Next, aiming at delivering TGFß, the only known factor reliably inducing chondrogenesis of BMSCs, in a spatially controlled way we functionalized the PEG-based hydrogel with TGFß3. We used the strategy introduced by Metzger et al. [148], in which streptavidin is covalently linked to the hydrogel network and biotinylated growth factors are used (Figure 10A). The release of biotinylated TGFß3 (bTGFß) samples (Figure 10B) from acellular hydrogels polymerized in absence and presence of streptavidin was monitored for one week. Whereas without streptavidin almost all of the added bTGFß3 was released, with streptavidin the hydrogels retained the majority of the bTGFß3 (Figure 10C). Less bTGFß3 was measured in the supernatant with the sample containing no non-biotinylated TGFß3 (bT3.2 in Figure 10B) indicating that basically only the non-biotinylated fraction was released from the streptavidin containing hydrogels. To test whether chondrogenesis occurs in functionalized hydrogels 0.5, 1 and 3 ng bTGFß3 /uL (corresponding to totally 5 / 10 / 30 ng of TGFß3 - a similar amount as used for the soluble stimulation) was immobilized in the hydrogels. Irrespective of the amount of bTGFß3 added to the hydrogel, the chondrogenesis reached similar levels as when delivered through the medium (Figure 10D and E). Furthermore, in absence of streptavidin, the single TGFß3 pulse was also sufficient to induce chondrogenesis efficiently (Figure 10D and E). In bi-layered constructs, in which only one part contained bTGFß3, pronounced chondrogenesis occurred in the bTGFß3 containing part, while in the other part at the boarder only a limited amount of GAG could be detected. Immobilization did not improve the localized differentiation, since also in absence of streptavidin, chondrogenic differentiation in the bTGFß3-deficient part did not occur in a more pronounced way (Figure 10F). In summary, neither biotinylation of TGFß3, nor its immobilization in the hydrogel compromised its bioactivity to induce chondrogenic differentiation of BMSCs, and immobilization proved not to be advantageous over simple addition to the hydrogel.
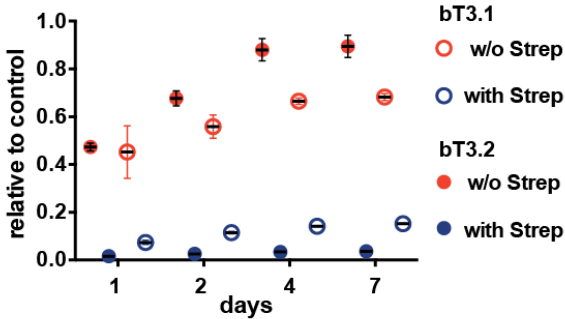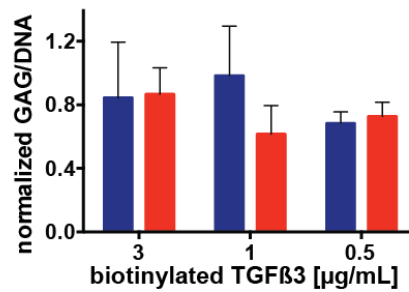
A Functionalization of hydrogels with TGFß3

8-armed MMP sensitive PEG-Lys

expanded BMSCs

Lys-RGD

8-armed PEG-Gln

factor XIII, Ca2+

biotinylated TGFß3

Gln-streptavidin

MMP-sensitve

B Mass spectrometry of biotinylated TGFß3 samples

bT3.1

pH7, 10x excess biotin:TGFß3 dimer

biotinylation degree / dimer:

0x   1x   2x   3x   4x   5x

20160422UB_8496_B 112 (1.929)

TOF MS ES+
1.46e5

100

%

25425.5
25899.0
26372.5
25410.5   25884.0   25970.0   26846.5

mass

23000 23500 24000 24500 25000 25500 26000 26500 27000 27500 28000 28500

bT3.2

pH8, 20x excess biotin:TGFß3 dimer

20160606UB_8654_B 81 (1.400)

100

%

26373.50
26847.00
25900.00
27320.50
25426.50   26918.00   27794.00

23000 23500 24000 24500 25000 25500 26000 26500 27000 27500 28000 28500 29000

C bTGFß3 release from acellular hydrogels

relative to control

days

bT3.1
w/o Strep
with Strep
bT3.2
w/o Strep
with Strep

D GAG accumulation versus bTGFß3 content

normalized GAG/DNA

biotinylated TGFß3 [µg/mL]

E In vitro culture comparing differential bTGFß3 delivery

soluble bTGFß3   immobilized bTGF3 (1 µg/mL)   non-immobilized bTGFß3 (1 µg/mL)

F Biphasic hydrogels

no   + bTGFß3

Immobilization

−

+
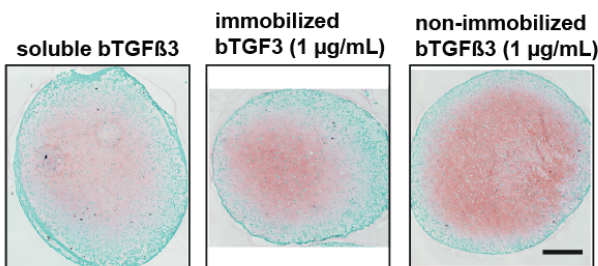
Figure 10: Immobilized TGFß3 in the hydrogel induced chondrogenic differentiation of BMSCs to the same extent as when delivered soluble. A) Scheme of the functionalizati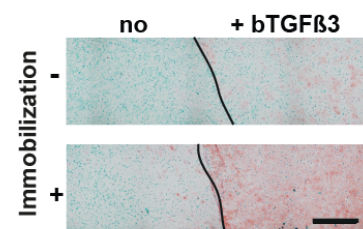on strategy. TGFß3 was immobilized by incorporating streptavidin covalently in the hydrogel network and using biotinylated (b)TGFß3. **B)** bTGFß3 variants (bT3.1 and bT3.2) were analyzed by time of flight mass spectrometry to determine the degree of biotinylation per dimer. **C)** bTGFß3 release from acellular hydrogels with and without streptavidin into the supernatant was determined by ELISA and normalized to the total amount added to the hydrogel. N=2, 4 replicates each. **D-E)** BMSCs were cultured for two weeks in hydrogels with immobilized or non-immobilized bTGFß3 (bT3.1) at 0.5, 1 and 3 µg/mL and soluble bTGFß3 (bT3.1). GAG/DNA was quantified and normalized to the control (bTGFß3 added to the medium). Immobilized (blue) and non-immobilized (red) bTGFß3 (D). N=3, 2 replicates each. Representative images of SafO/FG staining of cultures with 1 µg/mL (non-)immobilized and soluble TGFß3 are shown (E). **F)** Bi-layered hydrogels composed of a part with immobilized or non-immobilized bTGFß3, cultured in ChM in absence of soluble TGFß3. Representative images of SafO/GF staining of paraffin sections are shown. N=3, 1-3 replicates each. Scale bars: 200µm.

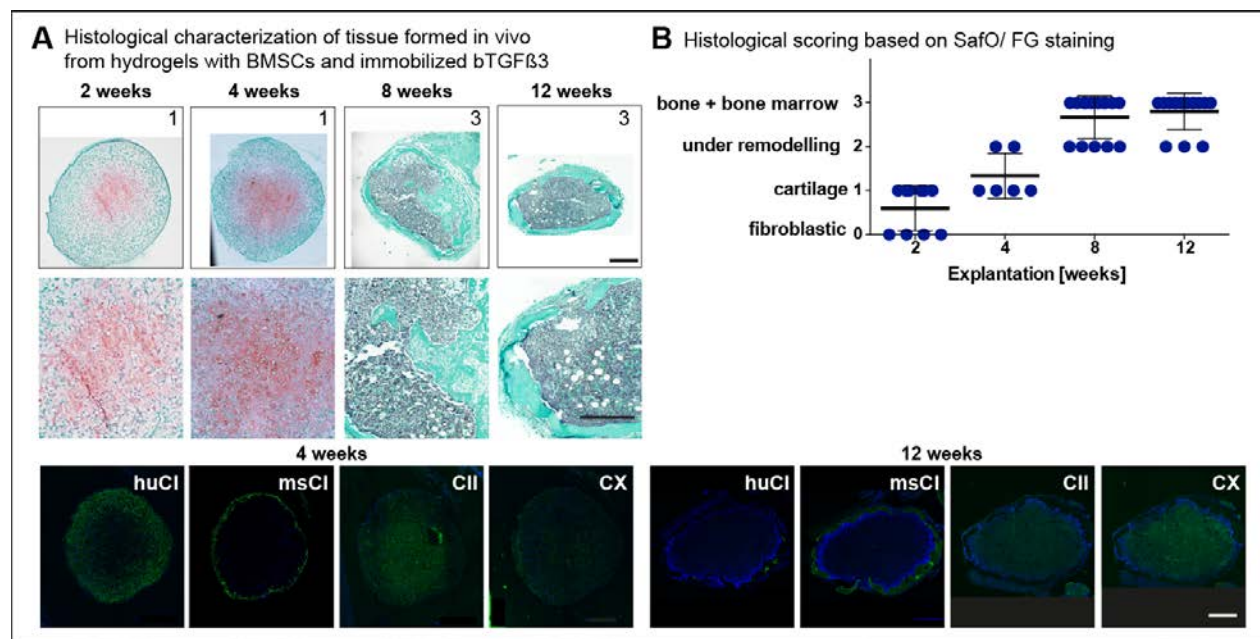## 3.1.2.2 Ectopic implantation of TGFß3-functionalyzed PEG hydrogels

Figure 11: BMSCs in TGFß3-functionalyzed PEG hydrogels efficiently underwent endochondral ossification in vivo without an in vitro pre-culture step. A) 20-25x 10^6 cells/mL BMSCs were encapsulated in hydrogels containing immobilized TGFß3 at a concentration of 1 µg/mL hydrogel (corresponding to 10 -20 ng per 10-20 µL hydrogel) and were directly implanted subcutaneously in nude mice. Constructs were explanted after 2 (N=2, 2-4 replicates), 4 (N=3, 2 replicates), 8 (N=7, 2-3 replicates) and 12 weeks (N=8, 2-4 replicates), respectively and paraffin sections were analyzed by SafO/FG staining and IF for CoII (human and mouse specific), II, X. Scale bars: 200 µm. **B)** Histological scoring obtained by valuing the SafO/FG stained sections with a number of 0-3 based on their maturation grade (see Table 3).

Because TGFß3 is the main inducer of chondrogenesis, we hypothesized that delivering TGFß3 in the hydrogel is enough to steer endochondral ossification in vivo without the prerequisite in vitro pre-culture step. For that purpose, hydrogels containing 1µg/mL immobilized TGFß3 (corresponding to 10-20 ng TGF ß3 per hydrogel) were implanted subcutaneously in nude mice immediately after cell encapsulation. After two to four weeks, chondrogenesis was observed as seen by positivity for SafO staining, the rounded cell morphology and the presence of ColII, and X (Figure 11A). After four to eight weeks cartilage tissue remodeling to bone was observed, an increased area of the tissue was positive for ColI and partially infiltrated by bone marrow. After eight to twelve weeks full ossicles developed consisting of a cortical bone rim with typical spindle shaped osteocytes enclosing bone marrow (Figure 11A). While the ColI in ECM denser regions percolating the ColX positive areas with big rounded cells was of human origin, the more mature bone tissue forming the rim of the constructs was exclusively of mouse origin indicating that the recruited mouse cells were mainly responsible for bone formation in situ.
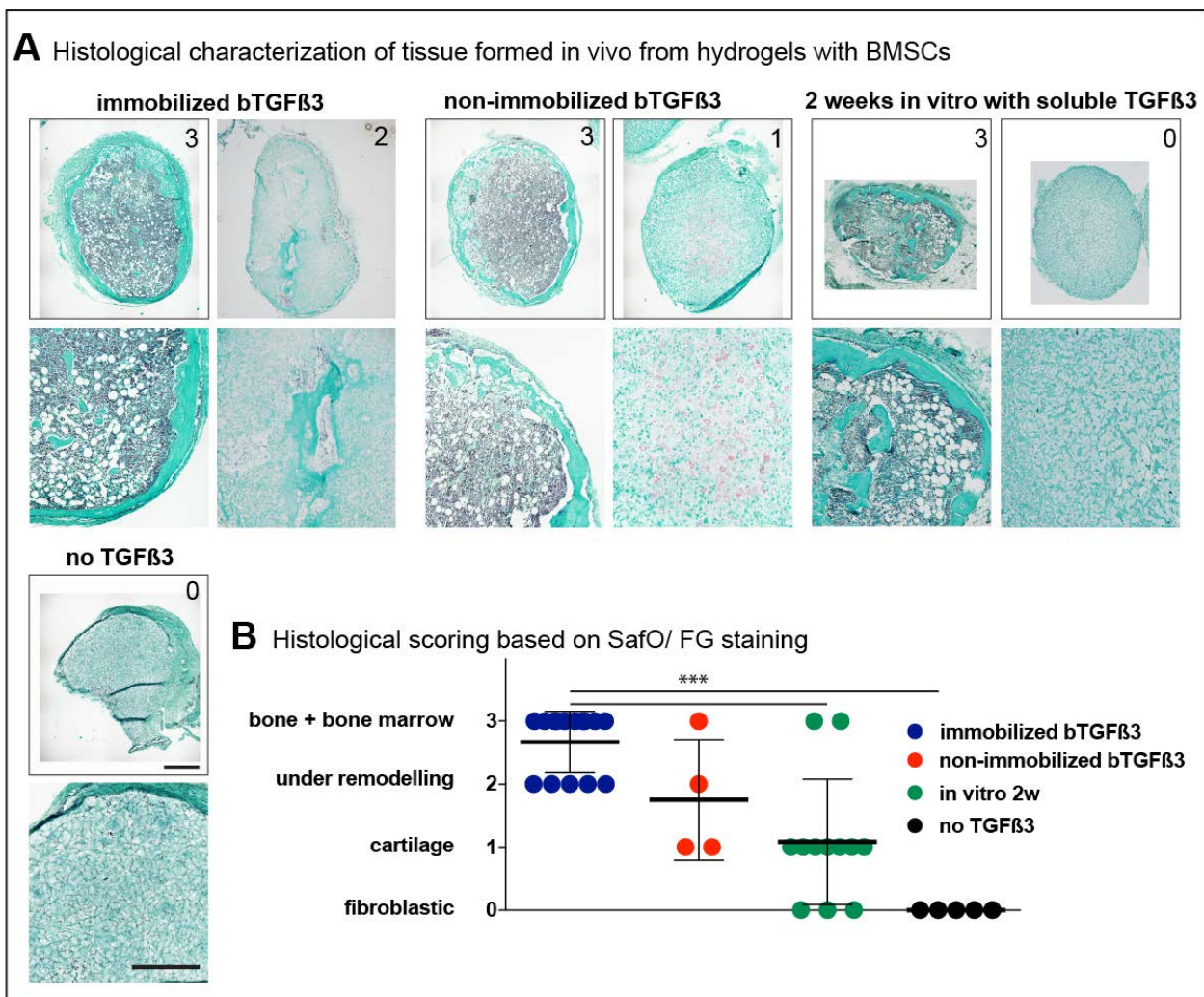

A Histological characterization of tissue formed in vivo from hydrogels with BMSCs

B Histological scoring based on SafO/ FG staining

Figure 12: Ossicle formation in PEG hydrogels with immobilized TGFß3 was more efficient than in non-functionalized hydrogels after two weeks of in vitro pre-culture in ChM. A) BMSCs were encapsulated in PEG hydrogels containing 1µg/mL immobilized TGFß3 (N=7, 2-4 replicates), 1 µg/mL non-immobilized TGFß3 (N=2, 2 replicates), and without TGFß3 after two weeks culture in ChM (N=3, 4 replicates) or directly implanted (N=3, 2 replicates) and explanted after eight weeks. SafO/FG stainings of representative replicates of the best and the worst replicate per condition are shown. Numbers on the images indicate their histological score. Scale bar: 200 µm. **B)** Histological scoring obtained by valuing the SafO/FG stained sections with a number of 0-3 based on their maturation grade (see Table 1). Unpaired t-test, ***P-value ≤0.0001.

The SafO/FG stained sections were evaluated with a histological score (Figure 11B). While from two to eight weeks the constructs were of increased maturation and in the majority of the cases after eight weeks full ossicles had developed with marginal remodeling tissue left, there was no improvement observed anymore from eight to twelve weeks implantation time (Figure 11B). Addition of TGFß3 to the hydrogels without immobilization also induced endochondral ossification and the formation of ossicles, however, by trend with lower efficiency compared to the immobilized condition (Figure 12A and B). Clearly, the efficiency of ossicle formation of non-functionalized hydrogels, which were implanted after two weeks in vitro chondrogenic culture was significantly lower compared to the immobilized TGFß3 condition (Figure 12A and B). In summary, the TGFß3 presented in the hydrogel (either immobilized or non-immobilized) induced efficiently endochondral ossification of unprimed BMSCs demonstrating that the in vitro pre-culture step can be omitted.

3.1.3 Cartilaginous layer

3.1.3.1 Blocking VEGF by either by utilizing sFLK expressing BMSCs or by functionalization of the hydrogel with sFLK.

Previous results showed that BMSCs stably expressing a soluble variant of mouse VEGFR2 (sFLK-1) spontaneously formed cartilaginous tissue upon immediate ectopic implantation without showing hypertrophic features like ColX [132]. We anticipated to reproduce this finding with sFLK-1-functionalized hydrogels instead of genetically modified BMSCs for the cartilaginous layer of the osteochondral construct. As a first step, sFLK expressing BMSCs were assessed in the hydrogel for their chondrogenic differentiation properties. Transduction of one fresh BMSC

donor with retrovirus expressing sFLK-1 and a truncated version of mouse CD8a resulted in an efficiency of 45 % (Figure 13A), 40 % lower than observed by Marsano et al. [132].
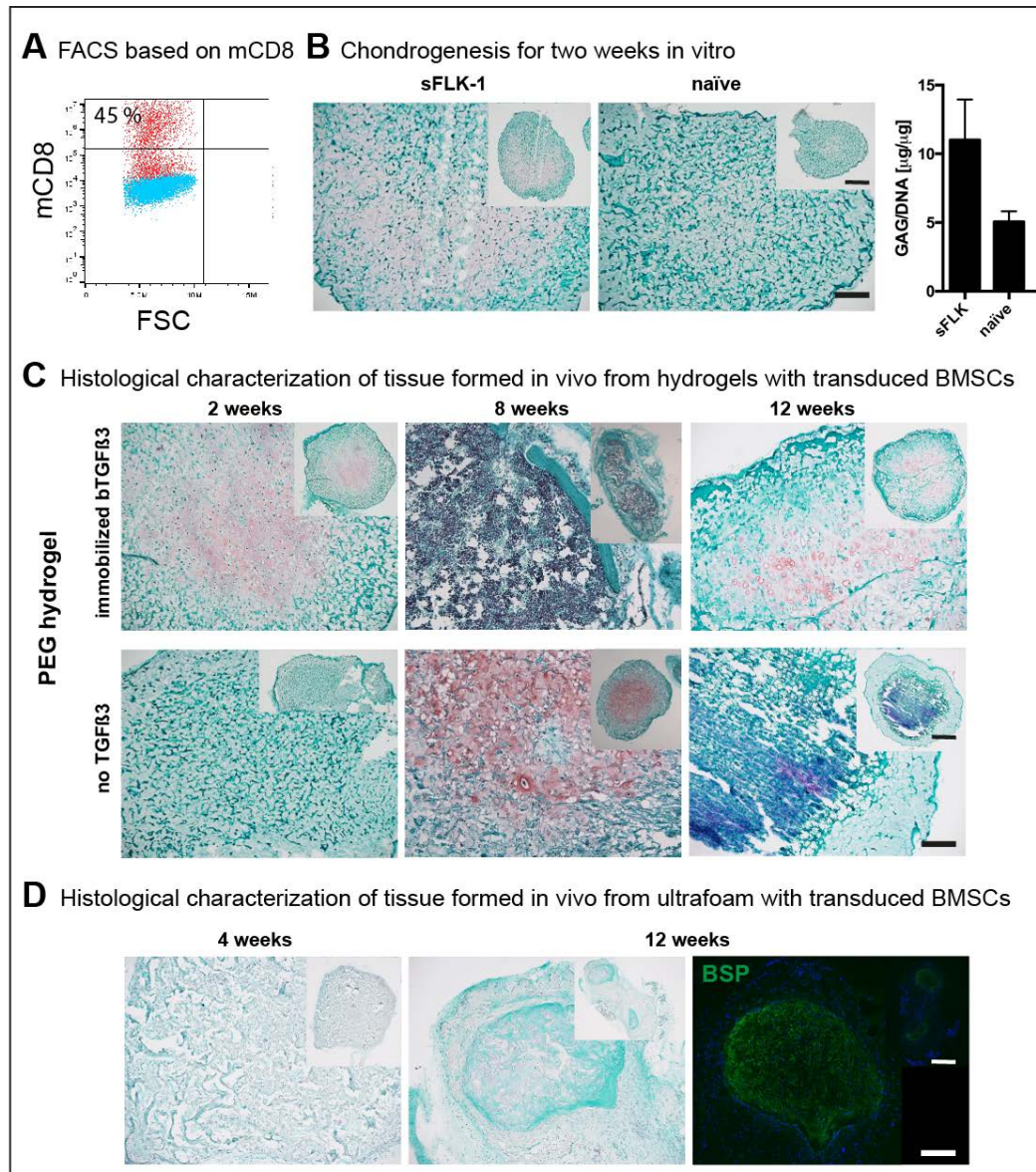

Figure 13: BMSCs over expressing sFLK did not undergo (spontaneous) stable chondrogenesis upon ectopic implantation. A) Flow cytometric analysis of transduced cells stained for mouse CD8a to determine the transduction efficiency. **B)** SafO/FG staining of paraffin sections and GAG/DNA quantification of transduced and control BMSCs after two weeks of culture in ChM in PEG hydrogels. **C)** sFLK-1-expressing cells were encapsulated in hydrogels with and without 1µg/mL immobilized bTGFß3 and immediately implanted. SafO/FG staining of cryosections from explants after 2, 8 and 12 weeks are shown. N=1, 2 replicates each**. D)** sFLK-1-expressing cells were seeded in ultrafoam and after one day of culture in vitro in CM implanted in nude mice. SafO/FG staining of cryosections from explants after four and twelve weeks and IF staining for BSP after twelve weeks are shown. Scale bars: 500 µm (low) and 200 µm (high magnification). N=1, 4 replicates each.

In expansion conditions the cells secreted 752 +/- 550 ng/10^6 cells/24 h, the big standard deviation originated from the high dependency on the cell density when the supernatant was withdrawn. Strangely, in Marsano et al. [132] the average secretion of sFLK-1 was determined with 1.37+/- 0.14 ng/10^6 cells/24 h cells to be 2 magnitudes lower. The transduction procedure did not impair the in vitro chondrogenic differentiation potential of the cells (Figure 13B). 0.25x 10^6 cells of sFLK-BMSCs were encapsulated in hydrogels with and without immobilized TGFß3. The reason for utilizing also the TGFß3-functionalized hydrogels was, that in previous experiments with two formerly transduced sFLK-1 expressing donors, no chondrogenesis was observed at all. Therefore, it was hypothesized that the TGFß3 could be the trigger for differentiation and the secretion of sFLK-1 could still prevent transformation into bone tissue. In case of the empty hydrogels, after two weeks no chondrogenic differentiation was observed, after eight weeks 1/2 replicates underwent chondrogenic differentiation and finally after twelve weeks, both replicates did not show any signs of chondrogenesis, but were calcified similarly to the no-TGFß3 controls with naïve cells (Figure 13C). In contrast, in presence of immobilized bTGFß3 clearly the cells underwent chondrogenesis after two weeks and one full ossicle was formed after eight weeks, while after twelve weeks both replicates were composed of cartilaginous matrix. Unfortunately, the type of the cartilage could not be determined (Figure 13C). As a control to exclude any unexpected effects of the PEG hydrogel, the cells were also seeded in ultrafoam following the method of Marsano et al. [132]. After four weeks, in none of the four replicates were signs of chondrogenesis observed and after twelve weeks in all four replicates GAG positive areas could be found, however, these regions were of hypertrophic phenotype since also BSP could be detected and the GAG positive parts were surrounded by denser FG positive matrix suggesting that these constructs were in the process of endochondral ossification (Figure 13D). In summary, the sFLK-1 expression induced spontaneous differentiation to some extent, however, not of a stable cartilage phenotype. It could be due to the fact that more than half of the cells did not express sFLK-1 and that the secreted amount of sFLK was not sufficient.

Therefore, the remaining cells were sorted according to CD8a expression that resulted in the positive population with more than 90 % CD8a+ cells and a negative subset with one quarter of the cells still expressing CD8a (Figure 14A). In vitro both populations were chondrogenic (Figure 14B) and the amount of sFLK determined in the medium was on average five times higher in the positive compared to the negative subpopulation (Figure 14C) indicating that the percentage of

CD8a^{+} cells reflected the amount of secreted sFLK-1. Upon eight weeks implantation, positively and negatively sorted cells formed fibrocartilage with little SafO positivity and expression of ColII, I and X throughout the construct (Figure 14D). There was no obvious difference between the two subpopulations visible indicating that the amount of sFLK produced by the cells might not have influenced the differentiation outcome and that there must be other reasons for the discrepancy to the findings of Marsano et al. [132].
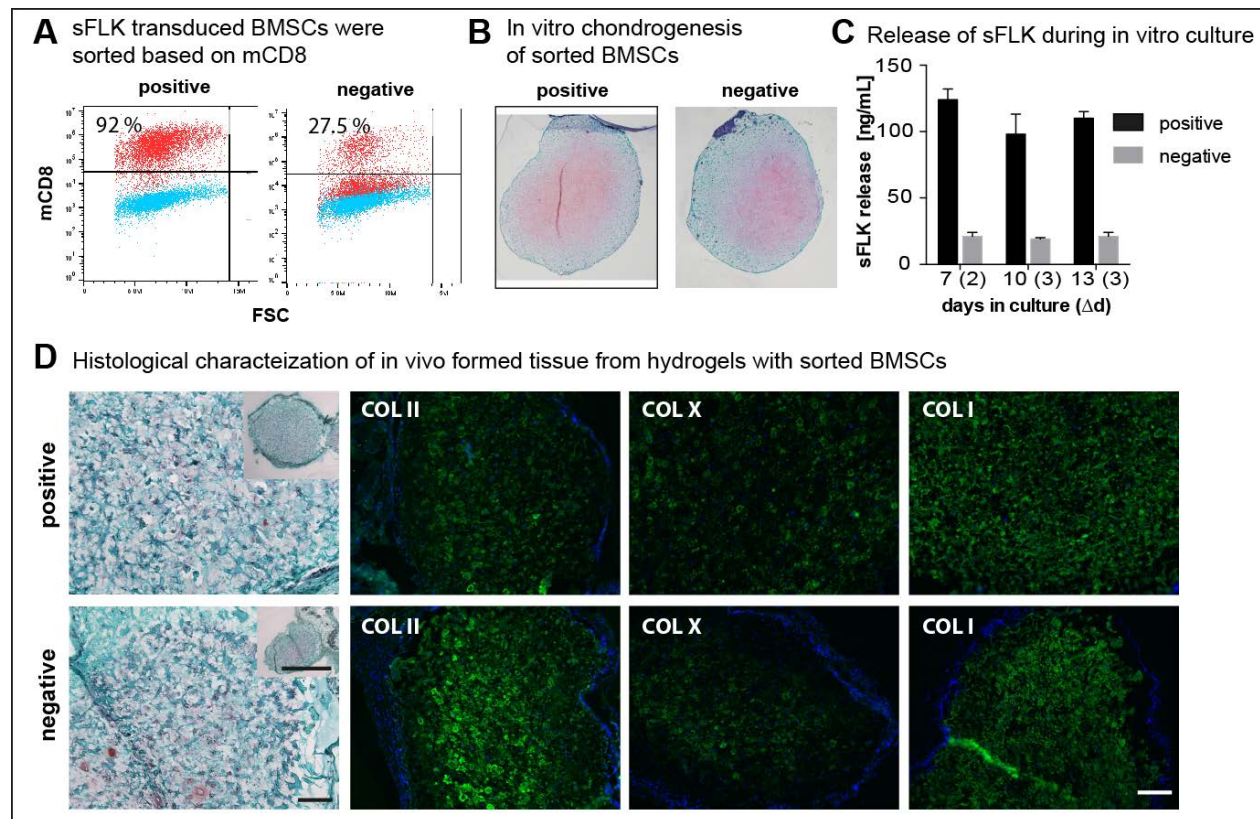

Figure 14: Enriched sFLK over-expressing BMSCs populations did not undergo spontaneous in vivo chondrogenesis. A) Flow cytometric analysis of expanded transduced cells that were sorted based on mouse CD8a. **B)** SafO/FG staining of paraffin sections of the CD8a^{+} and CD8a^{-} cells after 2 weeks culture in PEG hydrogels in ChM. **C)** Secretion of sFLK-1 by the CD8a^{+} and CD8a^{-} cells during chondrogenic culture measured by ELISA. The number in the bracket indicates the time between the two medium changes. Values are the mean of four replicates. **D)** Sorted cell populations were encapsulated in non-functionalized PEG hydrogels and explanted after eight weeks. Paraffin sections were analysed by SafO/FG staining and IF staining for ColI (human specific), II and X. Scale bars: 500 µm (low) and 200 µm (high magnification).

For hydrogel functionalization, since sFLK-1 is commercially available as FC tagged fusion protein, an affinity binding strategy based on covalent incorporation of ZZ-peptide was selected [197]. In order to measure the immobilization efficiency of sFLK in the hydrogel, capture and release assays were performed with fluorescently labeled protein. There was no difference

observed in terms of fluorescence measured in the supernatants withdrawn from hydrogels containing ZZ-peptide and from those without in the capture (Figure 15A) and neither in the release assay (Figure 15B) indicating that sFLK-FC could not be bound to the ZZ-peptide containing hydrogels. Alternatively, the functionalization with bevacizumab/avastin - a monoclonal VEGF antibody used in cancer treatment and bearing a FC domain - was tested. From hydrogels with ZZ peptide and loaded with 100 ng bevacizumab, after 7 days the cumulative release was approximately 35 %, while in absence of ZZ peptide all the loaded bevacizumab was released (Figure 15C). This experiment was only conducted once, but clearly proposed bevacizumab to be the favorable candidate for generating a VEGF scavenging hydrogel. However, considering that the results with the sFLK expressing cells implanted in PEG hydrogels were not promising, we decided not to continue with further characterization of the bevacizumab-functionalized hydrogels and their potential to induce chondrogenesis of BMSCs.
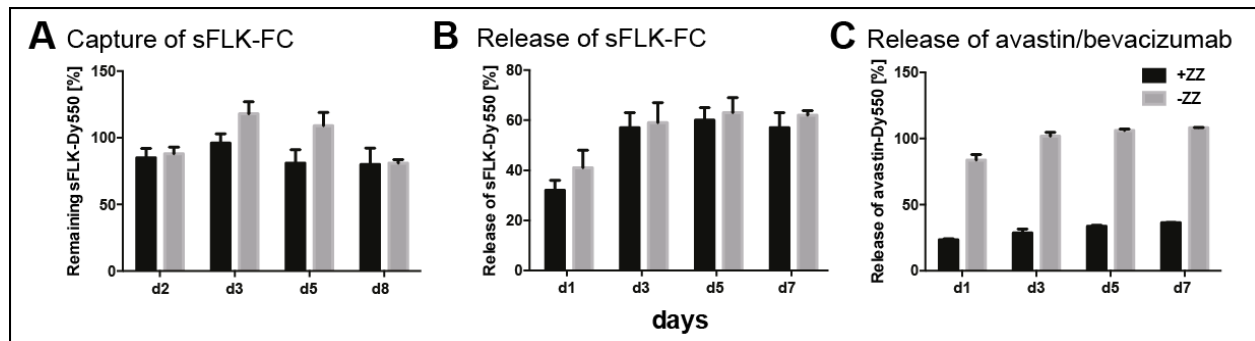

Figure 15: Dy550 labeled sFLK-1 could not, while labeled bevacizumab could be immobilized by ZZ peptide in the PEG hydrogel. A) PEG hydrogels were generated in presence (+ZZ) and absence of ZZ-peptide (-ZZ) and immersed in serum-free medium containing 500 ng/mL labeled sFLK-1-FC. At the indicated time points supernatant was withdrawn and fluorescence was measured and compared to the condition without hydrogels. **B)** Hydrogels with and without ZZ-peptide were generated in presence of 100 ng labeled sFLK-1-FC-Dy550 and immersed in SFM. Medium was changed at the indicated time points and fluorescence was measured and compared to the control without hydrogel containing 100 ng of sFLK. **C)** The same assay as in B) was performed with labeled bevacizumab (avastin). N=1, 4 replicates each.

3.1.3.2 Nasal chondrocytes (NCs)

In contrast to BMSCs, NCs have robust re-differentiation potential and are therefore a suitable cell source for the cartilaginous layer of an osteochondral construct. In order to determine the best conditions to induce chondrogenesis of NCs in PEG hydrogels, various cell numbers in combination with and without RGD, as well as soluble and immobilized bTGFß3 in vitro were

tested. Clearly with decreasing cell density the total amount of GAG produced by NCs unrelated to the RGD concentration was diminished similarly to with BMSCs. With different RGD concentrations, the variance of GAG accumulation was bigger than observed with BMSCs, but still there was no significant difference observable (Figure 16A).
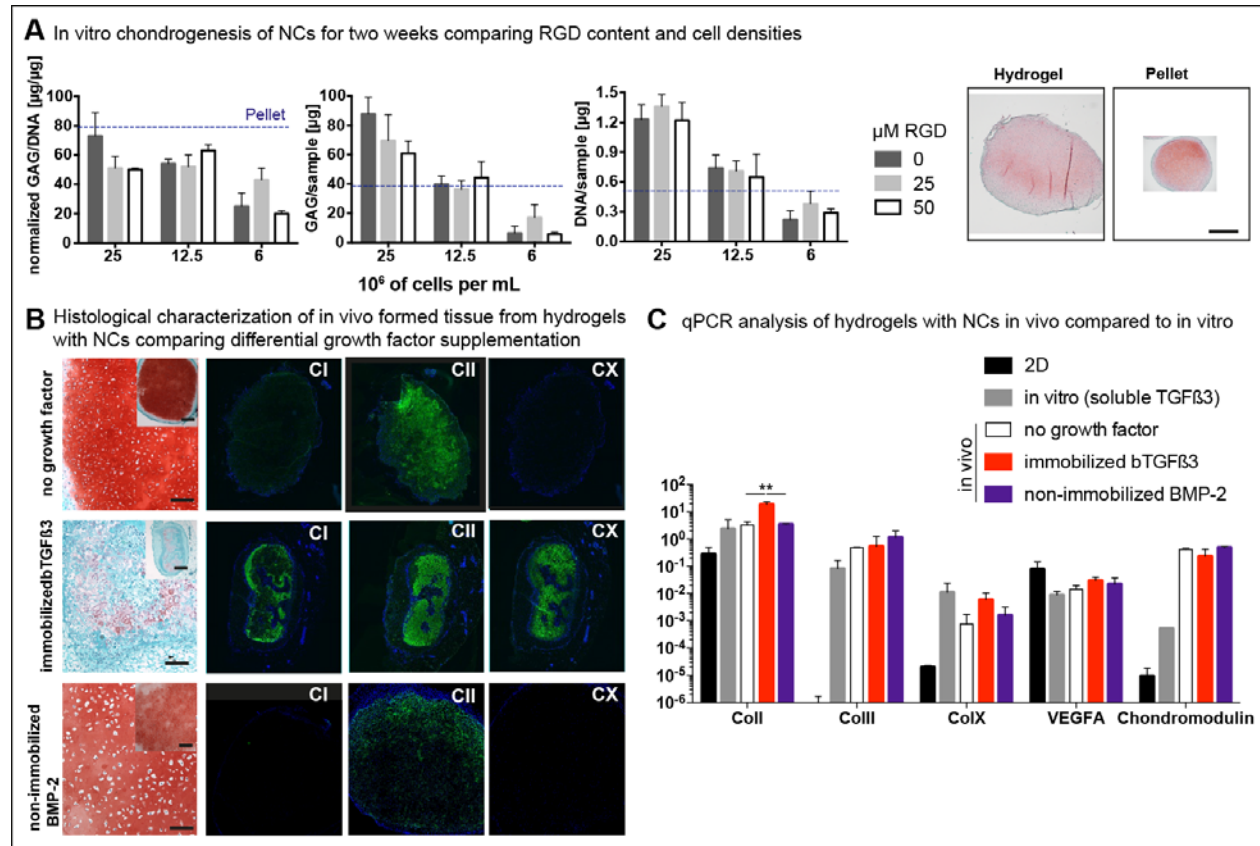

Figure 16: Chondrogenesis by NCs in vivo does not necessitate TGFß3. A) 6, 12.5 and 25x 10^6 NCs were encapsulated in hydrogels containing 0, 25 or 50 µM RGD, cultured for two weeks in ChM and GAG and DNA content was determined. The blue line represents the average value from culture as pellets with 0.25x 10^6 cells. SafO/FG staining of paraffin sections of a representative hydrogel with 0.25x 10^6 cells and 25 µM RGD and of a pellet are shown. Scale bar: 200 µm. N=1, 3 replicates. **B)** Hydrogels containing 0.25x 10^6 cells and 25 µM RGD in absence of any growth factor, in presence of immobilized TGFß3 and non-immobilized BMP-2 at 10 µg/mL were directly after cell encapsulation implanted subcutaneously and analyzed after eight weeks by SafO/FG and IF staining for ColI (human specific), II and X. N=2 for immobilized bTGFß and without TGFß and N=1 for BMP-2, 2 replicates each. **C)** The in B) mentioned constructs were implanted for three weeks and analyzed by qPCR for gene expression of ColI, II, X, VEGFA and chondromodulin as shown normalized to GAPDH. As a reference the cells after 2D expansion and in vitro constructs cultured in ChM were used. N=2, 2-3 replicates. **P-value: <0.0001.

For elucidation of the optimal condition for in vivo re-differentiation, hydrogels without a growth factor, with immobilized bTGFß and with non-immobilized BMP-2 (see section 3.1.4.3 for the reason) were implanted immediately after cell encapsulation. After eight weeks the NCs formed

a cartilage tissue rich in GAG and collagen type II and absent of collagen type X without TGFß3 (Figure 16B). In contrast, the cells in hydrogels with immobilized bTGFß3 seemed to have undergone hypertrophic differentiation, since the SafO positive regions were heavily intercalated by FG and collagen type I positive areas as well as abundant collagen type X was detected (Figure 16B). Furthermore, addition of BMP-2 to single layered hydrogels with NCs did not influence their cartilage forming capacity (Figure 16B). These findings hinted that TGFß3 unlike in in vitro [85] caused hypertrophic differentiation of NCs. In order to consolidate these results and to assess whether immobilized TGFß had an effect on the angiogenic properties of the implants, qPCR of early explants (after three weeks) was conducted. Gene expression analysis of the various collagens showed that ColI was indeed significantly higher expressed in the immobilized TGFß3 condition, by trend ColX was higher compared to the no growth factor and the BMP-2, but similarly expressed compared to the in vitro condition and ColII was not differentially expressed (Figure 16C). Chondromodulin - a potent anti-angiogenic molecule in cartilage [198] - was not differentially expressed in the no growth factor or BMP-2 versus the TGFß3 condition, but generally up-regulated in the in vivo conditions compared to the in vitro control group. In addition, there was no difference in vascular endothelial growth factor (VEGF) expression observed (Figure 16C) indicating that altered pro-/ anti-angiogenic properties did not account for the observed phenotype of NCs in presence of TGFß3. Taken together, the results demonstrated that TGFß3 is not needed, but rather detrimental for in vivo chondrogenesis by NCs.

3.1.4 Generation of an osteochondral construct by the combination of BMSCs with NCs in bi-layered PEG hydrogels

For the generation of an osteochondral construct directly in vivo we investigated the potential of bi-layered hydrogels containing BMSCs undergoing endochondral ossification with NCs undergoing spontaneous re-differentiation to form a bone-cartilage composite. Thus, a hydrogel disc with TGFß3 containing BMSCs was joined with a non-functionalized hydrogel disc containing NCs expressing green fluorescent protein (GFP) for tracking the respective layers upon implantation (Figure 18A). After four weeks, strong chondrogenic differentiation in the BMSC- and the NC-layer was observed and throughout the constructs ColI and X were expressed (Figure 18C).
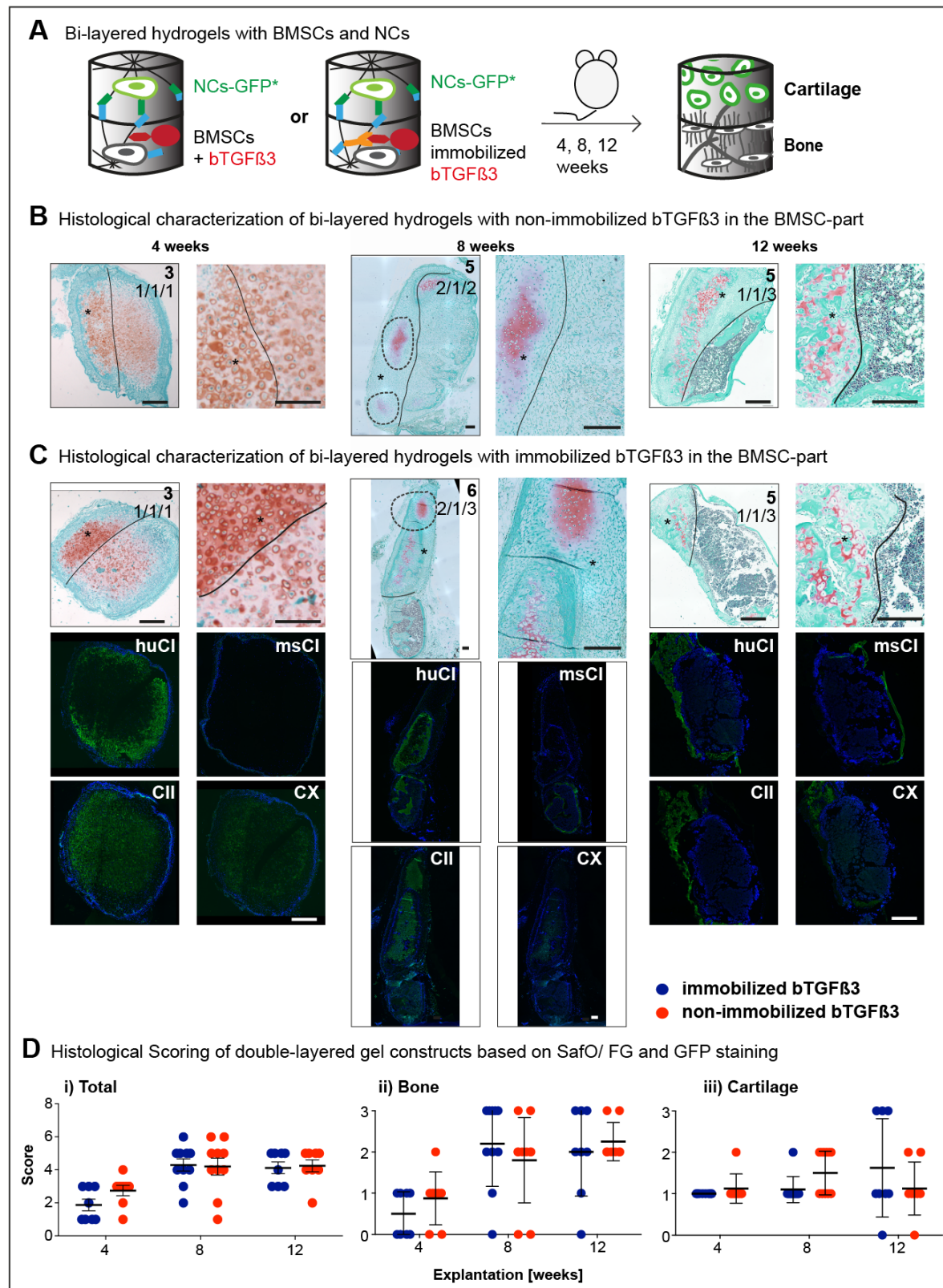
Figure 17: Combination of the TGFß3-functionalized hydrogel containing BMSCs with a non-functionalized hydrogel layer containing NCs resulted in the generation of bone tissue adjacent to cartilage with

hypertrophic traits. A) 20-25x 10^6/mL BMSCs were encapsulated in hydrogels containing immobilized bTGFß3, non-immobilized bTGFß3 and put on an additional layer containing 20-25x 10^6/mL NCs devoid of bTGFß3, and directly implanted subcutaneously in nude mice. **B-C)** Constructs were explanted after 4, 8 and 12 weeks, respectively and paraffin sections were analyzed by SafO/FG staining and IF for CoII (human and mouse specific), II, X (C). The number on the SafO/FG stained images indicates the given histological score. The line in the SafO/FG images marks the border between the BMSC- and the NC-part (*), based on IF against GFP. Dashed encircled areas were identified as stable cartilage. Scale bars: 200 µm. **D)** Constructs were scored based on SafO/FG and GFP staining. N=3, 2-4 replicates each time point and donor.

After eight to twelve weeks SafO positive hypertrophic cartilage was undergoing remodeling in the BMSC-part and in some constructs cortical bone developed and a major part was filled with a hematopoietic compartment (Figure 18B and C). Similar to the BMSC only constructs, the CoII of mature bone surrounding bone marrow was of mouse origin. In the NC part the developed cartilage acquired hypertrophic traits as observed by the increased abundance of dense FG and collagen type I positive tissue within the GAG rich area and presence of collagen type X (Figure 18C). A stable cartilage-like phenotype was rarely observed in certain areas of some constructs. It was observed in constructs, of which the two discs presumably had been displaced and the initial interface between the two cell types was diminished (Figure 18B and C).
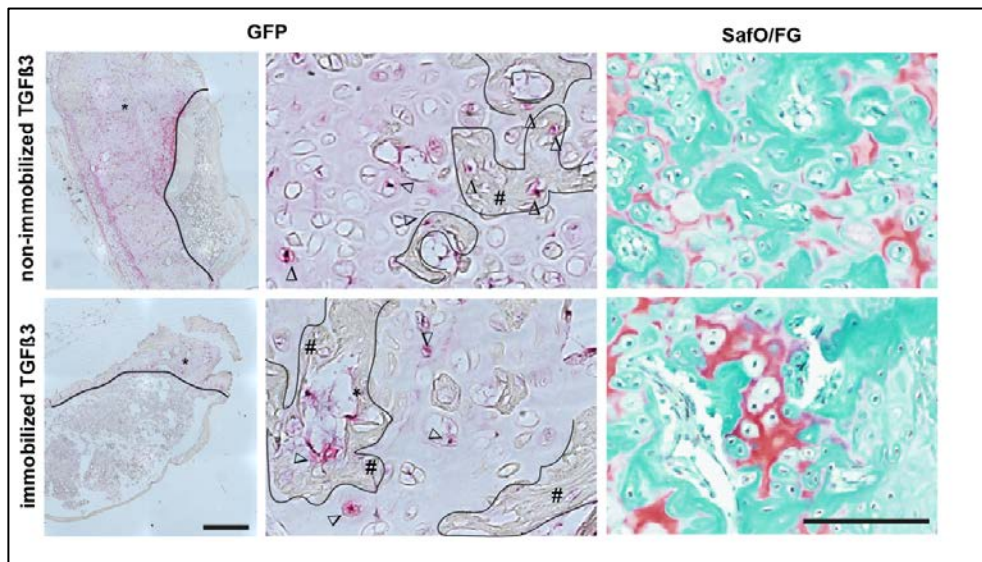
Figure 18: Precise localization of GFP positive NCs was difficult to observe. Immunohistochemistry (IHC) against GFP in 12 weeks explants shown in Figure 18B and C. Δ indicate GFP positive cells outside and inside, and # GFP-negative cells inside FG/CoII rich areas. Scale bars: 200 µm (low magnification), 50 µm (high magnification).

The GFP staining facilitated to clearly assign the NC and the BMSC derived hydrogel parts, however was not specific enough to indicate, whether there were NCs within the FG and human collagen type I rich pre-bone tissue present (Figure 19). With respect of confining an

endochondral phenotype to the BMSC layer no difference was observed whether TGFß3 was immobilized or not, thus the formation of biphasic tissue consisting of stable cartilage and bone was not improved by the immobilization of TGFß3 (Figure 18D i and iii). Immobilization of TGFß3 did not improve either the efficiency of bone tissue formation in the BMSC-part (Figure 18D ii). However, bone formation efficiency was generally lower in the bi-layered constructs than in the single-layered configuration. Namely, after eight and twelve weeks > 50 % of the constructs did not contain a bone layer that consisted of at least a small area of cortical bone and bone marrow (Figure 18D ii). Taken together, TGFß3 triggered endochondral ossification of BMSCs in bi-layered hydrogels, but to a lower efficiency than in single-layered hydrogels, while NCs formed cartilaginous tissue displaying some hypertrophic traits.
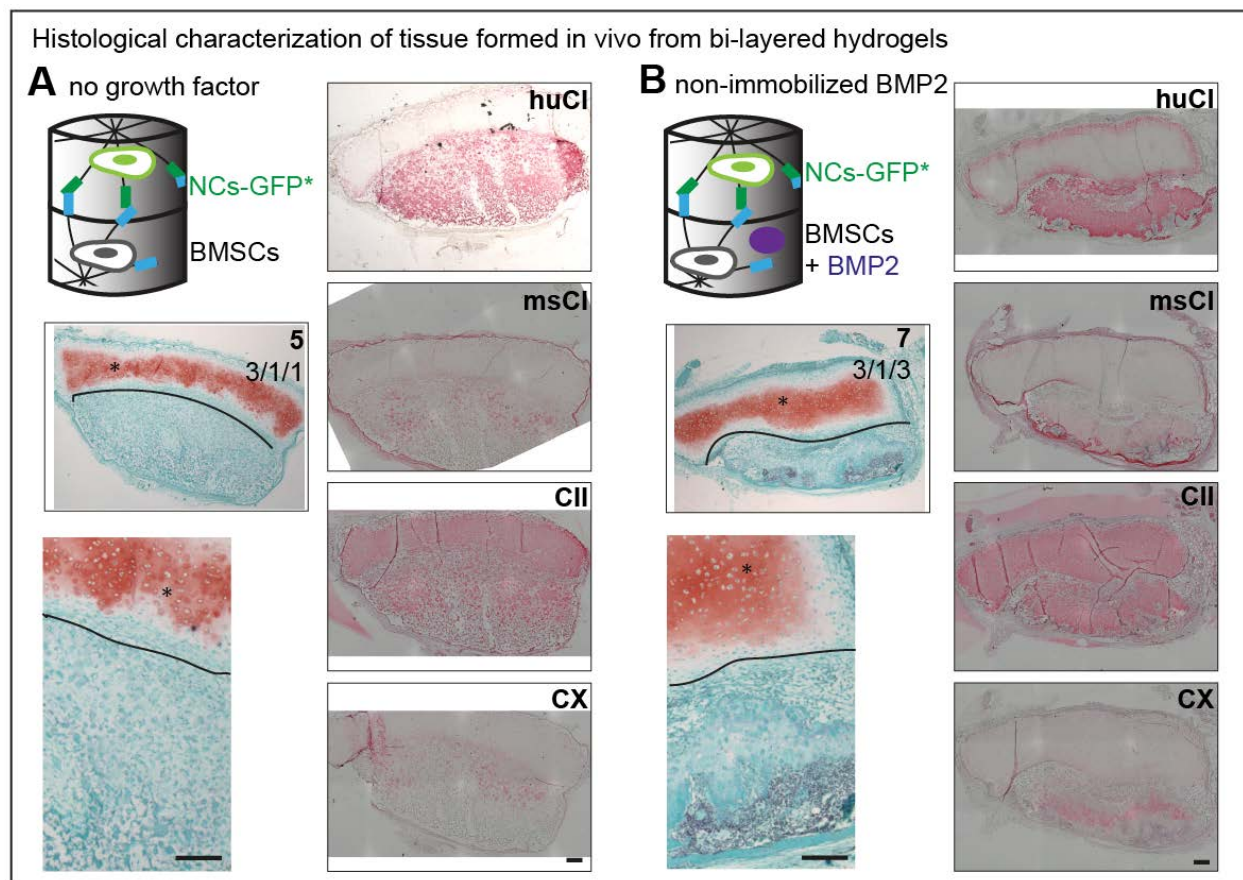
Figure 19: Without TGFß3 in the BMSC-layer, NCs formed hyaline cartilage. BMSCs were encapsulated in a non-functionalized PEG hydrogel (A), in a hydrogel containing non-immobilized BMP-2 at a concentration of 10µg/mL (B) and put on an additional layer containing NCs. **A-B)** hydrogels were implanted subcutaneously for eight weeks. Representative paraffin sections stained by SafO/FG and IHC for ColI (human and mouse specific), II and X are shown. The number on the SafO/FG stained images indicates the given histological score. Scale bars: 200 µm. N=1, 4 replicates.

In single-layered hydrogels containing immobilized bTGFß3 NCs acquired a hypertrophic phenotype (Figure 16B). Since in bi-layered hydrogels the TGFß was added not to the NC-, but to the BMSC-part it could also be that the proximity to the osteogenically differentiation BMSCs caused hypertrophic differentiation of the NCs in the bi-layered hydrogels. To differentiate this possibility from the TGFß3 as a cause of their hypertrophy, constructs either devoid of TGFß3 or containing BMP-2 as an alternative growth factor to induce endochondral ossification of BMSCs were fabricated (Figure 20A and B). Clearly, eight weeks after implantation in hydrogels without TGFß3 NCs formed cartilage absent of ColI and ColX (Figure 20A). Interestingly, in the BMSC-layer although only very limited amounts of GAG were detected, there was positivity for ColX and II, indicating that the proximity to the NCs may have induced differentiation of BMSCs also in absence of TGFß3 (Figure 20A). Hydrogels containing non-immobilized BMP-2 in the BMSC-layer developed into constructs with a clear biphasic configuration, in which NCs formed a SafO and ColII positive tissue without ColX, while the BMSCs underwent endochondral ossification as seen by the presence of a ColX rich matrix adjacent to bone marrow and cortical bone (Figure 20B). The stable NC-derived cartilage was not in direct contact with the bone, but it was separated from the bone by a big area of hypertrophic cartilage from the BMSC part and bone marrow. Furthermore, a BMSC derived fibrotic layer marked the interface (Figure 20B). Summarizing, these results suggested that the TGFß3 emanating from the BMSC-part induced hypertrophic differentiation of NCs, while BMP-2 allowed the development of stable hyaline cartilage adjacent to endochondral bone.

3.1.5 Discussion

The generation of cartilage bone composite tissues that is envisioned to repair osteochondral defects is challenged by the localized induction of cell differentiation as well as their proper integration [17]. To achieve this, many different approaches have been implemented such as separate in vitro pre-culture [183, 187], composite scaffold materials and architectures [188, 196] or differential growth factor functionalization [77, 194] utilizing no [77, 194], one [188, 196] or two types of cells [183, 187]. So far none of the strategies has proven to be superior to the other in terms of the generation of tissue composites resembling the native architecture. Here, we demonstrated that TGFß induced endochondral ossification by BMSCs occurred in a localized way and concomitantly with spontaneous re-differentiation of NCs in a bi-layered PEG based hydrogel. Unexpectedly, the cartilage formed by NCs acquired hypertrophic traits under the

influence of TGFß3 from the neighboring layer and replacement of TGFß3 with BMP-2 in the BMSC-part allowed the formation of stable cartilage by NCs.

Previous studies demonstrated that covalently immobilized or affinity bound TGFß elicited chondrogenesis of encapsulated BMSCs and/or articular chondrocytes in various scaffold systems in vitro [153, 163, 164] to a similar or better degree than the soluble control and also in vivo within three weeks [165]. Here, immobilization of TGFß3 in the PEG hydrogel induced very efficiently chondrogenesis and subsequent bone formation. Compared to non-immobilized TGFß3 the bone formation occurred with higher efficiency indicating that a longer exposure to TGFß3 may be beneficial. This is in contrast with a previous study, where addition of TGFß-loaded gelatin microspheres alone to BMSCs sheaths was not sufficient to induce bone formation orthotopically to any comparable extent as when additionally BMP-2 was added [182]. Thus, future studies involving elucidation of the time period and amount of TGFß required for the highest efficacy are warranted to improve scaffold mediated delivery modes, to optimally deploy TGFß and to reduce costs and side effects. Current approaches to generate bone tissue through endochondral ossification had relied on a lengthy in vitro pre-culture of two to six weeks to produce a chondrogenic template prior to implantation [114, 115, 173-177]. Our study demonstrated that by delivering a chondroinductive stimulus with the scaffold the in vitro pre-culture step can be circumvented. From a clinical point of view, optimization of the fabrication procedure including the shortening of the in vitro pre-differentiation step and designing effective scaffold systems facilitate faster and more efficient generation of grafts.

Mouse and human specific ColI staining revealed that the bone collar was composed solely of mouse collagen, while the tissue undergoing remodeling only contained human ColI indicating that the (secondary) bone may have been deposited through the vasculature recruited mouse osteoprogenitors and the ECM secreted by human cells may have served as a template. In native endochondral ossification hypertrophic chondrocytes can transdifferentiate to osteoblasts and together with directly differentiated osteoblasts from the perichondrium build up bone [46, 47]. Various previous studies using different scaffold systems and implantation sites reported differential origin of the newly formed bone [115, 174, 180, 182, 199]. Yet it remains to be clarified what is the relative impact of the construct size, the scaffold composition, the pre-culture step and the implantation site in determining the origin of the final bone derived by endochondral ossification. Consequently, in future studies only labeled cells should be utilized in order to

determine the temporal sequence of cellular contributions. While for clinical applications the origin of the cells does not play a major role as long as the bone formation occurs efficiently, however, for humanized bone organ models to study hematological malignancies with patient derived cells in vivo [200, 201] it is critical that the bone formed is of human origin. Thus, this system at the moment would not be suited as a humanized bone model and research is required to find out how to trigger the graft derived cells to generate bone. Furthermore, if indeed the recruited cells contribute more to the final bone, systemic or scaffold delivered administration of chemokines such as stromal derived factor 1 (SDF-1), platelet derived growth factor BB (PDGF BB) or insulin growth factor 1 (IGF-1) may foster stem cell mobilization [202] and could be of benefit for translation.

We observed lower efficiency of bone formation in bi-layered hydrogels (independent on the immobilization of TGFß3) compared to the single layered immobilized TGFß3 condition. It could be related to the decreased surface accessibility and consequently less efficient vascularization because one side of the hydrogel disc containing BMSCs was covered by the second disc containing NCs.

We showed that NCs under the influence of TGFß3 underwent hypertrophic differentiation, this means in case of bi-layered gels by the TGFß3 emanating from the neighboring layer. The main reason for TGFß3 immobilization was the refinement of its spatially specific delivery. Intriguingly, there was no difference in terms of abundance and distribution of stable and hypertrophic cartilage formed between the immobilized and non-immobilized TGFß3 condition suggesting that increased leakage of TGFß to the NC-part by the absence of immobilization could not account for the cartilage phenotype formed by NCs. Likewise, in in vitro culture assays with bi-layered hydrogels chondrogenesis by BMSCs was induced only in the layer with TGFß irrespective of its immobilization indicating no leakage to the TGFß devoid layer. Alternatively, the immobilization strategy might not have sufficed to confine TGFß3 only to the BMSC-part. Moreover, it could not be excluded that due to active remodeling of the BMSC-layer increased MMP activity also caused increased cleavage of the MMP sites in the hydrogel, which resulted in higher release of the streptavidin-TGFß complex diminishing the effect of immobilization.

It remains elusive why the NCs under the influence of TGFß3 in the hydrogel differentiated as hypertrophic chondrocytes. It has not been described yet that TGFß induces hypertrophic differentiation of (nasal) chondrocytes. In contrast to a previous study that showed that NCs despite of being hypertrophically primed after in vitro culture in hypertrophic medium reverted back to a stable cartilage phenotype upon subcutaneous implantation [203], expression of the anti-angiogenic factor chondromodulin that was attributed to be the reason for the phenotypic switch in the former study, was not decreased in the TGFß3 compared to the no growth factor and the BMP-2 condition. The histological pictures of the NCs under the influence of TGFß strongly reminded to those derived from osteoarthritic cartilage. However, it is known from murine osteoarthritic models that excessive TGFß along the cartilaginous-osseous junction rather induces osteophyte formation (bony islands within the cartilage evolved through endochondral ossification of periosteal cells) than having a direct effect on the hypertrophic like phenotype of osteoarthritic chondrocytes [204]. Furthermore, generally TGFß signaling is essential in the joints to maintain a stable hyaline cartilage phenotype and to protect articular chondrocytes from undergoing hypertrophy [204].

Previous studies using the subcutaneous model to generate fully differentiated bi-layered tissues have been hampered by either incomplete maturation of the osseous tissue and/or hypertrophic differentiation of the cartilaginous part due to suboptimal cell source selection, insufficient stimuli or insufficient in vivo maturation time [185-189]. By utilization of BMP-2 in the osseous layer hyaline cartilage developed next to endochondral bone and is herewith the first study to our knowledge convincingly showing newly generated bone next to newly formed cartilage in an ectopic environment. Unlike the natural cartilaginous-osseous junction, which consists of a relatively thin layer of calcified ColX positive cartilage [2, 205], we observed between the bone and the NC derived stable cartilage a large area of BMSC derived hypertrophic cartilage and to lesser extent also bone marrow.

It remains to be elucidated how the formation of an interface including calcified cartilage more closely resembling the native one can be achieved. Future investigations may i) include the optimization of the system such as adjusted growth factor delivery and/or fabrication of the hydrogel interface e.g. through differential physicochemical features of the hydrogel in the osseous phase at the interface to the cartilage [206] that could serve as foci for bone ECM deposition, ii) address whether interface formation can occur in a self-governed way driven by

the cross-talk between the adjacent cells with the commitment to form endochondral bone or stable cartilage, respectively, and the concomitant tissue development or iii) whether the mechanical parameter absent in the ectopic model will be required. To this end, also a study at an orthotopic site necessitates to be conducted.

3.2 Part II - Identification of a BMSC subpopulation with a superior chondrogenic differentiation capacity

3.2.1 Transcriptomic analysis of single-cell derived clones

In order to find marker molecules that could select for BMSC with higher chondrogenic capacity (CC) we isolated and expanded single cell derived clones (N=5 donors) and correlated their gene expression profile with their chondrogenic in vitro differentiation potential (Figure 8). The overall clonal efficiency was 23.2 ± 11.5 %. Clones were expanded for 28 ± 2 days, with a mean proliferation rate of 0.7 ± 0.1 doublings/day (Figure 21A, 22A). As expected, chondrogenic differentiation occurred to a different extent among the clones (Figure 21B-C and Figure 22B-C) and the percentage of clones with high chondrogenic capacity (CC), defined based on a Bern score ≥ 3.0, ranged from 13 to 50 %, depending on the donor. 14 clones generated from donor 1 (batch 1) and 20 clones from donors 2-4 (batch 2) were subjected to RNA sequencing.

Differential gene expression analysis (DGA) on all the 14 clones selected for donor 1 (batch 1) demonstrated that clones with high and low CC separated in two clusters, with 58 genes significantly differentially expressed (adjusted P. value <0.05) (Figure 21D). In order to reduce the confounding effect of the different proliferation rates, in an additional analysis only clones with a similar proliferation rate (0.67-0.70, 9 out of 14) were taken into account (Figure 21E), while outliers in terms of proliferation rate were discarded. Interestingly, the clustering became more prominent and the number of significantly differentially expressed genes rose to 1771 (Figure 21E). This demonstrated that clones with a closer proliferation rate shared more common gene expression patterns and that the different doubling times introduced more heterogeneity eventually masking the putative similarities among clones with equal CC. Amid the significant genes (fold up-regulation > 12 in clones with high CC), there were extracellular matrix proteins, which are important components of the cartilage ECM such as hyaluronan and proteoglycan link protein (HAPLN1), aggrecan (ACAN) and cartilage oligomeric matrix protein (COMP) (Figure 21F). Moreover, several surface markers (NCAM1/CD56, VACAM1/CD106, ALCAM/CD166, ITGA1/CD49a) were significantly higher and two were significantly lower expressed (ENG/CD105 and CSF1R/CD115) in the clones with high CC, with CD56 having the highest fold change (Figure 21F).

A Proliferation rate of clones

B Chondrogenic capacity

Clones included for DGA

Clones excluded from DGA

D Differential gene expression profile of batch 1

High CC   Low CC

C SafO/FG staining of clones subjected to RNAsequencing

E Differential gene expression profile of clones with similar proliferation rate of batch 1

Low CC   High CC

proliferation rate 0.7 0.67

F Heat map of selected significantly differentially expressed genes

c12 c19 c35 c49 c50   c16 c17 c28 c44

High CC   Low CC

NCAM1, ITGA1, VCAM1, ALCAM, CSF1R, ENG, ROR2* — Surface markers

HAPLN1, COMP, ACAN — Cartilage ECM proteins

EFEMP1, FGF2, GDF6, SNX19, NOV, SOX6, PTHLH, TGFB1 — Genes associated with chondrogenic differentiation

G Expression of NCAM1 by qPCR

NCAM1 versus GAPDH

H Signaling pathways with differentially expressed genes

predicted pathway activity:
- activated
- inhibited
- unpredictable
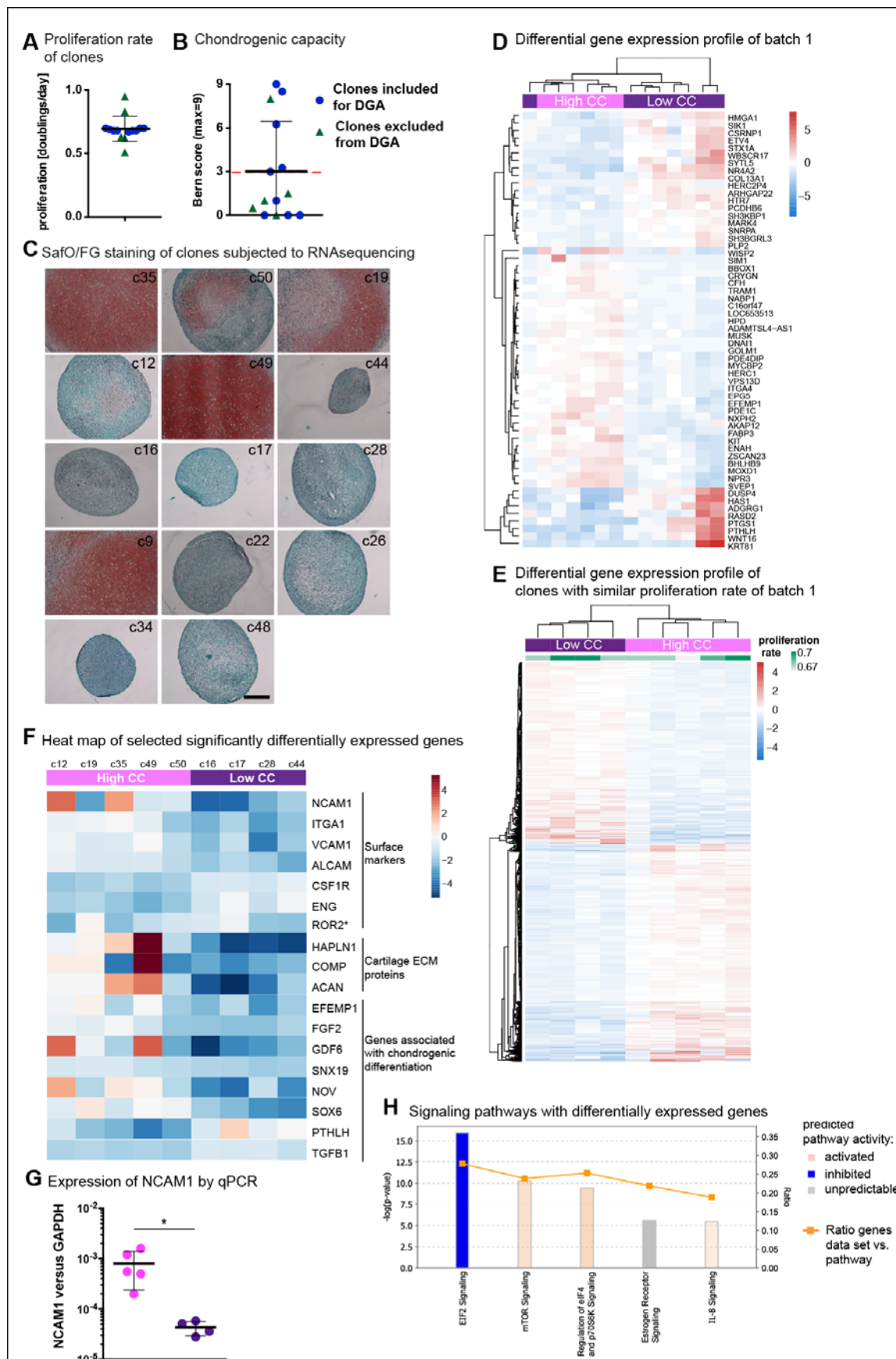
Ratio genes data set vs. pathway

71

Figure 20: Gene expression and chondrogenic capacity correlated and was more pronounced if proliferation outlier clones were excluded. A) Proliferation rate of single cell derived clones. **B-C)** Clones were cultured as pellets (1-2 replicates) in chondrogenic medium (ChM) for three weeks and assessed histologically. Bern score was used to evaluate the SafO/FG stained sections (B). Scale bar: 200 µm. Bern scores: c35: 8.5, c50: 3.25, c19: 6.25, c12: 3.0, c49: 9, c44: 0, c16: 0, c17: 0, c28: 0, c9: 8, c22: 1, c26: 0.5, c34: 0, c48: 1.5. Clones with a Bern score ≥ 3 (red dashed line) were assigned to have a high CC. **D)** Differential gene expression analysis (DGA) comparing clones with low and high CC. **E)** DGA of clones with a similar proliferation rate (c35-c28). **F)** Heatmap of surface markers (*ROR2 was not on the list from the DGA, but was identified by a previous study [207]), cartilage ECM proteins and genes associated with chondrogenic differentiation identified by ingenuity pathway analysis (IPA) that were among the significant genes of the subset analysis of batch 1. **G)** Gene expression of NCAM1 in clones analyzed by qPCR and normalized to GAPDH. Unpaired t-test, *P-value = 0.04. **H)** Differentially expressed genes involved in canonical signaling pathways as determined by IPA. Bar height indicates P-value as calculated by Fisher's exact test right-tailed that is indicative for the probability of association of the data set and the pathway.

The significant up-regulation of CD56 in clones with high CC was also confirmed by qPCR (Figure 21G). Ingenuity pathway analysis (IPA) showed that downstream targets of PDGFBB signaling were down-regulated, targets of TGFß signaling were down- and upregulated to equal degrees in clones of high CC, and that genes implicated in chondrogenesis were rather increased (Figure 21F). Among the pathways with the highest coverage of differentially expressed genes there were EIF2, estrogen, mTOR, eIF4, and IL8 signaling pathways, the first presumably being deactivated and the latter three activated in clones with high CC (Figure 21H).

Clones from three additional donors were combined and subjected to RNA sequencing (batch 2) (Figure 22) that was performed in order to validate the discovered genes in batch 1 to be related to the CC in a less donor dependent manner. Principle component analysis (PCA) showed that all clones grouped according to the donor origin, clones from the batch 2 were furthest apart from the clones of batch 1 (Figure 22D). Since the number of samples per donor was low, the differential gene expression analysis was done for all the clones irrespective of their proliferation rate. The big dissimilarity of the clones from different donors suggested that the donor-to-donor variability is bigger than the clone of high CC to low CC variability. This was confirmed by DGA, which yielded six significantly differentially expressed genes (Figure 22E). None of these six genes overlapped with the genes found in batch 1 (independent whether all clones or the subset with similar proliferation rate was taken into account). Plotting the counted reads of CD56 mRNAs, it was visible that there was a trend of higher expression in clones with high CC (Figure 22F). This trend was confirmed by qPCR analysis and again the variability was too high and therefore did not reach significance (Figure 22F). Furthermore, clonal populations were also

assessed by flow cytometry for CD56, the trend of a higher frequency of CD56$^+$ cells among the clones with higher CC was also here apparent, but not significant (Figure 22G). Taken together, NCAM1/CD56, VACAM1/CD106, ALCAM/CD166, ITGA1/CD49a were identified by RNA sequencing as putative markers for clones with high CC. However, donor-to-donor variability masked the confirmation of these surface markers to be significantly up-regulated in clones of high CC from various donors and masked the identification of further putative marker genes.
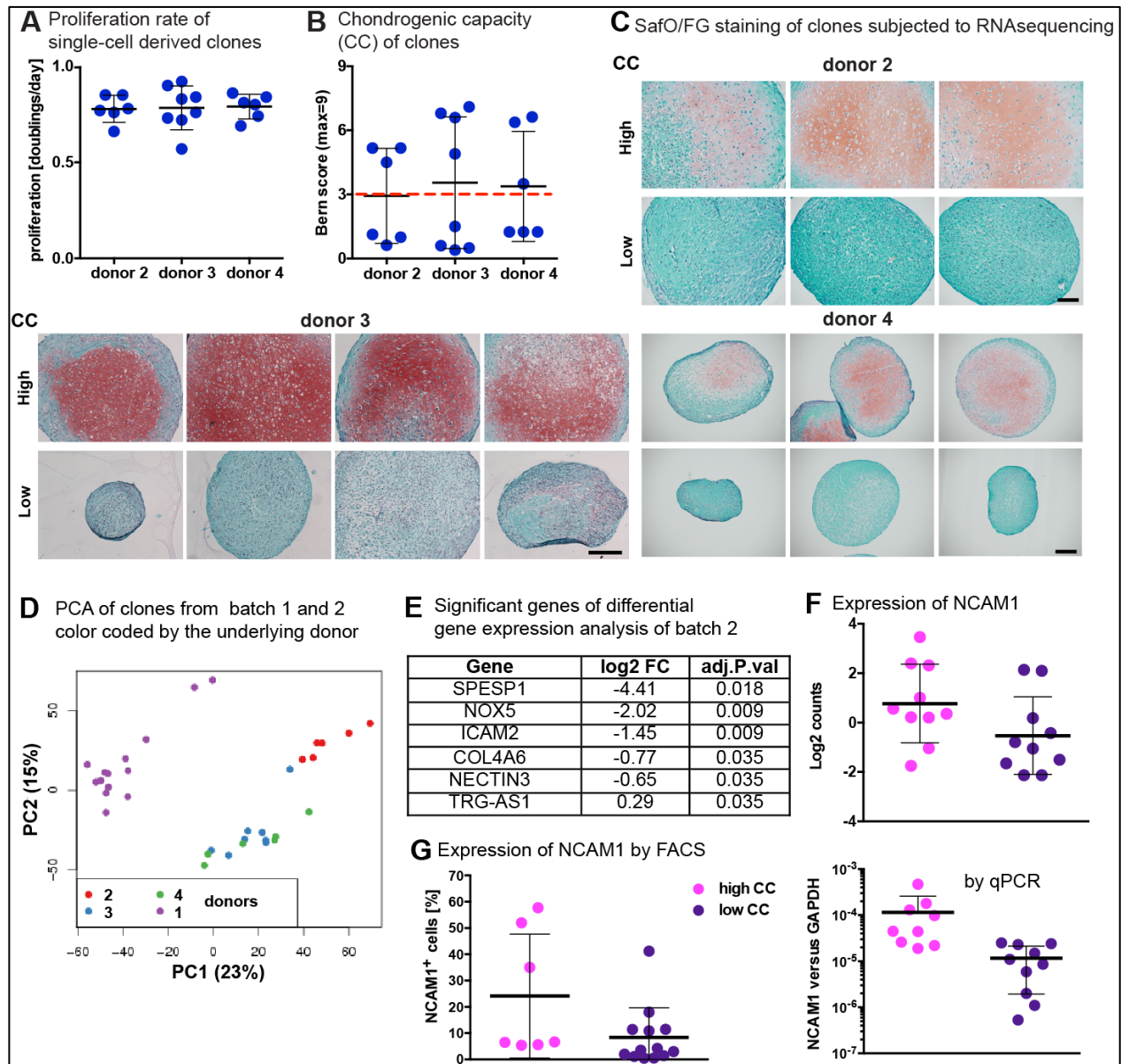

Gene	log2 FC	adj.P.val
SPESP1	-4.41	0.018
NOX5	-2.02	0.009
ICAM2	-1.45	0.009
COL4A6	-0.77	0.035
NECTIN3	-0.65	0.035
TRG-AS1	0.29	0.035

Figure 21: Transcriptomic analysis of clones from other three donors did not confirm the data of the first batch. A) Proliferation rate of clones. **B)** Bern score of clones after three weeks in culture in ChM. Clones with a Bern score ≥3 (red dashed line) were considered as clones with high CC. **C)** SafO/FG staining of paraffin sections. 1-2 replicates per clone. Scale bar: 200 µm. **D)** Principal component analysis (PCA) comparing clones of all tested

different donors (batch 1 and 2). **B)** Significantly differentially expressed genes of batch 2 (adjusted p value < 0.05). **C)** NCAM1 expression by counted reads from the RNA sequencing (upper graph) and by qPCR in batch 2 clones. **G)** Clonal populations of donor 2 and 3 were assessed by flow cytometry before subjection to the chondrogenic culture for the frequency of CD56^{+} cells.

3.2.2 Sorting of expanded multiclonal BMSCs based on CD56/NCAM1

Aiming at finding surface marker(s) that select for BMSCs with higher CC within the bulk, expanded multiclonal BMSCs (P1) were analyzed for the surface markers found to be up-regulated in clones with high CC in batch 1. CD49a, CD105 and CD166 were expressed in all of the cells, while on average 93.9 +/- 7.1 % of the cells were positive for CD106 (N=7 donors) and the frequency of CD56^{+} cells ranged between 1 and 35% with an average of 13 +/- 11% CD56^{+} cells (N=12 donors) (Figure 23). Previously it was reported that cultured unfractionated BMSCs (passage 2) were 100% positive for CD166, while for CD106 two populations remained [208] and the frequency of cells positive for CD56 in P2-P3 cells was determined between 24-89% [209]. Markers exhibiting high and stable expression profiles are unlikely to be unique markers of BMSCs with high chondrogenic potential. Instead markers with low expression, reflecting the low presence of chondrogenic clones in the total BMSCs population are more likely to be unique markers of chondrogenic BMSCs [210]. Therefore, we pursued CD56 for comparative studies of CC.
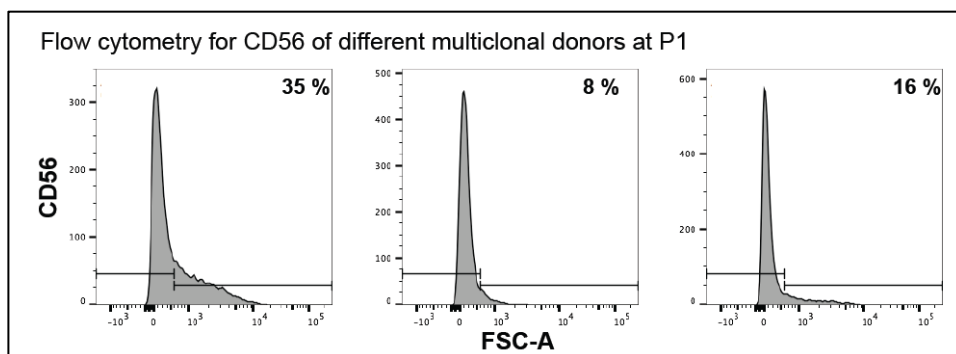

Figure 22: CD56^{+} cells as determined by flow cytometry in multiclonal populations at P1 were present to different extents among donors. Three donors representing the range of CD56^{+} cell frequencies are displayed (N=23).

CD56 or NCAM1 (neural cell adhesion molecule) originally discovered in neurons is a immunoglobulin-like domain containing transmembrane glycoprotein engaged in homophilic cell-cell contact and heterophilic cell-ECM adhesion and is expressed in adult organisms by various

tissue cells [211]. It is expressed on uncultured [208] and cultured adult human BMSCs [209] and in-situ CD56 was detected rather to be co-expressed on CD271^{+} bone-lining MSCs than at perivascular location [212]. Experiments in vivo and in vitro with chicken limb bud progenitor cells demonstrated that NCAM by mediating cell condensation at the onset of chondrogenic differentiation is important for the quality of the chondrogenesis [213, 214]. The functional implication of CD56 during chondrogenesis further motivated us to determine the chondrogenic potential of CD56^{+} cells.
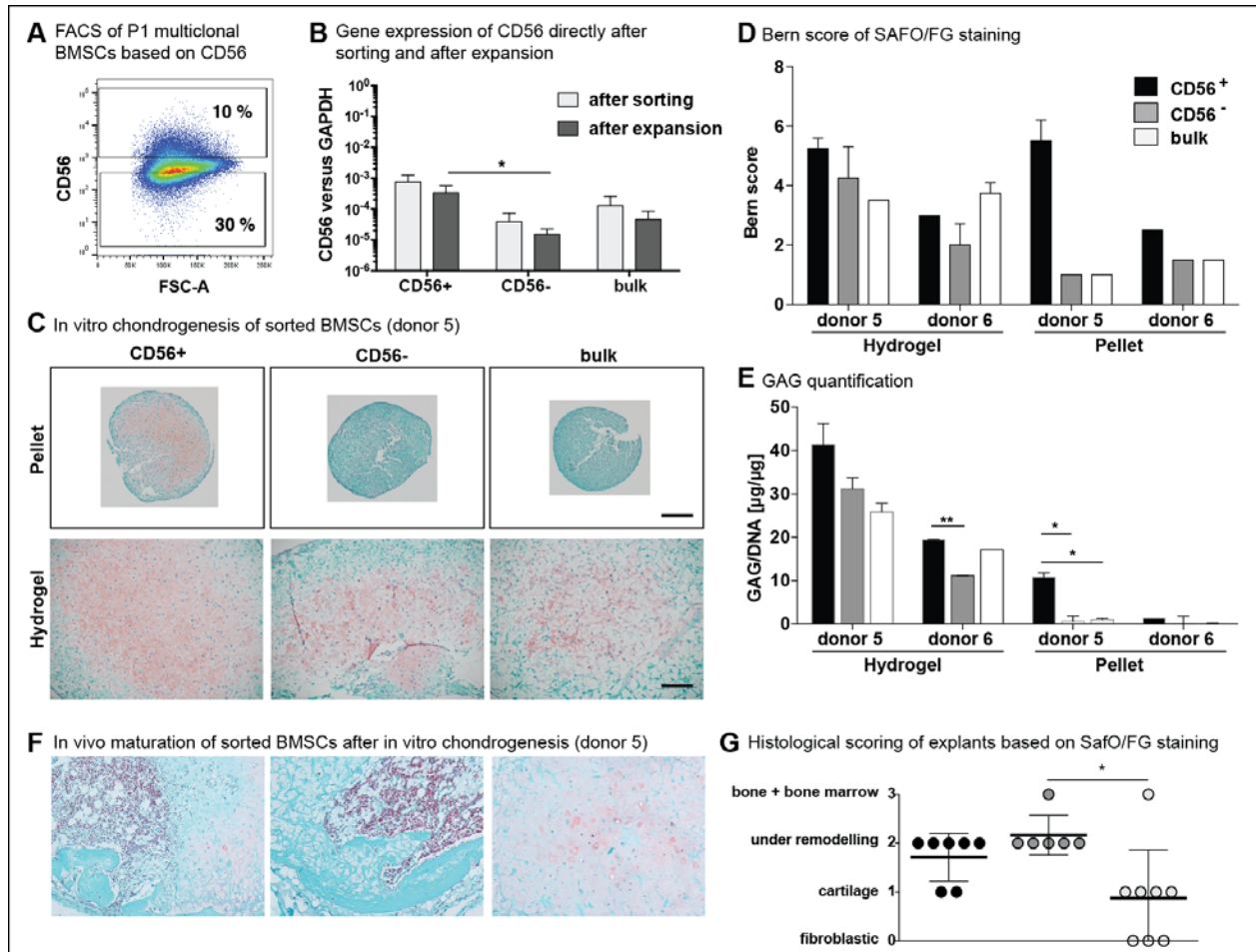

Figure 23: Enriching for CD56^{+} cells resulted in a trend of higher chondrogenesis. A) Representative FACS plot of CD56 stained P1 cells. The squares indicate the populations, which were sorted as CD56^{+} and CD56^{-}. **B)** Gene expression of CD56 normalized to GAPDH directly after sorting (N=3) and after expansion (N=5). Paired t-test, *P-value = 0.04 **C-E)** Sorted populations and as a control the unsorted ones were cultured for two weeks in ChM as pellets and in PEG hydrogels. N=2, 1-2 replicates each culture condition and cell subset. SafO/FG staining of paraffin sections of donor 5 are shown. Scale bar: 200 μm (C). Semi-quantification of SafO/FG stained sections by Bern score (D) and quantification of accumulated GAG/DNA represented for every donor and culture system separately. Paired t-test, **P value = 0.00017, *P value = < 0.05 (E). **F-G)** In vitro cultured hydrogels were subcutaneously implanted in

immunocompromised mice. SafO/FG staining, representative replicates of donor 5 are shown (F) and histological score (G). N=2, 2-4 replicates each cell subset. Scale bar: 200 μm. Paired t-test, **P value= 0.001.

To verify the potential of CD56 to select for BMSCs with high CC, P1 expanded BMSCs were sorted (Figure 24A) and CD56 positive and negative sub-populations were tested in chondrogenic cultures, using unsorted BMSCs as a control (Figure 24C-E). The gene expression levels of CD56 directly after sorting and after expansion were more than one order of magnitude higher in the CD56+ cells as compared to the negative ones and the unsorted cells showed an intermediate expression level (Figure 24B). This demonstrated that the sorted populations clearly differed in terms of CD56 mRNA amounts. Interestingly, the expression levels were slightly lower after expansion in all cell populations (Figure 24B). Two donors could be assessed in terms of chondrogenic potential in two separate experiments as pellet and PEG based hydrogel cultures. For both donors for all cell populations the chondrogenesis took place to a very limited extent as pellet cultures and at an intermediate to good level in the PEG hydrogels. There was a trend that chondrogenesis of CD56+ cells was better compared to the negative and the bulk (Figure 24C-E), however, as measured by GAG quantification it was significantly better only in case of donor 5 when cultured as pellets and in case of donor 6 when cultured in hydrogels, but there the difference was only visible between positively and negatively sorted populations (Figure 24E). These observations were also reflected in the histological analysis (Figure 24D). Because sole enrichment of a BMSC population with higher CC (without adaptation of the differentiation conditions) is very unlikely to decrease the inherent tendency of BMSCs to form (pre-)hypertrophic chondrocytes, we implanted the in vitro cultured hydrogels subcutaneously to assess their bone formation potential. After eight weeks, there was no difference between positively and negatively sorted cells (Figure 24F-G). Interestingly, the negative cells developed significantly more into mature ossicles than the bulk cells (Figure 24G).
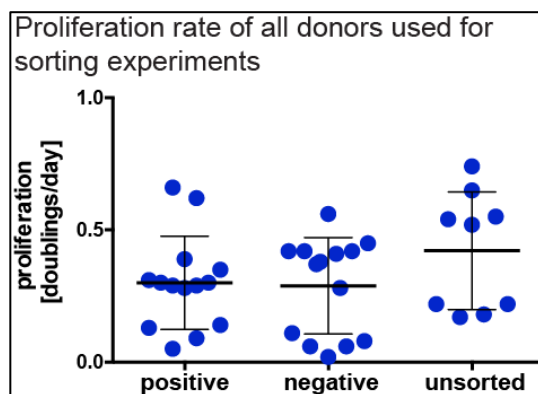

Figure 24: Relatively low proliferation rate of multiclonal BMSCs irrespective of sorting. The proliferation rate was calculated by using the plated cell number and the total number of cells counted at the end of the expansion phase. In general, cells were expanded on average for 8 days. N=15.

In summary, despite of the trend of better chondrogenesis by CD56$^+$ compared to the CD56$^-$ cells, due to the donor and also the intra-replicate variability it was not possible to draw a conclusion whether enrichment for CD56 could improve the BMSCs chondrogenic differentiation capacity. It would be mandatory to assess more technical replicates and more donors, however, a big problem encountered was that these donors did not proliferate sufficiently and it was often not possible to retrieve enough cells. With average proliferation rates of 0.30 +/- 0.18 for the positive, 0.29 +/- 0.18 for the negative and 0.42 +/- 0.22 doublings/day for the unsorted populations, respectively, they proliferated 2-3 times lower than usually observed with BMSCs at P0-3. Comparing to the proliferation rate of unsorted cells the FACS process did not seem to be the cause for the slow proliferation, even though the sorted cells proliferated a bit less (Figure 25).

In order to better characterize the heterogeneity within the CD56 sorted cell populations, single cells from P1-expanded BMSCs sorted based on CD56 were collected and expanded (Figure 26A). 10.4 % of the CD56$^+$ and 5.9 % of the CD56$^-$ derived clones with appreciable proliferation rates were retrieved. Clones were expanded for on average 24.15 ± 2.66 and 22.93 ± 3.63 days and showed a mean proliferation rate of 0.81 ± 0.11 and 0.86 ± 0.14 doublings/day, respectively (Figure 26B). The gene expression of CD56 at the end of the expansion phase was inconsistent with the clone origin - derivation from CD56$^+$ or CD56$^-$ sorted single cell – and it did not correlate with the CC of the underlying clone (Figure 26C). After expansion clones were subjected to in vitro tri-lineage differentiation assays. Regarding chondrogenic potential, 1 clone out of 11 and 4 clones out of 22 showed high CC within the CD56$^-$ and CD56$^+$derived clones, respectively, not resulting in a significant difference between the two subpopulation derived clones (Figure 26D). The CD56$^+$ clones were marginally osteogenic and adipogenic, while with the exception of one clone all CD56$^-$ clones were osteogenic (Figure 26E) and the majority underwent adipogenesis (Figure 26F), as measured by alizarin red staining for calcification and oil red staining for the accumulation of fat droplets, respectively. In conclusion, the big discrepancy in osteogenic and adipogenic differentiation potential suggested that the CD56$^+$ and CD56$^-$ are indeed two distinct cell populations.

A FACS based on CD56 of P1-BMSCs for the isolation of single cells

B Proliferation rate of clones

C CD56 gene expression of clones after expansion

D Chondrogenic differentiation

E Adipogenic differentiation
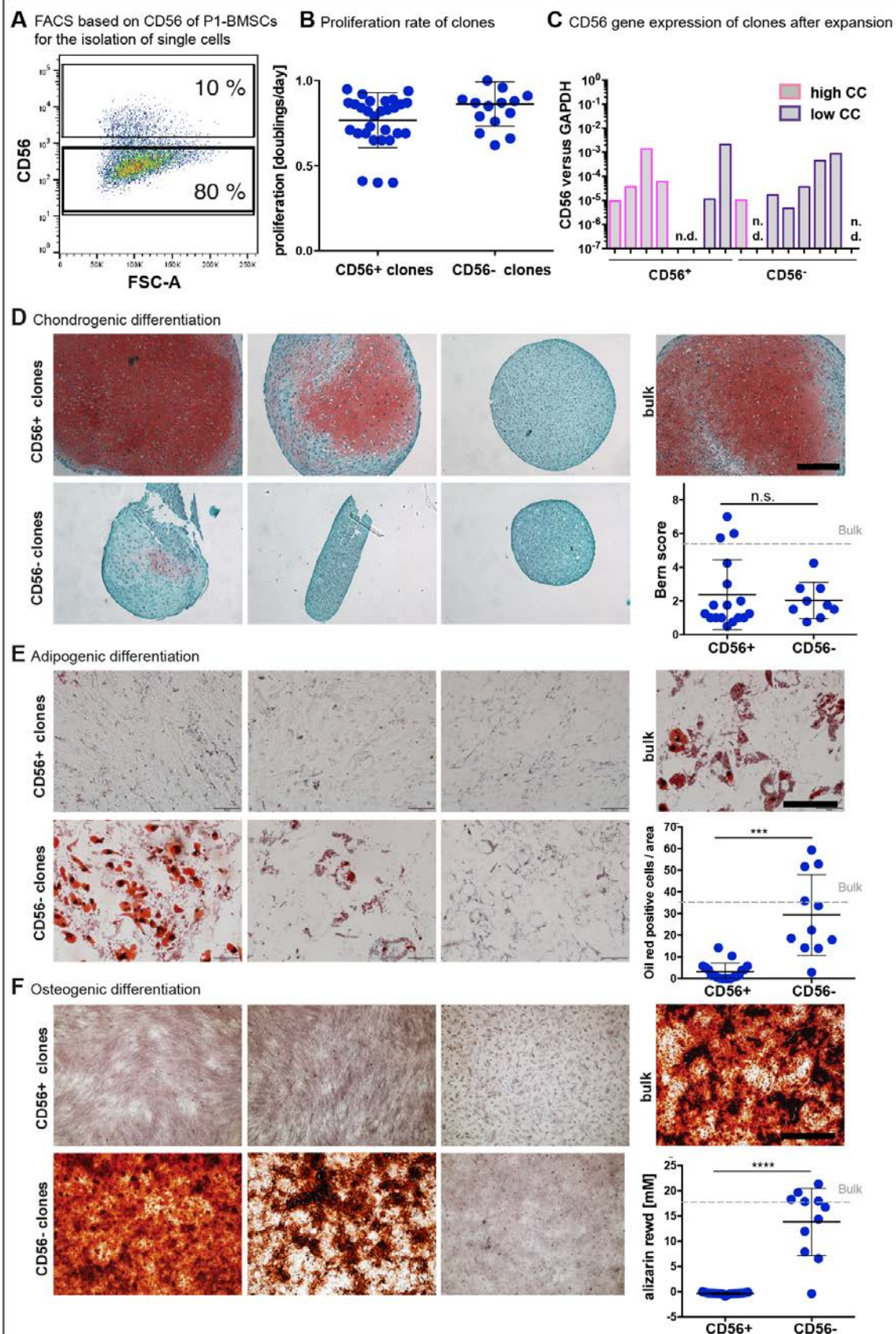
F Osteogenic differentiation

Figure 25: CD56⁺ and CD56⁻ single cell derived clones differed clearly in terms of adipogenic and osteogenic, but not chondrogenic differentiation potential. A) P1-expanded BMSCs were single cell sorted based on CD56 protein expression. **B)** Proliferation rate of CD56 positive and negative clones. **C)** Gene expression by qPCR of CD56 normalized to GAPDH after expansion. **D)** Clones were cultured for three weeks in ChM. SafO/FG staining of paraffin sections are shown and the CC was evaluated by using the Bern score. **E)** Adipogenic differentiation for three weeks. Staining for oil red and quantification by counting the cells clearly containing lipid droplets. **F)** Osteogenic differentiation for three weeks. Staining for alizarin red and colorimetric quantification thereof. Unpaired t-test, P value = ***0.0009, ****<0.0001. The gray line corresponds to the average value measured by P3 unsorted cells. Because often there was no single clone representative for all clones within one population, the best, intermediate and worst clone are presented from left to right. Scale bars: 200 µm.

3.2.3 Discussion

BMSCs are considered as promising therapeutic candidate for cell-based articular cartilage repair and regeneration strategies. However, their application in the routine clinical practice is hampered by their large inter- and intra-donor variability in terms of proliferative and (chondrogenic) differentiation potential [116, 210]. In this study, we explored the existence of predictive markers identifying BMSCs subsets with high chondrogenic capacity (CC), starting from analyzing the molecular signature of clones with differential CC derived from single BMSCs. Transcriptomic data from one donor gave a clear cut difference between clones with high and low CC and hinted NCAM/CD56 as a marker to prospectively isolate a subpopulation of BMSCs with superior chondrogenic potential. BMSCs' donor-to-donor variability still remained the main obstacle impeding the possibility to draw final conclusions on the applicability of exploiting transcriptomic data from a very small number of donors and of the translational potential of CD56 as a selection marker.

Aiming to overcome the heterogeneity of bulk BMSCs isolated from bone marrow aspirates we investigated whether gene expression correlates with the CC of individual single BMSC-derived clones. Differential gene expression analysis resulted in the segregation of clones with high and low CC indicating a correlation between the gene expression profile and the CC of the underlying clone. Surprisingly, the segregation of the two groups was even more prominent when clones with a different proliferation rate than the average (proliferation outliers) were excluded from the analysis. These results suggested that differences in proliferation of individual clones might have introduced randomization of the gene expression profile according to

chondrogenic capacity. Additional clones from three different donors were subjected to RNA sequencing (batch 2) in order to assess, whether the results obtained by the transcriptomic analysis of batch 1 are donor-independent. The segregation of clones with high and low CC was poor and the results from batch 2 could not corroborate the findings from the first one. Of note, in batch 2 it was not possible to exclude proliferation outliers due to the low number of clones available from each donor. Overall, our analysis suggested that donor-to-donor variability exceeded the gene expression difference based on CC, masking the putative similarities among clones with similar chondrogenic potential. It could not be excluded that variable culture conditions such as the duration of expansion or different cellular confluence states at the time of harvest introduced additional variance. The difficulty in extrapolating predictive markers from differential gene expression analysis between single BMSC- derived clones was reported previously with a bovine bone marrow donor [199]. Our results highlighted the requirement for a more comprehensive analysis, considering a significant higher number of donors and clones per donor, what stands in contrast to the study of Dickinson et al [207].

Interestingly, when excluding the proliferation rate as a confounding effect in the analysis of batch 1, three cartilage ECM proteins (HAPLN1, COMP and ACAN), and most importantly several surface markers were found to be significantly up-regulated in clones with high CC. Among them, NCAM1/CD56 was the surface marker with the highest fold change difference between clones with high and low CC. Moreover, CD56+ cells were present at varying low to intermediate frequencies in different donors of heterogeneous BMSC populations. Together with N-cadherin, CD56 has previously been demonstrated to be an important mediator for cell-cell adhesion during pre-chondrogenic condensation of chondroprogenitors in limb bud development [213-215]. Because the initial condensation phase is also critical for triggering in vitro chondrogenesis of adult BMSCs [216-218], enrichment of cells with high CD56 expression might be beneficial. CD56+ sorted cells from expanded multiclonal BMSCs did not exhibit unequivocally a higher chondrogenic potential compared to the bulk or the CD56- cells, although a trend along this line was visible. The non-significance was attributed mainly to the low tested donor number and technical replicates due to low proliferation rates of the (sorted) cells.

To further investigate the heterogeneity within the CD56 sorted cell populations, single CD56+/- cell-derived clones were compared in tri-lineage differentiation assays. A clear distinction between the two subpopulations was evident in terms of osteogenic and adipogenic

differentiation capacity (good in CD56- clones and absent in CD56+ ones), while the difference in chondrogenesis was less conclusive. Previously, Battula et al. sorted CD56+ MSCs from CD45 depleted human bone marrow in combination with MSCA-1 and CD271. Interestingly, the authors observed higher CFU-Fs and better chondrogenic in vitro differentiation compared to the CD271+MSCA-1+CD56- cells and better adipogenic differentiation of CD56- cells at multiclonal and clonal level [102]. Since our results overlapped with this precedent study, although different sorting times were applied (post- versus pre-expansion), it may indicate that CD56 expression identifies a certain cell subpopulation not only in naïve BMSCs, but also in expanded cells, what would underline the relevance of CD56+ as a prospective marker. Moreover, the non-significant difference of in vitro chondrogenesis between the CD56+ and CD56- cell subsets does not exclude a potential more significant difference at an in vivo orthotopic site [207]. A very recent report identified ROR2 (a Wnt receptor) as a putative marker for cells with increased CC by transcriptomic comparison of clones with differing CC from one human bone marrow donor. The expression of ROR2 in cultured BMSCs was induced by high cell density expansion to varying degrees. The positively sorted cells showed increased chondrogenic potential in vitro and in a sheep full thickness cartilage defect; the differences being more pronounced in vivo than in vitro [207]. In our transcriptomic data ROR2 was detected at low levels and was not differentially expressed in clones with high and low CC, conversely CD56 was not part of the data set of Dickinson et al. [207]. The cell density at the time of the RNA harvest could account for the discrepancy between our and their results. Nevertheless, it would be interesting to elucidate the relationship of CD56+ and ROR2+ cells after expansion.

From a translational point of view, the most important criteria for the applicability of a selection strategy is the cell yield that can be achieved with it. The decision to analyze and sort expanded and not freshly isolated or minimally expanded cells could have been a caveat of this study. Surface marker expression is known to be affected by in vitro culture conditions and most probably does not correspond any more to that of certain naïve subpopulations [90, 208, 219]. Therefore, analysis of cell-subpopulations cultured for a minimal time just to retrieve enough material for bulk RNA analysis and comparing them to the in vitro and in vivo differentiation potential of their counterparts expanded for longer times, eventually combined with index sorting to generate single cell derived clones instead of simple manual seeding, as well as single cell RNA sequencing could be more successful in finding the markers for a true chondroprogenitor population within human bone marrow and could uncover if at all it is existing.

4 Conclusions

By exploiting the cell intrinsic propensities of bone marrow derived mesenchymal stromal cells and nasal chondrocytes, in combination with the cell-degradable PEG based hydrogel system this study demonstrated that without the need of a prolonged in vitro-pre-differentiation step a cartilage-bone composite could be generated at an ectopic site. The PEG hydrogel provided for both tissues an ideal environment to evolve and allowed for localized growth factor functionalization. Specifically, delivering TGFß3 in an immobilized fashion in the PEG hydrogel induced formation of faithful bone organoids by BMSCs directly in vivo. In bi-layered gels, we observed that the TGFß3 emanating from the BMSC-layer triggered NCs to acquire hypertrophic traits. Utilization of BMP-2 instead of TGFß3 allowed the formation of stable cartilage next to endochondral bone demonstrating unequivocally the ability of the here-used system for the generation of osteochondral composites. A future study in an orthotopic animal model will be needed to unearth the potential clinical relevance of these bi-layered hydrogels containing BMSCs and NCs in the context of osteochondral repair.

Given that single cell derived clones generated from one bone marrow donor show differential chondrogenic differentiation capacity highlighting the cell heterogeneity within cultured BMSCs, our study compared the transcriptional profile of clones with high and low chondrogenic capacity in order to find selective markers for prospective isolation of a cell subset with superior chondrogenic potential within the bulk BMSCs. Differential gene expression analysis resulted in a segregation of clones with differential chondrogenic capacity and proposed NCAM1/CD56 to be such a selective marker. By trend, from multiclonal BMSCs sorted CD56$^+$ cells displayed a higher chondrogenesis than the CD56$^-$ cells, however, analysis of more donors are needed in order to confirm these data. Further RNA sequencing of clones from other donors resulted in a very poor clustering indicating the importance to analyze a very high number of donors and clones for reliable marker identification. Moreover, to exclude confounding effects of extensive expansion and varying culture conditions it would be important to analyze the transcriptome and prospectively sort BMSCs at a very early time point, while performing functional assays on their expanded progeny.

5 Materials and methods

If not otherwise stated all reagents were purchased from Sigma. Cell culture media and supplements are from Gibco.

Cell isolation and expansion

Bone marrow aspirates and cartilage tissue biopsies were obtained from patients after informed consent during surgical procedures in accordance with the local ethical committee (University Hospital Basel; Prof. Dr. Kummer; approval date 26/03/2007 Ref Number 78/07). Human mesenchymal stromal cells were isolated from bone marrow aspirates (n=23; mean age: 33.7 ± 10 years, part I and n=11; mean age: 40 ± 13 years, 8:3 male: female for part II) by plating 0.1-0.13x10^6 of nucleated cells/cm^2 in alpha-MEM with 10 % FBS, 100 mM HEPES buffer, 1mM sodium pyruvate, 100 IU/mL penicillin, 100 µg/mL streptomycin and 0.29 mg/mL glutamate, supplemented with 5 ng/mL FGF2 (BioTechne) (complete medium, CM) and expanded in the same medium for one to two passages more before using them for chondrogenic and endochondral assays or expanding them for one passage more for sorting experiments.

Nasal chondrocytes were isolated from minced nasal cartilage septum biopsies, taken from three donors (female, 26; male, 52; male, 41) by digestion in 0.15 % type II collagenase (Worthington) for 22 hours at 37˚C. NCs were expanded in DMEM, 4.5 g/L glucose, with 10 % FBS, 100 mM HEPES buffer, 1mM sodium pyruvate, 100 IU/mL penicillin, 100 µg/mL streptomycin and 0.29 mg/mL glutamate, supplemented with 1 ng/mL TGFß1 (BioTechne) and 5 ng/mL FGF2 (BioTechne).

Generation of single-cell derived clones

1x10^4 nucleated cells from five fresh bone marrow aspirates (23 years, male; 38 years, male; 49 years, female; 30 years, female; 38 years, male) were seeded in 96 well plates. It is expected that the frequency of clonogenic cells is approximately 1/10^4. After one week the wells were checked for colony growth, wells without cells and wells where it seemed that two or more cells gave rise to a colony were discarded. Clones were expanded in CM and when a high enough cell number was reached (minimum 0.8x10^6 cells) they were subjected to RNA isolation for transcriptomic analysis, chondrogenic assays and flow cytometry in case of donor 2 and 3. If a clone stopped growing or showed morphological signs of senescence, it was discarded.

For the clonal study of CD56$^+$ and CD56$^-$ one P1-expanded donor (age: 33 years, male) was sorted based on CD56 expression and single cells were put into 6x 96 well plates and processed as described above. The CD56$^+$ cells gave rise to so many clones that after 20 days the clones, which were not confluent that time, were discarded. After expansion the clones were tested in tri-lineage in vitro differentiation assays.

Lentiviral transduction for GFP

Lentivirus with GFP was produced as described in Miot et al. [220] by co-transfection of 12 µg of pWPXL-EGFP, 12 µg of pCMVΔR8.91 and 5 µg of pMD.2G in 2.5x 10^6 293T cells using Fugene 6 (Roche) in DMEM, 10 % FBS, 100 U/mL penicillin and 100 µg/mL streptomycin (CMT). After two and three days the supernatant was collected and filtered through 0.45 µm pore size filters. For transduction of NCs, passage 2 cells were seeded at a density of 5100 cells/cm^2 24 hours prior to virus addition. Transduction was facilitated with 2µg/mL polybren. 3 days after transduction the cells were analysed by flow cytometry (with accuri, BD) for expression of GFP and the percentage of transduced cells was determined in FlowJow.

Retroviral transduction of BMSCs with sFLK-1

For the generation of the retroviral vector containing mouse extracellular domain of VEGFR2 (sFLK-1) fused to a IgG2 derived FC domain and linked through an internal ribosomal entry site to a truncated version of mouse CD8a, phoenix cells (kept in CM at 32°C) were transfected with the respective plasmids using Fugene 6 (Roche). The supernatant was harvested two times on day two, day three and four, and filtered through a 0.45 µm pore size filter. One fresh bone marrow aspirate (50, female) was cultured for 6 days at an initial density of 10^5 nucleated cells before transduction. The BMSCs were transduced with the filtered supernatant six times during three days with polybrene. The transduction efficiency was determined by flow cytometric analysis for mouse CD8 and secretion of sFLK was determined by culturing BMSCs in 60-mm dishes for 4 hours in 1 mL CM. After filtration through 0.45 µm pore size filters sFLK in supernatants was quantified with the ELISA DuoSet$^®$ immunoassay kit (R&D systems) according to the user's manual. sFLK transduced cells and the corresponding non transduced control cells were subjected to chondrogenic in vitro and in vivo assays at passage 3.

Chondrogenic differentiation

For chondrogenic pellet cultures, 0.25 M cells were centrifuged for 5 minutes at 1000 rpm in 0.25 mL serum-free medium consisting of DMEM, 4.5 g/mL glucose with 100 mM HEPES buffer, 1mM sodium pyruvate, 100 IU/mL penicillin, 100 µg/mL streptomycin and 0.29 mg/mL glutamate, 1.25 µg/mL human serum albumin (HSA), insulin-transferrin-selen (Gibco), linoleic acid, supplemented with 0.1 mM ascorbic acid 2-phosphate, 10^{-7} dexamethasone and 10 ng /mL TGFß3 (Novartis) (ChM). Pellets were cultured for two weeks if not otherwise stated and the medium was changed twice a week.

Adipogenic differentiation

$4x10^4$ of cells were seeded into 12 well plates (1-3 replicates depending on the available cell number) and cultured for 2 weeks in adipogenic differentiation medium containing CM based on DMEM, 4.5g/L glucose supplemented with 10 ug/mL methyl-iso buthyl xanthine, 10 ug/mL insulin Actrapid HM, 0.1 mM indomethacin and 10^{-4} M dexamethasone and for one week in CM containing insulin. After the culture the cells were fixed for 10 min in formalin and stained with oil red. For semi-quantitative analysis, three pictures per well were taken with a 20x objective and cells clearly showing oil droplet accumulation were counted.

Osteogenic differentiation

$4x10^4$ of cells were seeded into 12 well plates (1-3 replicates depending on the available cell number) and cultured for 3 weeks in osteogenic differentiation medium containing CM based on alpha-MEM supplemented with 0.1 mM ascorbic acids, beta-glycero-phosphate and 10^{-6} dexamethasone. Afterwards the cells were fixed for 10 min in formalin and stained with alizarin red. For quantitation purposes, after image acquisition the alizarin red was solubilized by incubation in 10 % acetic acid at room temperature and at 85 °C, and the with 10 % ammonium hydroxide neutralized supernatants were optically measured at a wavelength of 405.

Fabrication of PEG hydrogels

PEG hydrogels were generated as previously described [146, 221]. Briefly, an equimolar ratio of 8-armed PEG equipped with peptides that allow for cross-linkage by transglutaminase factor XIII and cell mediated degradation (PEG-MMP$_{sensitive}$-Lys and PEG-Gln) at a concentration for 1.5%

w/v hydrogels was polymerized by addition of 10 U/mL of factor XIII in 50 mM Tris buffer, pH7.6 in presence of 50 mM $CaCl_2$, and 25 µM RGD-Lys, 1 ng/µL bTGFß3, 10 ng/µL BMP-2 and/or 100 µM streptavidin-Gln as specified in the text. 0.2-0.25x10^6 cells/1mL were encapsulated if not otherwise stated. Single-layered hydrogel discs of 10 or 20 µL were formed sandwiched between hydrophobically coated (SigmaCote) glass slides with 1 mm spacers for 30 min at 37°C. The metallic head was used for locally inhibiting the polymerization of the hydrogel using electrochemical methods [222], resulting in a thin layer of non-polymerised hydrogel in the vicinity of the metallic head, insuring the easy and reproducible detachment of the head. The so-produced first hydrogel disc was then put on top of a 15-µL drop of hydrogel mix forming the second layer. Polymerization and disc combination was allowed for 20 minutes at 37°C in the sandwich of two hydrophobically coated glass slides with a spacer of 2.8 mm. Hydrogels were cultured in ChM containing TGFß3 and in case of TGFß functionalization in ChM without TGFß supplementation for two weeks with a medium change twice - trice a week, or kept in serum-free medium without supplements until implanted subcutaneously (< 4 hours). For the formation of biphasic hydrogels side-by side, the first hydrogel disc (25 µL) was polymerized for 5- 10 minutes in one half of a PDMS mold of 8 x 2 mm in dimension placed on the hydrophobic glass slide and the other part (25 µL) was added in the second half and gelation was completed for 20 minutes at 37°C. Hydrogels were either cultured in ChM for 2 weeks with a medium change 2-3 times/weeks, or kept in serum-free medium without supplements until implanted subcutaneously (< 4 hours). When bTGFß3 was added to the hydrogel TGFß3 was omitted in the medium.

Biotinylation of TGFß3:

Dimeric TGFß3 (Novartis) was biotinylated in 6 M urea, 20 mM HEPES buffer at pH 7 or 8, respectively, on ice for 60 minutes using EZ- Link NHS-PEG$_4$-biotin reagent (Thermo Scientific) at a 10 or 20 fold molar excess over the protein dimer concentration as stated in the text. The reaction was stopped by addition of 1 M Tris buffer, pH 7.6 to a final concentration of 20 mM. For removal of unreacted biotin reagent the TGFß3 was dialyzed in ZelluTrans, 3500 MWCO (ROTH) into fresh urea buffer for 24 hours at 4°C. The degree of biotinylation was checked by time of flight mass spectrometry performed by the functional genomic center Zürich.

Acellular release assay and ELISA quantification of TGFß3

20 µL hydrogels were formed in absence or presence of 100 µM streptavidin-Gln and with 20 ng of bTGFß3 in eppendorf tubes, after 30 minutes covered with 500 µL serum-free medium and incubated at 37˚C for 7 days. At indicated time points the medium was replaced with fresh one. The amount of released bTGFß3 was measured by ELISA (DuoSet, human TGFß3, R&D systems) following the manufacturer's protocol and normalized to the control medium, to which 20 ng of bTGFß3 was directly added.

Acellular capture and relase assay with sFLK-1 and bevacizumab

Recombinant sFLK-1-FC (R&D systems) or bevacizumab (avastin) (Roche) was labeled with DyLight 550 antibody labeling kit (Thermo Scientific) following the instructions of the manufacturer. For capture, 20 µL hydrogels were formed in presence and absence of ZZ-Lys directly in eppendorf tubes, after 30 minutes 500 µL SFM (devoid of phenol red) containing 500 ng/mL labeled sFLK-FC and 50 µL of supernatant was withdrawn and substituted with fresh medium for one week at the indicated time points. As a control, medium was added to tubes without hydrogels. For release, 20 µL of hydrogels with and without ZZ-peptide and 100 ng labeled sFLK-FC or bevacizumab, respectively was directly polymerized in eppendorf tubes and after 30 minutes 500 µL of SFM was added and incubated for one week at 37˚C. The medium was replaced completely at the indicated time points. As a control 100 ng of labeled protein was added to 500 µL SFM without a hydrogel. For determination of remaining or released labeled protein the supernatants were measured with the plate reader Synergy H1 at emission/excitation 526/576 nm and normalized to the controls.

Characterization of hydrogels generated with copper alloy

Single and bi-layered hydrogels generated with different concentrations of HSA (0-500 µM) and 25 µM Cy3-Lys were imaged in a drop of tris buffer on a glass slide by confocal scanning laser microscopy (LSM710, Zeiss). Z-stacks with 30 µm distance were taken from top to bottom in the middle of the hydrogel with the 10x objective. The average fluorescent Z-intensity was extracted with ImageJ and normalized to the intensity measured in control hydrogels that were prepared between two glass slides in order to compensate for the fluorescence loss in deeper layers.

Ectopic implantation in mice

Gel constructs without any in vitro culture unless stated differently in the text were implanted in subcutaneous pouches (four per animal) in the back of female athymic CD-1 nu/nu mice (Charles River Laboratories), >5 weeks of age. Animals were sacrificed for construct retrieval after 2, 3, 4, 8 or 12 weeks as stated in the text. All animal procedures were reviewed and approved by the Swiss Federal Veterinary Office (BS 1797).

Cytofluorometry and fluorescently activated cell sorting (FACS)

BMSCs at different passages were analyzed using the fluorophore-conjugated antibodies against the following surface markers: CD49a, mouse CD8 (Becton Dickinson), CD56, CD105, CD106, CD166 (BioLegendes). The cells after trypsinization were stained for 20 minutes at 4°C in FACS buffer (PBS, 2 % FBS, 2.5 mM EDTA) and measured with a Fortessa flow cytometer (Becton Dickinson). The data was processed in FlowJow. For sorting, the cells were trypsinized and stained in FACS buffer for 20 minutes at 4°C with an anti CD56-APC, (BioLegends) or an anti mouse-CD8a-APC antibody (Becton Dickinson) and sorted using Aria (Becton Dickinson). 3.3×10^3 unsorted, negatively and positively sorted cells/cm^2 were plated and expanded until confluent or not more than 12 days before testing in chondrogenic assays.

Quantification of glycosamino glycan (GAG) and DNA

Pellets and hydrogels were digested with 1mg/mL protease K in 50 mM Tris with 1mM EDTA, 1mM iodoacetamide and 10 mg/mL pepstatin-A for 16 h at 56° C. For glycosaminoglycan quantification, the method of Barbosa et al. [223] was employed. Briefly, diluted or undiluted digested constructs (depending on SafO intensity) were incubated with 1 ml of DMMB solution (16 mg/L dimethylmethylene blue (DMMB), 6 mM sodium formate, 200 mM GuHCL, pH 3.0) on a shaker at room temperature for 30 minutes. Precipitated DMMB-GAG complexes were centrifuged and supernatants were discarded. Complexes were dissolved in decomplexion solution (4 M GuHCL, 50 mM Na-Acetate, 10% Propan-1-ol, pH 6.8) at 60°C, absorption was measured at 656 nm and GAG concentrations were calculated using a standard curve prepared with purified bovine chondroitin sulfate. DNA content was measured by using the CyQuant® Cell Proliferation Assay Kit (Molecular Probes) according the instructions of the manufacturer.

Histological and immunofluorescence staining

Pellets and hydrogels after in vitro culture or upon explantation, respectively, were fixed in 4 % paraformaldehyde, dehydrated, embedded in paraffin with the help of histogel (Thermo Scientific) and 5 μm thick sections were cut (Microm HM 430 or Microm HM 340E). Alternatively, fixed hydrogels were frozen in O.C.T. (VWR) with the help of a cartridge filled with methylbutane and dipped in liquid nitrogen and 7-10 μm thick cryosections (Cryostat Leica CM1950) were made. In vivo samples after fixation were decalcified in 15 % EDTA, pH 7 if required. Safranin-O/fast green staining with hematoxylin (J.T. Baker) nuclear counterstaining was performed to analyze chondrogenic and bone tissue formation. For semi-quantitative assessment of chondrogenesis the Bern score according to Grogan et al. [224] was determined. For immunofluorescence (IF) or immunohistochemical (IHC) staining after dehydration, the sections were subjected to enzymatic epitope retrieval at 37°C first with 2 mg/mL hyaluronidase and then with 1 mg/mL pronase (Roche), blocked with 5 % bovine serum albumin and the following primary antibodies were used: ColI, human specific, ab138492; ColI, mouse-specific, ab21286; ColII, human and mouse specific ab34712; ColX, human specific, ab49945, BSP, ab52128 and GFP, ab6673 (abcam). The immunobinding was detected in the case of IF with Alexa Fluor 488 or 564 conjugated secondary antibodies (Invitrogen) and DAPI was used as a nuclear counterstain, and for IHC with biotinylated secondary antibodies (Dako), the VECTASTAIN® ABC kit (vector laboratories) and VECTOR Red Alkaline phosphatase substrate kit (vector laboratories) for detection, hematoxylin (J.T. Baker) was used as a counterstain. For ColX staining in order to reduce mouse background staining, the primary antibody was pre-incubated with double the concentration of goat derived anti-mouse Fab fragments (Jackson Immuno Research) for 20 minutes and blocked with 10 % normal mouse serum (Jackson Immuno Research) for 10 minutes following the technique of [225]. The sections were visualized using a wide field microscope (Olympus BX61 or BX63) and images were processed with ImageJ. For semi-quantitation of the in vivo differentiation efficiency of single layered hydrogel constructs, SafO/FG stained sections were assigned with a score between 0-3 based on the criteria of bone in Table 3. For double-layered constructs the scoring based on SafO/FG stained sections and GFP labeling, was divided into evaluation of the cartilage part (identified by the prevalent presence of GFP-positive cells) and the bone part (identified by the absence of GFP-positive cells) by a number of 0-3 and an additional value of one was assigned if the constructs kept a bi-phasic configuration, resulting in a maximum score of 7 (Table 3).

Part	Parameters	Score
Cartilage	Undifferentiated/ fibroblastic	0
	Hypertrophic cartilage	1
	Mix of hyaline-like and hypertrophic cartilage	2
	Hyaline-like cartilage	3
Two-layer configuration	Two layers disassembled or bi-phasic configuration lost	0
	Bi-phasic configuration visible	1
Bone	Undifferentiated/ fibroblastic	0
	Hypertrophic cartilage	1
	Cartilage under remodelling	2
	Cortical bone and bone marrow	3
	Maximum	**7**

Table 3: Parameters included in the histological scoring of double layered constructs. Based on the SafO/FG staining and GFP immunofluorescence the bone and the cartilage part were evaluated with a number from 0-3, respectively and the interface between 0-1, resulting in a maximum score of 7. Hyaline cartilage score for the cartilage part was only assigned if there was no hypertrophic cartilage tissue was present at all.

RNA sequencing

Based on SafO/FG staining the clones were evaluated and divided into two groups, clones with a Bern score ≥ 3 were classified to have a high CC and clones with a Bern score < 3 as clones of low CC. The batch 1 analysis included 14 clones of donor 1 (6 of high CC) and batch 2 seven clones of donor 2 (3 of high CC), eight of donor 3 (4 of high CC) and six clones of donor 4 (3 of high CC). For mRNA isolation the protocol of the column-based quick-RNA min-prep (ZymoResearch) was followed. mRNA was quantified by using nanodrop and its quality was determined with the help of the 2100 bioanalyzer (Agilent technologies). 300 ng of DNase-

digested mRNA was used for library preparation with TruSeq Stranded Total RNA Kit with Ribo-Zero Gold (Illumina). Libraries were run on the fragment analyzer (Advanced Analytical) for quality control and were adjusted to equal concentrations. Sequencing was performed with a HighSeq 2500, with single end reads of 50 base lengths. The data was analyzed in R with the help of the Bioconductor package for determination of differentially expressed genes considering the chondrogenic capacity of the clones. All genes with an adjusted P-value <0.05 were considered to be significantly differentially expressed. For batch 1 two different approaches were tested: only a sub-set of clones was compared based on similar proliferation rates or all clones were analyzed in an unbiased way without accounting for the proliferation rate. For batch 2, the data were analyzed without considering the proliferation rate and the donors were considered as co-variable. The significantly differentially expressed genes of the subset analysis of batch 1 were additionally compared to the panel of QUIAGEN surface markers to identify surface markers and to identify involved pathways analyzed by ingenuity pathway analysis (QUIAGEN).

Quantitative real-time PCR

The mRNA was isolated as described in the RNA sequencing paragraph except that the DNA digestion was not performed. cDNA was generated with random primer (Promega) and the kit of SuperScript reverse transcriptase III (Thermo Scientific). For qPCR the TaqMan™ assay on demand system based on FAM and Tamra (Thermo Scientific) was used. Samples from the clonal studies and the sorting experiments were analyzed for expression of CD56 (NCAM1) (Hs00941830) and as reference gene GAPDH (Hs02758991) was used. PEG hydrogel samples from in vivo and in vitro experiments were digested for 45 minutes in 0.15 % type II collagenase (Worthington) at 37° C prior to RNA isolation. They were analyzed with the following TaqMan™ primers: ColI (Hs00164004), ColII (Hs00264051), ColX (Hs001666657), VEGFA (Hs00900055), chondromodulin (Hs0017087).

Statistical analysis

Statistical analysis was performed with Graph Pad Prism 6 software. Statistical significance was considered with a P-value < 0.05. All the data are shown as average +/- standard deviation. N indicates number of donors tested and analyzed.

References

1. Sophia Fox, A.J., A. Bedi, and S.A. Rodeo, *The basic science of articular cartilage: structure, composition, and function.* Sports Health, 2009. **1**(6): p. 461-8.

2. Hunziker, E.B., T.M. Quinn, and H.J. Häuselmann, *Quantitative structural organization of normal adult human articular cartilage.* Osteoarthritis and Cartilage, 2002. **10**(7): p. 564-572.

3. Changoor, A., et al., *Structural characteristics of the collagen network in human normal, degraded and repair articular cartilages observed in polarized light and scanning electron microscopies.* Osteoarthritis Cartilage, 2011. **19**(12): p. 1458-68.

4. Decker, R.S., E. Koyama, and M. Pacifici, *Genesis and morphogenesis of limb synovial joints and articular cartilage.* Matrix Biol, 2014. **39**: p. 5-10.

5. Decker, R.S., E. Koyama, and M. Pacifici, *Articular Cartilage: Structural and Developmental Intricacies and Questions.* Curr Osteoporos Rep, 2015. **13**(6): p. 407-14.

6. Iwamoto, M., et al., *Toward regeneration of articular cartilage.* Birth Defects Res C Embryo Today, 2013. **99**(3): p. 192-202.

7. Guo, X., et al., *Wnt/beta-catenin signaling is sufficient and necessary for synovial joint formation.* Genes Dev, 2004. **18**(19): p. 2404-17.

8. Hartmann, C. and C.J. Tabin, *Wnt-14 plays a pivotal role in inducing synovial joint formation in the developing appendicular skeleton.* Cell, 2001. **104**(3): p. 341-51.

9. Spater, D., et al., *Wnt9a signaling is required for joint integrity and regulation of Ihh during chondrogenesis.* Development, 2006. **133**(15): p. 3039-49.

10. Koyama, E., et al., *Synovial joint formation during mouse limb skeletogenesis: roles of Indian hedgehog signaling.* Ann N Y Acad Sci, 2007. **1116**: p. 100-12.

11. Brunet, L.J., et al., *Noggin, cartilage morphogenesis, and joint formation in the mammalian skeleton.* Science, 1998. **280**(5368): p. 1455-7.

12. Koyama, E., et al., *A distinct cohort of progenitor cells participates in synovial joint and articular cartilage formation during mouse limb skeletogenesis.* Dev Biol, 2008. **316**(1): p. 62-73.

13. Shwartz, Y., et al., *Joint Development Involves a Continuous Influx of Gdf5-Positive Cells.* Cell Rep, 2016. **15**(12): p. 2577-87.

14. Decker, R.S., et al., *Cell origin, volume and arrangement are drivers of articular cartilage formation, morphogenesis and response to injury in mouse limbs.* Developmental Biology, 2017. **426**(1): p. 56-68.

15. Ray, A., et al., *Precise spatial restriction of BMP signaling is essential for articular cartilage differentiation.* Development, 2015. **142**(6): p. 1169-79.

16. Kozhemyakina, E., et al., *Identification of a Prg4-expressing articular cartilage progenitor cell population in mice.* Arthritis Rheumatol, 2015. **67**(5): p. 1261-73.

17. Lopa, S. and H. Madry, *Bioinspired scaffolds for osteochondral regeneration.* Tissue Eng Part A, 2014. **20**(15-16): p. 2052-76.

18. Catterall, J.B., et al., *Aspartic acid racemization reveals a high turnover state in knee compared with hip osteoarthritic cartilage.* Osteoarthritis Cartilage, 2016. **24**(2): p. 374-81.

19. Albrecht, C., et al., *Gene expression and cell differentiation in matrix-associated chondrocyte transplantation grafts: a comparative study.* Osteoarthritis Cartilage, 2011. **19**(10): p. 1219-27.

20.   Zlotnicki, J.P., et al., *Biologic Treatments for Sports Injuries II Think Tank-Current Concepts, Future Research, and Barriers to Advancement, Part 3: Articular Cartilage.* Orthop J Sports Med, 2016. **4**(4): p. 2325967116642433.

21.   Mundi, R., et al., *Cartilage Restoration of the Knee: A Systematic Review and Meta-analysis of Level 1 Studies.* Am J Sports Med, 2016. **44**(7): p. 1888-95.

22.   Kraeutler, M.J., et al., *Microfracture Versus Autologous Chondrocyte Implantation for Articular Cartilage Lesions in the Knee: A Systematic Review of 5-Year Outcomes.* Am J Sports Med, 2017: p. 363546517701912.

23.   Katagiri, H., L.F. Mendes, and F.P. Luyten, *Definition of a Critical Size Osteochondral Knee Defect and its Negative Effect on the Surrounding Articular Cartilage in the Rat.* Osteoarthritis Cartilage, 2017. **25**(9): p. 1531-1540.

24.   Luo, Z., et al., *Mechano growth factor (MGF) and transforming growth factor (TGF)-beta3 functionalized silk scaffolds enhance articular hyaline cartilage regeneration in rabbit model.* Biomaterials, 2015. **52**: p. 463-75.

25.   Zhang, W., et al., *The use of type 1 collagen scaffold containing stromal cell-derived factor-1 to create a matrix environment conducive to partial-thickness cartilage defects repair.* Biomaterials, 2013. **34**(3): p. 713-23.

26.   Huang, H., et al., *A functional biphasic biomaterial homing mesenchymal stem cells for in vivo cartilage regeneration.* Biomaterials, 2014. **35**(36): p. 9608-19.

27.   Longobardi, L., et al., *TGF-beta type II receptor/MCP-5 axis: at the crossroad between joint and growth plate development.* Dev Cell, 2012. **23**(1): p. 71-81.

28.   Rho, J.Y., L. Kuhn-Spearing, and P. Zioupos, *Mechanical properties and the hierarchical structure of bone.* Med Eng Phys, 1998. **20**(2): p. 92-102.

29.   Olszta, M.J., et al., *Bone structure and formation: A new perspective.* Materials Science and Engineering: R: Reports, 2007. **58**(3-5): p. 77-116.

30.   Teti, A., *Bone development: overview of bone cells and signaling.* Curr Osteoporos Rep, 2011. **9**(4): p. 264-73.

31.   Wang, Y., et al., *The predominant role of collagen in the nucleation, growth, structure and orientation of bone apatite.* Nat Mater, 2012. **11**(8): p. 724-33.

32.   Clarke, B., *Normal bone anatomy and physiology.* Clin J Am Soc Nephrol, 2008. **3 Suppl 3**: p. S131-9.

33.   Berendsen, A.D. and B.R. Olsen, *Bone development.* Bone, 2015. **80**: p. 14-8.

34.   Summerbell, D., J.H. Lewis, and L. Wolpert, *Positional information in chick limb morphogenesis.* Nature, 1973. **244**(5417): p. 492-6.

35.   Saunders, J.W., Jr., *The proximo-distal sequence of origin of the parts of the chick wing and the role of the ectoderm.* J Exp Zool, 1948. **108**(3): p. 363-403.

36.   Tickle, C., *The number of polarizing region cells required to specify additional digits in the developing chick wing.* Nature, 1981. **289**(5795): p. 295-8.

37.   Zeller, R., J. Lopez-Rios, and A. Zuniga, *Vertebrate limb bud development: moving towards integrative analysis of organogenesis.* Nat Rev Genet, 2009. **10**(12): p. 845-58.

38.   ten Berge, D., et al., *Wnt and FGF signals interact to coordinate growth with cell fate specification during limb development.* Development, 2008. **135**(19): p. 3247-57.

39.   Akiyama, H., et al., *The transcription factor Sox9 has essential roles in successive steps of the chondrocyte differentiation pathway and is required for expression of Sox5 and Sox6.* Genes Dev, 2002. **16**(21): p. 2813-28.

40. Vortkamp, A., et al., *Regulation of rate of cartilage differentiation by Indian hedgehog and PTH-related protein.* Science, 1996. **273**(5275): p. 613-22.

41. Long, F. and D.M. Ornitz, *Development of the endochondral skeleton.* Cold Spring Harb Perspect Biol, 2013. **5**(1): p. a008334.

42. Dy, P., et al., *Sox9 directs hypertrophic maturation and blocks osteoblast differentiation of growth plate chondrocytes.* Dev Cell, 2012. **22**(3): p. 597-609.

43. Amarilio, R., et al., *HIF1alpha regulation of Sox9 is necessary to maintain differentiation of hypoxic prechondrogenic cells during early skeletogenesis.* Development, 2007. **134**(21): p. 3917-28.

44. Gerber, H.P., et al., *VEGF couples hypertrophic cartilage remodeling, ossification and angiogenesis during endochondral bone formation.* Nat Med, 1999. **5**(6): p. 623-8.

45. Houben, A., et al., *beta-catenin activity in late hypertrophic chondrocytes locally orchestrates osteoblastogenesis and osteoclastogenesis.* Development, 2016. **143**(20): p. 3826-3838.

46. Yang, L., et al., *Hypertrophic chondrocytes can become osteoblasts and osteocytes in endochondral bone formation.* Proc Natl Acad Sci U S A, 2014. **111**(33): p. 12097-102.

47. Park, J., et al., *Dual pathways to endochondral osteoblasts: a novel chondrocyte-derived osteoprogenitor cell identified in hypertrophic cartilage.* Biol Open, 2015. **4**(5): p. 608-21.

48. Hung, I.H., et al., *FGF9 regulates early hypertrophic chondrocyte differentiation and skeletal vascularization in the developing stylopod.* Dev Biol, 2007. **307**(2): p. 300-13.

49. Liu, Z., et al., *Coordination of chondrogenesis and osteogenesis by fibroblast growth factor 18.* Genes Dev, 2002. **16**(7): p. 859-69.

50. Shu, B., et al., *BMP2, but not BMP4, is crucial for chondrocyte proliferation and maturation during endochondral bone development.* J Cell Sci, 2011. **124**(Pt 20): p. 3428-40.

51. Yoon, B.S., et al., *BMPs regulate multiple aspects of growth-plate chondrogenesis through opposing actions on FGF pathways.* Development, 2006. **133**(23): p. 4667-78.

52. Kozhemyakina, E., A.B. Lassar, and E. Zelzer, *A pathway to bone: signaling molecules and transcription factors involved in chondrocyte development and maturation.* Development, 2015. **142**(5): p. 817-31.

53. Nakashima, K., et al., *The novel zinc finger-containing transcription factor osterix is required for osteoblast differentiation and bone formation.* Cell, 2002. **108**(1): p. 17-29.

54. Day, T.F., et al., *Wnt/beta-catenin signaling in mesenchymal progenitors controls osteoblast and chondrocyte differentiation during vertebrate skeletogenesis.* Dev Cell, 2005. **8**(5): p. 739-50.

55. Bandyopadhyay, A., et al., *Genetic analysis of the roles of BMP2, BMP4, and BMP7 in limb patterning and skeletogenesis.* PLoS Genet, 2006. **2**(12): p. e216.

56. Blumer, M.J., S. Longato, and H. Fritsch, *Structure, formation and role of cartilage canals in the developing bone.* Ann Anat, 2008. **190**(4): p. 305-15.

57. Xing, W., et al., *Epiphyseal chondrocyte secondary ossification centers require thyroid hormone activation of Indian hedgehog and osterix signaling.* J Bone Miner Res, 2014. **29**(10): p. 2262-75.

58. Wang, Y., et al., *IGF-I Signaling in Osterix-Expressing Cells Regulates Secondary Ossification Center Formation, Growth Plate Maturation, and Metaphyseal Formation During Postnatal Bone Development.* J Bone Miner Res, 2015. **30**(12): p. 2239-48.

59. Allerstorfer, D., et al., *VEGF and its role in the early development of the long bone epiphysis.* J Anat, 2010. **216**(5): p. 611-24.

60. Percival, C.J. and J.T. Richtsmeier, *Angiogenesis and intramembranous osteogenesis.* Dev Dyn, 2013. **242**(8): p. 909-22.

61. Schindeler, A., et al., *Bone remodeling during fracture repair: The cellular picture.* Semin Cell Dev Biol, 2008. **19**(5): p. 459-66.

62. Phillips, A.M., *Overview of the fracture healing cascade.* Injury, 2005. **36 Suppl 3**: p. S5-7.

63. Wang, T., X. Zhang, and D.D. Bikle, *Osteogenic Differentiation of Periosteal Cells During Fracture Healing.* J Cell Physiol, 2017. **232**(5): p. 913-921.

64. Chan, C.K., et al., *Identification and specification of the mouse skeletal stem cell.* Cell, 2015. **160**(1-2): p. 285-98.

65. Marecic, O., et al., *Identification and characterization of an injury-induced skeletal progenitor.* Proc Natl Acad Sci U S A, 2015. **112**(32): p. 9920-5.

66. Rux, D.R., et al., *Regionally Restricted Hox Function in Adult Bone Marrow Multipotent Mesenchymal Stem/Stromal Cells.* Dev Cell, 2016. **39**(6): p. 653-666.

67. Aponte-Tinao, L.A., et al., *Should fractures in massive intercalary bone allografts of the lower limb be treated with ORIF or with a new allograft?* Clin Orthop Relat Res, 2015. **473**(3): p. 805-11.

68. Aponte-Tinao, L.A., et al., *What Are the Risk Factors and Management Options for Infection After Reconstruction With Massive Bone Allografts?* Clin Orthop Relat Res, 2016. **474**(3): p. 669-73.

69. Sen, M.K. and T. Miclau, *Autologous iliac crest bone graft: should it still be the gold standard for treating nonunions?* Injury, 2007. **38 Suppl 1**: p. S75-80.

70. Skalak, R.F.C.F., Tissue Engineering, 1988.

71. Langer, R. and J.P. Vacanti, *Tissue engineering.* Science, 1993. **260**(5110): p. 920-6.

72. Saxer, F., et al., *Implantation of Stromal Vascular Fraction Progenitors at Bone Fracture Sites: From a Rat Model to a First-in-Man Study.* Stem Cells, 2016. **34**(12): p. 2956-2966.

73. Niederauer, G.G., et al., *Evaluation of multiphase implants for repair of focal osteochondral defects in goats.* Biomaterials, 2000. **21**(24): p. 2561-74.

74. Kon, E., et al., *Orderly osteochondral regeneration in a sheep model using a novel nano-composite multilayered biomaterial.* J Orthop Res, 2010. **28**(1): p. 116-24.

75. Kon, E., et al., *Osteochondral regeneration using a novel aragonite-hyaluronate bi-phasic scaffold in a goat model.* Knee Surg Sports Traumatol Arthrosc, 2014. **22**(6): p. 1452-64.

76. Reyes, R., et al., *Cartilage repair by local delivery of transforming growth factor-β1 or bone morphogenetic protein-2 from a novel, segmented polyurethane/polylactic-co-glycolic bilayered scaffold.* Journal of Biomedical Materials Research Part A, 2014. **102**(4): p. 1110-1120.

77. Lu, S., et al., *Dual growth factor delivery from bilayered, biodegradable hydrogel composites for spatially-guided osteochondral tissue repair.* Biomaterials, 2014. **35**(31): p. 8829-39.

78. Getgood, A., et al., *Osteochondral tissue engineering using a biphasic collagen/GAG scaffold containing rhFGF18 or BMP-7 in an ovine model.* J Exp Orthop, 2014. **1**(1): p. 13.

79. Bourgine, P.E., et al., *Osteoinductivity of engineered cartilaginous templates devitalized by inducible apoptosis.* Proc Natl Acad Sci U S A, 2014. **111**(49): p. 17426-31.

80. Tonnarelli, B., et al., *Re-engineering development to instruct tissue regeneration.* Curr Top Dev Biol, 2014. **108**: p. 319-38.

81. Occhetta, P., et al., *Learn, simplify and implement: developmental re-engineering strategies for cartilage repai.* Swiss Med Wkly, 2016. **146**: p. w14346.

82. Mhanna, R., et al., *Chondrocyte culture in three dimensional alginate sulfate hydrogels promotes proliferation while maintaining expression of chondrogenic markers.* Tissue Eng Part A, 2014. **20**(9-10): p. 1454-64.

83. Popko, M., et al., *Histological structure of the nasal cartilages and their perichondrial envelope. I. The septal and lobular cartilage.* Rhinology, 2007. **45**(2): p. 148-52.

84. Rotter, N., et al., *Age-related changes in the composition and mechanical properties of human nasal cartilage.* Arch Biochem Biophys, 2002. **403**(1): p. 132-40.

85. Kafienah, W., et al., *Three-dimensional tissue engineering of hyaline cartilage: comparison of adult nasal and articular chondrocytes.* Tissue Eng, 2002. **8**(5): p. 817-26.

86. Shafiee, A., et al., *Evaluation and comparison of the in vitro characteristics and chondrogenic capacity of four adult stem/progenitor cells for cartilage cell-based repair.* J Biomed Mater Res A, 2016. **104**(3): p. 600-610.

87. Pelttari, K., et al., *Adult human neural crest-derived cells for articular cartilage repair.* Sci Transl Med, 2014. **6**(251): p. 251ra119.

88. Mumme, M., et al., *Nasal chondrocyte-based engineered autologous cartilage tissue for repair of articular cartilage defects: an observational first-in-human trial.* Lancet, 2016. **388**(10055): p. 1985-1994.

89. Elsaesser, A.F., et al., *Characterization of a migrative subpopulation of adult human nasoseptal chondrocytes with progenitor cell features and their potential for in vivo cartilage regeneration strategies.* Cell Biosci, 2016. **6**: p. 11.

90. Bianco, P., *"Mesenchymal" stem cells.* Annu Rev Cell Dev Biol, 2014. **30**: p. 677-704.

91. Dominici, M., et al., *Minimal criteria for defining multipotent mesenchymal stromal cells. The International Society for Cellular Therapy position statement.* Cytotherapy, 2006. **8**(4): p. 315-7.

92. Friedenstein, A.J., S. Piatetzky, II, and K.V. Petrakova, *Osteogenesis in transplants of bone marrow cells.* J Embryol Exp Morphol, 1966. **16**(3): p. 381-90.

93. Friedenstein, A.J., et al., *Origin of bone marrow stromal mechanocytes in radiochimeras and heterotopic transplants.* Exp Hematol, 1978. **6**(5): p. 440-4.

94. Friedenstein, A.J., *Stromal mechanisms of bone marrow: cloning in vitro and retransplantation in vivo.* Haematol Blood Transfus, 1980. **25**: p. 19-29.

95. Owen, M., *Marrow stromal stem cells.* J Cell Sci Suppl, 1988. **10**: p. 63-76.

96. Owen, M. and A.J. Friedenstein, *Stromal stem cells: marrow-derived osteogenic precursors.* Ciba Found Symp, 1988. **136**: p. 42-60.

97. Simmons, P.J. and B. Torok-Storb, *Identification of stromal cell precursors in human bone marrow by a novel monoclonal antibody, STRO-1.* Blood, 1991. **78**(1): p. 55-62.

98. Quirici, N., et al., *Isolation of bone marrow mesenchymal stem cells by anti-nerve growth factor receptor antibodies.* Exp Hematol, 2002. **30**(7): p. 783-91.

99. Deschaseaux, F., et al., *Direct selection of human bone marrow mesenchymal stem cells using an anti-CD49a antibody reveals their CD45med,low phenotype.* Br J Haematol, 2003. **122**(3): p. 506-17.

100. Sacchetti, B., et al., *Self-renewing osteoprogenitors in bone marrow sinusoids can organize a hematopoietic microenvironment.* Cell, 2007. **131**(2): p. 324-36.

101. Tormin, A., et al., *CD146 expression on primary nonhematopoietic bone marrow stem cells is correlated with in situ localization.* Blood, 2011. **117**(19): p. 5067-77.

102. Battula, V.L., et al., *Isolation of functionally distinct mesenchymal stem cell subsets using antibodies against CD56, CD271, and mesenchymal stem cell antigen-1.* Haematologica, 2009. **94**(2): p. 173-84.

103. Mabuchi, Y., et al., *LNGFR(+)THY-1(+)VCAM-1(hi+) cells reveal functionally distinct subpopulations in mesenchymal stem cells.* Stem Cell Reports, 2013. **1**(2): p. 152-65.

104. Li, H., et al., *Low/negative expression of PDGFR-alpha identifies the candidate primary mesenchymal stromal cells in adult human bone marrow.* Stem Cell Reports, 2014. **3**(6): p. 965-74.

105. Ghazanfari, R., et al., *Human Non-hematopoietic CD271pos/CD140alow/neg Bone Marrow Stroma Cells Fulfill Stringent Stem Cell Criteria in Serial Transplantations.* Stem Cells Dev, 2016.

106. Morikawa, S., et al., *Prospective identification, isolation, and systemic transplantation of multipotent mesenchymal stem cells in murine bone marrow.* J Exp Med, 2009. **206**(11): p. 2483-96.

107. Mendez-Ferrer, S., et al., *Mesenchymal and haematopoietic stem cells form a unique bone marrow niche.* Nature, 2010. **466**(7308): p. 829-34.

108. Pinho, S., et al., *PDGFRalpha and CD51 mark human nestin+ sphere-forming mesenchymal stem cells capable of hematopoietic progenitor cell expansion.* J Exp Med, 2013. **210**(7): p. 1351-67.

109. Nusspaumer, G., et al., *Ontogenic Identification and Analysis of Mesenchymal Stromal Cell Populations during Mouse Limb and Long Bone Development.* Stem Cell Reports, 2017.

110. Zhou, B.O., et al., *Leptin-receptor-expressing mesenchymal stromal cells represent the main source of bone formed by adult bone marrow.* Cell Stem Cell, 2014. **15**(2): p. 154-68.

111. Worthley, D.L., et al., *Gremlin 1 identifies a skeletal stem cell with bone, cartilage, and reticular stromal potential.* Cell, 2015. **160**(1-2): p. 269-84.

112. Yoo, J.U., et al., *The chondrogenic potential of human bone-marrow-derived mesenchymal progenitor cells.* J Bone Joint Surg Am, 1998. **80**(12): p. 1745-57.

113. Pelttari, K., et al., *Premature induction of hypertrophy during in vitro chondrogenesis of human mesenchymal stem cells correlates with calcification and vascular invasion after ectopic transplantation in SCID mice.* Arthritis Rheum, 2006. **54**(10): p. 3254-66.

114. Scotti, C., et al., *Recapitulation of endochondral bone formation using human adult mesenchymal stem cells as a paradigm for developmental engineering.* Proc Natl Acad Sci U S A, 2010. **107**(16): p. 7251-6.

115. Scotti, C., et al., *Engineering of a functional bone organ through endochondral ossification.* Proc Natl Acad Sci U S A, 2013. **110**(10): p. 3997-4002.

116. Pittenger, M.F., et al., *Multilineage potential of adult human mesenchymal stem cells.* Science, 1999. **284**(5411): p. 143-7.

117. Wakitani, S. and T. Yamamoto, *Response of the donor and recipient cells in mesenchymal cell transplantation to cartilage defect.* Microsc Res Tech, 2002. **58**(1): p. 14-8.

118. Kuroda, R., et al., *Treatment of a full-thickness articular cartilage defect in the femoral condyle of an athlete with autologous bone-marrow stromal cells.* Osteoarthritis Cartilage, 2007. **15**(2): p. 226-31.

119. Nejadnik, H., et al., *Autologous bone marrow-derived mesenchymal stem cells versus autologous chondrocyte implantation: an observational cohort study.* Am J Sports Med, 2010. **38**(6): p. 1110-6.

120. Buda, R., et al., *Osteochondral lesions of the knee: a new one-step repair technique with bone-marrow-derived cells.* J Bone Joint Surg Am, 2010. **92 Suppl 2**: p. 2-11.

121. Gobbi, A., et al., *One-Step Cartilage Repair with Bone Marrow Aspirate Concentrated Cells and Collagen Matrix in Full-Thickness Knee Cartilage Lesions: Results at 2-Year Follow-up.* Cartilage, 2011. **2**(3): p. 286-99.

122. Gigante, A., et al., *Use of collagen scaffold and autologous bone marrow concentrate as a one-step cartilage repair in the knee: histological results of second-look biopsies at 1 year follow-up.* Int J Immunopathol Pharmacol, 2011. **24**(1 Suppl 2): p. 69-72.

123. Skowronski, J., R. Skowronski, and M. Rutka, *Large cartilage lesions of the knee treated with bone marrow concentrate and collagen membrane--results.* Ortop Traumatol Rehabil, 2013. **15**(1): p. 69-76.

124. Guo, X., et al., *Repair of large articular cartilage defects with implants of autologous mesenchymal stem cells seeded into beta-tricalcium phosphate in a sheep model.* Tissue Eng, 2004. **10**(11-12): p. 1818-29.

125. Marquass, B., et al., *Matrix-associated implantation of predifferentiated mesenchymal stem cells versus articular chondrocytes: in vivo results of cartilage repair after 1 year.* Am J Sports Med, 2011. **39**(7): p. 1401-12.

126. Zscharnack, M., et al., *Repair of chronic osteochondral defects using predifferentiated mesenchymal stem cells in an ovine model.* Am J Sports Med, 2010. **38**(9): p. 1857-69.

127. Bornes, T.D., A.B. Adesida, and N.M. Jomha, *Mesenchymal stem cells in the treatment of traumatic articular cartilage defects: a comprehensive review.* Arthritis Res Ther, 2014. **16**(5): p. 432.

128. Weiss, S., et al., *Impact of growth factors and PTHrP on early and late chondrogenic differentiation of human mesenchymal stem cells.* J Cell Physiol, 2010. **223**(1): p. 84-93.

129. Bian, L., et al., *Dynamic compressive loading enhances cartilage matrix synthesis and distribution and suppresses hypertrophy in hMSC-laden hyaluronic acid hydrogels.* Tissue Eng Part A, 2012. **18**(7-8): p. 715-24.

130. Leijten, J.C., et al., *Gremlin 1, frizzled-related protein, and Dkk-1 are key regulators of human articular cartilage homeostasis.* Arthritis Rheum, 2012. **64**(10): p. 3302-12.

131. Leijten, J., et al., *Metabolic programming of mesenchymal stromal cells by oxygen tension directs chondrogenic cell fate.* Proc Natl Acad Sci U S A, 2014. **111**(38): p. 13954-9.

132. Marsano, A., et al., *Spontaneous In Vivo Chondrogenesis of Bone Marrow-Derived Mesenchymal Progenitor Cells by Blocking Vascular Endothelial Growth Factor Signaling.* Stem Cells Transl Med, 2016. **5**(12): p. 1730-1738.

133. Narcisi, R., et al., *Long-term expansion, enhanced chondrogenic potential, and suppression of endochondral ossification of adult human MSCs via WNT signaling modulation.* Stem Cell Reports, 2015. **4**(3): p. 459-72.

134. Correa, D., et al., *Sequential exposure to fibroblast growth factors (FGF) 2, 9 and 18 enhances hMSC chondrogenic differentiation.* Osteoarthritis Cartilage, 2015. **23**(3): p. 443-53.

135. Ng, J.J., et al., *Recapitulation of physiological spatiotemporal signals promotes in vitro formation of phenotypically stable human articular cartilage.* Proc Natl Acad Sci U S A, 2017. **114**(10): p. 2556-2561.

136. Oldershaw, R.A., et al., *Directed differentiation of human embryonic stem cells toward chondrocytes.* Nat Biotechnol, 2010. **28**(11): p. 1187-94.

137. Craft, A.M., et al., *Specification of chondrocytes and cartilage tissues from embryonic stem cells.* Development, 2013. **140**(12): p. 2597-610.

138. Craft, A.M., et al., *Generation of articular chondrocytes from human pluripotent stem cells.* Nat Biotechnol, 2015. **33**(6): p. 638-45.

139. Zhao, J., et al., *Small molecule-directed specification of sclerotome-like chondroprogenitors and induction of a somitic chondrogenesis program from embryonic stem cells.* Development, 2014. **141**(20): p. 3848-58.

140. Umeda, K., et al., *Long-term expandable SOX9+ chondrogenic ectomesenchymal cells from human pluripotent stem cells.* Stem Cell Reports, 2015. **4**(4): p. 712-26.

141. Yamashita, A., et al., *Generation of scaffoldless hyaline cartilaginous tissue from human iPSCs.* Stem Cell Reports, 2015. **4**(3): p. 404-18.

142. Liu, H., et al., *The potential of induced pluripotent stem cells as a tool to study skeletal dysplasias and cartilage-related pathologic conditions.* Osteoarthritis Cartilage, 2017. **25**(5): p. 616-624.

143. Yang, J., et al., *Cell-laden hydrogels for osteochondral and cartilage tissue engineering.* Acta Biomater, 2017. **57**: p. 1-25.

144. Slaughter, B.V., et al., *Hydrogels in regenerative medicine.* Adv Mater, 2009. **21**(32-33): p. 3307-29.

145. Lin, C.C., *Recent advances in crosslinking chemistry of biomimetic poly(ethylene glycol) hydrogels.* RSC Adv, 2015. **5**(50): p. 39844-398583.

146. Ehrbar, M., et al., *Biomolecular hydrogels formed and degraded via site-specific enzymatic reactions.* Biomacromolecules, 2007. **8**(10): p. 3000-7.

147. Ehrbar, M., et al., *Elucidating the role of matrix stiffness in 3D cell migration and remodeling.* Biophys J, 2011. **100**(2): p. 284-93.

148. Metzger, S., et al., *Modular poly(ethylene glycol) matrices for the controlled 3D-localized osteogenic differentiation of mesenchymal stem cells.* Adv Healthc Mater, 2015. **4**(4): p. 550-8.

149. Bryant, S.J., et al., *Encapsulating chondrocytes in degrading PEG hydrogels with high modulus: engineering gel structural changes to facilitate cartilaginous tissue production.* Biotechnol Bioeng, 2004. **86**(7): p. 747-55.

150. Park, Y., et al., *Bovine primary chondrocyte culture in synthetic matrix metalloproteinase-sensitive poly(ethylene glycol)-based hydrogels as a scaffold for cartilage repair.* Tissue Eng, 2004. **10**(3-4): p. 515-22.

151. Anderson, S.B., et al., *The performance of human mesenchymal stem cells encapsulated in cell-degradable polymer-peptide hydrogels.* Biomaterials, 2011. **32**(14): p. 3564-74.

152. Mhanna, R., et al., *GFOGER-modified MMP-sensitive polyethylene glycol hydrogels induce chondrogenic differentiation of human mesenchymal stem cells.* Tissue Eng Part A, 2014. **20**(7-8): p. 1165-74.

153. Sridhar, B.V., et al., *Development of a cellularly degradable PEG hydrogel to promote articular cartilage extracellular matrix deposition.* Adv Healthc Mater, 2015. **4**(5): p. 702-13.

154. Ruoslahti, E., *RGD and other recognition sequences for integrins.* Annu Rev Cell Dev Biol, 1996. **12**: p. 697-715.

155. Hesse, E., et al., *Peptide-functionalized starPEG/heparin hydrogels direct mitogenicity, cell morphology and cartilage matrix distribution in vitro and in vivo.* J Tissue Eng Regen Med, 2017.

156. Alakpa, Enateri V., et al., *Tunable Supramolecular Hydrogels for Selection of Lineage-Guiding Metabolites in Stem Cell Cultures.* Chem, 2016. **1**(2): p. 298-319.

157. Steinmetz, N.J., et al., *Mechanical loading regulates human MSC differentiation in a multi-layer hydrogel for osteochondral tissue engineering.* Acta Biomater, 2015. **21**: p. 142-53.

158. Reed, S. and B. Wu, *Sustained growth factor delivery in tissue engineering applications.* Ann Biomed Eng, 2014. **42**(7): p. 1528-36.

159. Belair, D.G., N.N. Le, and W.L. Murphy, *Design of growth factor sequestering biomaterials.* Chemical Communications, 2014. **50**(99): p. 15651-15668.

160. Vulic, K. and M.S. Shoichet, *Affinity-based drug delivery systems for tissue repair and regeneration.* Biomacromolecules, 2014. **15**(11): p. 3867-3880.

161. Metzger, S., et al., *Cell-Mediated Proteolytic Release of Growth Factors from Poly(Ethylene Glycol) Matrices.* Macromol Biosci, 2016. **16**(11): p. 1703-1713.

162.	Moghadam, M.N., et al., *Controlled release from a mechanically-stimulated thermosensitive self-heating composite hydrogel.* Biomaterials, 2014. **35**(1): p. 450-455.

163.	McCall, J.D., J.E. Luoma, and K.S. Anseth, *Covalently tethered transforming growth factor beta in PEG hydrogels promotes chondrogenic differentiation of encapsulated human mesenchymal stem cells.* Drug Deliv Transl Res, 2012. **2**(5): p. 305-12.

164.	Kopesky, P.W., et al., *Sustained delivery of bioactive TGF-beta1 from self-assembling peptide hydrogels induces chondrogenesis of encapsulated bone marrow stromal cells.* J Biomed Mater Res A, 2014. **102**(5): p. 1275-85.

165.	Re'em, T., et al., *Chondrogenesis of hMSC in affinity-bound TGF-beta scaffolds.* Biomaterials, 2012. **33**(3): p. 751-61.

166.	Chen, Y.G., *Endocytic regulation of TGF-beta signaling.* Cell Res, 2009. **19**(1): p. 58-70.

167.	Jenkins, G., *The role of proteases in transforming growth factor-beta activation.* Int J Biochem Cell Biol, 2008. **40**(6-7): p. 1068-78.

168.	Place, E.S., et al., *Latent TGF-beta hydrogels for cartilage tissue engineering.* Adv Healthc Mater, 2012. **1**(4): p. 480-4.

169.	Thompson, E.M., et al., *Recapitulating endochondral ossification: a promising route to in vivo bone regeneration.* J Tissue Eng Regen Med, 2015. **9**(8): p. 889-902.

170.	Romagnoli, C. and M.L. Brandi, *Adipose mesenchymal stem cells in the field of bone tissue engineering.* World J Stem Cells, 2014. **6**(2): p. 144-52.

171.	de Girolamo, L., et al., *Osteogenic differentiation of human adipose-derived stem cells: comparison of two different inductive media.* J Tissue Eng Regen Med, 2007. **1**(2): p. 154-7.

172.	Osinga, R., et al., *Generation of a Bone Organ by Human Adipose-Derived Stromal Cells Through Endochondral Ossification.* Stem Cells Transl Med, 2016. **5**(8): p. 1090-7.

173.	Janicki, P., et al., *Chondrogenic pre-induction of human mesenchymal stem cells on beta-TCP: enhanced bone quality by endochondral heterotopic bone formation.* Acta Biomater, 2010. **6**(8): p. 3292-301.

174.	Farrell, E., et al., *In-vivo generation of bone via endochondral ossification by in-vitro chondrogenic priming of adult human and rat mesenchymal stem cells.* BMC Musculoskelet Disord, 2011. **12**: p. 31.

175.	Sheehy, E.J., et al., *Tissue Engineering Whole Bones Through Endochondral Ossification: Regenerating the Distal Phalanx.* Biores Open Access, 2015. **4**(1): p. 229-41.

176.	Sheehy, E.J., et al., *Engineering cartilage or endochondral bone: a comparison of different naturally derived hydrogels.* Acta Biomater, 2015. **13**: p. 245-53.

177.	Yang, W., et al., *Effects of in vitro chondrogenic priming time of bone-marrow-derived mesenchymal stromal cells on in vivo endochondral bone formation.* Acta Biomater, 2015. **13**: p. 254-65.

178.	Harada, N., et al., *Bone regeneration in a massive rat femur defect through endochondral ossification achieved with chondrogenically differentiated MSCs in a degradable scaffold.* Biomaterials, 2014. **35**(27): p. 7800-10.

179.	van der Stok, J., et al., *Chondrogenically differentiated mesenchymal stromal cell pellets stimulate endochondral bone regeneration in critical-sized bone defects.* European Cells and Materials, 2014. **27**: p. 137-148.

180.	Bahney, C.S., et al., *Stem cell-derived endochondral cartilage stimulates bone healing by tissue transformation.* J Bone Miner Res, 2014. **29**(5): p. 1269-82.

181. Dang, P.N., et al., *Controlled Dual Growth Factor Delivery From Microparticles Incorporated Within Human Bone Marrow-Derived Mesenchymal Stem Cell Aggregates for Enhanced Bone Tissue Engineering via Endochondral Ossification.* Stem Cells Transl Med, 2016. **5**(2): p. 206-17.

182. Dang, P.N., et al., *Endochondral Ossification in Critical-Sized Bone Defects via Readily Implantable Scaffold-Free Stem Cell Constructs.* Stem Cells Transl Med, 2017. **6**(7): p. 1644-1659.

183. Schaefer, D., et al., *In vitro generation of osteochondral composites.* Biomaterials, 2000. **21**(24): p. 2599-606.

184. Cheng, H.W., et al., *In vitro generation of an osteochondral interface from mesenchymal stem cell-collagen microspheres.* Biomaterials, 2011. **32**(6): p. 1526-35.

185. Schek, R.M., et al., *Engineered osteochondral grafts using biphasic composite solid free-form fabricated scaffolds.* Tissue Eng, 2004. **10**(9-10): p. 1376-85.

186. Sheehy, E.J., et al., *Engineering osteochondral constructs through spatial regulation of endochondral ossification.* Acta Biomater, 2013. **9**(3): p. 5484-92.

187. Mesallati, T., et al., *Tissue engineering scaled-up, anatomically shaped osteochondral constructs for joint resurfacing.* Eur Cell Mater, 2015. **30**: p. 163-85; discussion 185-6.

188. Giannoni, P., et al., *Design and characterization of a tissue-engineered bilayer scaffold for osteochondral tissue repair.* J Tissue Eng Regen Med, 2015. **9**(10): p. 1182-92.

189. Sartori, M., et al., *A new bi-layered scaffold for osteochondral tissue regeneration: In vitro and in vivo preclinical investigations.* Mater Sci Eng C Mater Biol Appl, 2017. **70**(Pt 1): p. 101-111.

190. Guo, X., et al., *Repair of osteochondral defects with biodegradable hydrogel composites encapsulating marrow mesenchymal stem cells in a rabbit model.* Acta Biomater, 2010. **6**(1): p. 39-47.

191. Gao, J., et al., *Repair of osteochondral defect with tissue-engineered two-phase composite material of injectable calcium phosphate and hyaluronan sponge.* Tissue Eng, 2002. **8**(5): p. 827-37.

192. Tanaka, T., et al., *Use of a biphasic graft constructed with chondrocytes overlying a beta-tricalcium phosphate block in the treatment of rabbit osteochondral defects.* Tissue Eng, 2005. **11**(1-2): p. 331-9.

193. Bal, B.S., et al., *In vivo outcomes of tissue-engineered osteochondral grafts.* J Biomed Mater Res B Appl Biomater, 2010. **93**(1): p. 164-74.

194. Re'em, T., et al., *Simultaneous regeneration of articular cartilage and subchondral bone induced by spatially presented TGF-beta and BMP-4 in a bilayer affinity binding system.* Acta Biomater, 2012. **8**(9): p. 3283-93.

195. He, A., et al., *Repair of osteochondral defects with in vitro engineered cartilage based on autologous bone marrow stromal cells in a swine model.* Sci Rep, 2017. **7**: p. 40489.

196. Li, X., et al., *Osteogenesis and chondrogenesis of biomimetic integrated porous PVA/gel/V-n-HA/pa6 scaffolds and BMSCs construct in repair of articular osteochondral defect.* J Biomed Mater Res A, 2015. **103**(10): p. 3226-36.

197. Lienemann, P.S., et al., *A versatile approach to engineering biomolecule-presenting cellular microenvironments.* Adv Healthc Mater, 2013. **2**(2): p. 292-6.

198. Hiraki, Y. and C. Shukunami, *Chondromodulin-I as a novel cartilage-specific growth-modulating factor.* Pediatr Nephrol, 2000. **14**(7): p. 602-5.

199. Cote, A.J., et al., *Single-cell differences in matrix gene expression do not predict matrix deposition.* Nat Commun, 2016. **7**: p. 10865.

200. Holzapfel, B.M., et al., *Tissue engineered humanized bone supports human hematopoiesis in vivo.* Biomaterials, 2015. **61**: p. 103-14.

201. Reinisch, A., et al., *A humanized bone marrow ossicle xenotransplantation model enables improved engraftment of healthy and leukemic human hematopoietic cells.* Nat Med, 2016. **22**(7): p. 812-21.

202. Herrmann, M., S. Verrier, and M. Alini, *Strategies to Stimulate Mobilization and Homing of Endogenous Stem and Progenitor Cells for Bone Tissue Repair.* Front Bioeng Biotechnol, 2015. **3**: p. 79.

203. Pippenger, B.E., et al., *Bone-forming capacity of adult human nasal chondrocytes.* J Cell Mol Med, 2015. **19**(6): p. 1390-9.

204. Shen, J., S. Li, and D. Chen, *TGF-beta signaling and the development of osteoarthritis.* Bone Res, 2014. **2**.

205. Lyons, T.J., et al., *The normal human chondro-osseous junctional region: evidence for contact of uncalcified cartilage with subchondral bone and marrow spaces.* BMC Musculoskelet Disord, 2006. **7**: p. 52.

206. Huebsch, N., et al., *Matrix elasticity of void-forming hydrogels controls transplanted-stem-cell-mediated bone formation.* Nat Mater, 2015. **14**(12): p. 1269-77.

207. Dickinson, S.C., et al., *The Wnt5a Receptor, Receptor Tyrosine Kinase-Like Orphan Receptor 2, Is a Predictive Cell Surface Marker of Human Mesenchymal Stem Cells with an Enhanced Capacity for Chondrogenic Differentiation.* Stem Cells, 2017.

208. Buhring, H.J., et al., *Phenotypic characterization of distinct human bone marrow-derived MSC subsets.* Ann N Y Acad Sci, 2009. **1176**: p. 124-34.

209. Skog, M.S., et al., *Expression of neural cell adhesion molecule and polysialic acid in human bone marrow-derived mesenchymal stromal cells.* Stem Cell Res Ther, 2016. **7**(1): p. 113.

210. Muraglia, A., R. Cancedda, and R. Quarto, *Clonal mesenchymal progenitors from human bone marrow differentiate in vitro according to a hierarchical model.* J Cell Sci, 2000. **113 (Pt 7)**: p. 1161-6.

211. Ditlevsen, D.K., et al., *NCAM-induced intracellular signaling revisited.* J Neurosci Res, 2008. **86**(4): p. 727-43.

212. Harichandan, A., K. Sivasubramaniyan, and H.J. Buhring, *Prospective isolation and characterization of human bone marrow-derived MSCs.* Adv Biochem Eng Biotechnol, 2013. **129**: p. 1-17.

213. Widelitz, R.B., et al., *Adhesion molecules in skeletogenesis: II. Neural cell adhesion molecules mediate precartilaginous mesenchymal condensations and enhance chondrogenesis.* J Cell Physiol, 1993. **156**(2): p. 399-411.

214. Tavella, S., et al., *N-CAM and N-cadherin expression during in vitro chondrogenesis.* Exp Cell Res, 1994. **215**(2): p. 354-62.

215. Goldring, M.B., K. Tsuchimochi, and K. Ijiri, *The control of chondrogenesis.* J Cell Biochem, 2006. **97**(1): p. 33-44.

216. Younesi, M., V.M. Goldberg, and O. Akkus, *A micro-architecturally biomimetic collagen template for mesenchymal condensation based cartilage regeneration.* Acta Biomater, 2016. **30**: p. 212-221.

217. Vickers, S.M., T. Gotterbarm, and M. Spector, *Cross-linking affects cellular condensation and chondrogenesis in type II collagen-GAG scaffolds seeded with bone marrow-derived mesenchymal stem cells.* J Orthop Res, 2010. **28**(9): p. 1184-92.

218. Bian, L., et al., *Hydrogels that mimic developmentally relevant matrix and N-cadherin interactions enhance MSC chondrogenesis.* Proc Natl Acad Sci U S A, 2013. **110**(25): p. 10117-22.

219. Cleary, M.A., et al., *Expression of CD105 on expanded mesenchymal stem cells does not predict their chondrogenic potential.* Osteoarthritis Cartilage, 2016. **24**(5): p. 868-72.

220. Miot, S., et al., *In vitro and in vivo validation of human and goat chondrocyte labeling by green fluorescent protein lentivirus transduction.* Tissue Eng Part C Methods, 2010. **16**(1): p. 11-21.

221. Ehrbar, M., et al., *Enzymatic formation of modular cell-instructive fibrin analogs for tissue engineering.* Biomaterials, 2007. **28**(26): p. 3856-66.

222. Simona, B.R., et al., *Density gradients at hydrogel interfaces for enhanced cell penetration.* Biomater Sci, 2015. **3**(4): p. 586-91.

223. Barbosa, I., et al., *Improved and simple micro assay for sulfated glycosaminoglycans quantification in biological extracts and its use in skin and muscle tissue studies.* Glycobiology, 2003. **13**(9): p. 647-53.

224. Grogan, S.P., et al., *Visual histological grading system for the evaluation of in vitro-generated neocartilage.* Tissue Eng, 2006. **12**(8): p. 2141-9.

225. Goodpaster, T. and J. Randolph-Habecker, *A flexible mouse-on-mouse immunohistochemical staining technique adaptable to biotin-free reagents, immunofluorescence, and multiple antibody staining.* J Histochem Cytochem, 2014. **62**(3): p. 197-204.

Acknowledgements